

AD-A212 216

DTIC ACCESSION NUMBER

DTIC FILE COPY

PHOTOGRAPH THIS SHEET

LEVEL

INVENTORY

15th Leeds-Lyon Symposium on Tribology
The Tribological Design of Machine Elements

DOCUMENT IDENTIFICATION
SEPT 6th - 9th 1988

This document has been approved
for public release and sale in
distribution is unlimited.

DISTRIBUTION STATEMENT

ACCESSION FOR	
NTIS	GRA&I <input checked="" type="checkbox"/>
DTIC	TAB <input type="checkbox"/>
UNANNOUNCED	<input type="checkbox"/>
JUSTIFICATION	<i>per ltr</i>
BY	
DISTRIBUTION /	
AVAILABILITY CODES	
DIST	AVAIL AND/OR SPECIAL
<i>A-1</i>	

DISTRIBUTION STAMP



DTIC
ELECTE
SEP 13 1989

S E D

DATE ACCESSIONED

DATE RETURNED

REGISTERED OR CERTIFIED NO.

89 9 11 099

DATE RECEIVED IN DTIC

PHOTOGRAPH THIS SHEET AND RETURN TO DTIC-FDAC

AD-A212 216

15th LEEDS-LYON SYMPOSIUM ON TRIBOLOGY

"THE TRIBOLOGICAL DESIGN OF MACHINE ELEMENTS"

SEPTEMBER 6th - 9th 1988

DEDICATED TO THE LATE PROFESSOR F T BARWELL

INSTITUTE OF TRIBOLOGY
DEPARTMENT OF MECHANICAL ENGINEERING
UNIVERSITY OF LEEDS

SYNOPSIS OF PAPERS

SESSION 1 (Paper (i)) - TUESDAY 6th SEPTEMBER

KEYNOTE ADDRESS

THE TRIBOLOGICAL DESIGN OF MACHINE ELEMENTS

by

H S Cheng

(Walter P Murphy Professor of Mechanical Engineering)

(Northwestern University Evanston U S A)

The history of tribology indicates that many important tribological concepts and theories were stimulated by the needs of new machinery development, and the new tribological research findings, in turn, have helped to upgrade the design of more efficient and more reliable tribological elements. This mutual dependence is illustrated with some classical and recent examples.

Discussions are then given to the status of tribological design limits of counterformal as well as conformal contacts, and to the current needs to extend these limits to meet the requirements of future machineries in aerospace, automotive, and information processing industries.

SESSION II (Paper (i)) - WEDNESDAY 7th SEPTEMBER 1988

TRIBOLOGICAL DESIGN - THE AEROSPACE INDUSTRY

by

J Dominy

(Rolls-Royce plc, Derby, U K)

SYNOPSIS

The industrial definition of tribology tends to be somewhat wider than the classical "study of friction and wear". The interest of the industrial tribologist will extend beyond the behaviour of the contact itself to consider heat generation, cooling, component stressing and life.

In the case of the aero engine the most prominent tribological problem is bearings. The combination of load, speed and environment have caused the designer to use tool steels to meet the required life. A less obvious tribological application is that of the rubbing blade tip seals on compressors where any excessive wear directly affects the engine performance.

Gearboxes are common to both helicopters and turbo-prop engines. The applications are very different due to the very high ratio required for a helicopter and the different safety requirements since, in the case of the helicopter, the gearbox is fundamental to its operation. Efficiency has become of extreme importance in the aero engine gearbox, especially those for the very large (60,000 hp) engines projected for the next century. The weight, bulk and drag of the necessary cooling system are such that the concept only becomes viable if the losses can be maintained at less than 0.75% throughout the flight cycle.

It must be said that in most gearboxes and bearings, tribological design is a secondary consideration. This is partly due to the constraints placed on the designer by the environment and available lubricants but mainly to the requirement for the component not to suffer from major structural damage which is usually immediate, rather than surface damage, which can often be detected and is generally a more benign failure.

The tribology of airframes has tended to centre round flight controls and control bearings. Here again the rotary and fixed wing applications are different due to the requirement of the helicopter to transfer the control motion to the rotating blades. Tyres and brakes are continually developing as the weight and speed of large transport aircraft continues to increase.

Engine and gearbox lubricants have really only changed in detail in recent times due to the constraints of the specifications to which they are manufactured, the qualification requirements for any new lubricant and operator acceptance. Nevertheless, they are approaching their limits in terms of temperature capability and any significant improvement will necessitate new base stocks.

Industrial research into tribology has traditionally been in close association with the academic world, primarily due to the development of the principles of lubrication, particularly ehl, within the universities while the aerospace industry has applied the new science to its particular problems. This co-operation will continue but the restrictions on funding from both industrial and academic sources will mean increased selectivity and greater difficulty in supporting fundamental work.

TRIBOLOGICAL DESIGN - THE RAILWAYS

by

C Pritchard and T G Pearce

(British Railways Board, Derby U K)

SYNOPSIS

Introduction

In a paper reviewing the tribological aspects of railways, F T Barwell identified 47 interacting surfaces. Most are common to other industries but one, the interaction between steel wheel and steel rail, remains unique and fundamental to railways. An understanding of this interaction is crucial to many design processes, and forms the subject of this paper.

Lateral Guidance

The first requirements are that the wheels steer smoothly round curves while maintaining a stable path on straight track. Lateral suspension design thus calls for a knowledge of the steering mechanism. The two wheels on a common axle are coned (to a varying angle) so that axial displacement results in two different rolling radii and two different contact angles against the rails (Fig 1). A restoring force arises from the differences between the lateral reaction forces and the friction forces derived from "creepage" (the small mismatch between rotational and translational speeds) at the wheel/rail contacts (Fig 2).

Numerical calculations compute the positions and shapes of the contact areas and the normal stress distributions from which longitudinal, lateral and spin creep forces are compiled. The lateral suspension is then modelled, reacting to the changes in restoring force as the wheelset changes its attitude with time as it runs along the rail.

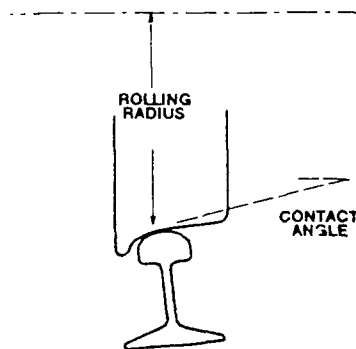


FIG. 1.

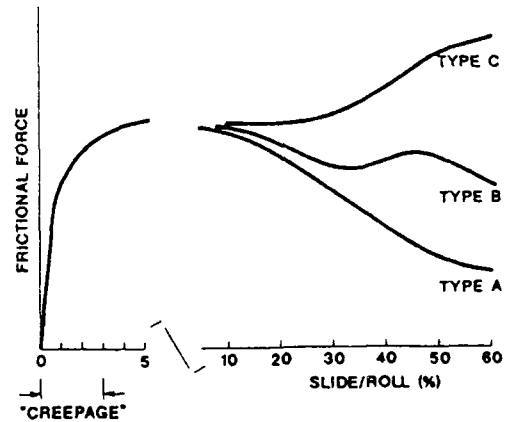


FIG. 2.

Measurements of Creepage

Measurements show that theoretical creep forces are approximately attained, even though the calculations assume that the friction coefficient in creepage is $\mu=0.60$ and the measured friction coefficient ("adhesion") varied from 0.40 to 0.15. It is suggested that the sliding conditions in "microslip" are different from those in the higher slip generated in adhesion measurements.

Wear

A requirement of the design process is to minimise wheel/rail wear. A wear number is invoked, the creep force T(Newtons) times the creepage Y. It is found that the wear rate of rails is proportional to TY over two ranges. For TY less than 200N wear is mild, above this value wear increases by a factor of 10 and debris is metallic. Water prolongs mild wear to TY's approaching 1000, while oils reduce mild wear by a factor of 10.

Surface Defects/Corrugations

As in all rolling contact devices, surface damage occurs other than wear. On rails, cracks form by a mechanism of rolling contact fatigue, initiating at small areas of local deformation ("squats") in the rail surface, sometimes at "corrugations" which form in a periodic wear pattern with a wavelength of 40-80mm.

Corrugations also cause noisy running. It is postulated that they are initiated by a stick-slip lateral motion of the rail, excited by a misaligned wheelset. This results in a periodic pattern of abrupt wear scars, each about 30mm long. The pattern becomes established if a vertical vibration of the rail is excited in phase with the scar spacing, and it is found that a spacing of twice the scar length gives rise to the largest vertical force fluctuations. Thus, when the natural frequency of vertical vibration, combined with traffic speed, provides a "wavelength" of about 60mm, corrugations are formed.

Braking and Traction

Braking and traction make considerable demands on the adhesion coefficient, which ranges between about 0.40 and 0.10, with occasional excursions down to 0.07 (0.02 on damp, rusty or leaf affected track). When adhesion is inadequate, control systems in the past have "dumped" power so as to prevent wheel or rail damage. More recently, wheel slide protection (WSP) and traction control devices are designed not only to prevent damage but also to control the slide/roll ratio where friction is highest. Some assume an optimum slide ratio, some "peak seek". Measurements of the friction characteristics show at least three types of behaviour (Fig 2), and friction is also increased by "conditioning" in sustained high slip. The way in which control should respond to such a diverse pattern is a current topic for debate.

Conclusions

A considerable tribological understanding of the interactions at the wheel/rail interface is required if the design of railway running gear and of braking and traction control is to be properly optimised.

SESSION II (Paper (iii)) - WEDNESDAY 7th SEPTEMBER

TRIBOLOGICAL DESIGN - THE AUTOMOTIVE INDUSTRY

by

P A Willermet

(Ford Motor Co. Dearborn, U S A)

SYNOPSIS

Rapid and continuing change within the automotive industry demands continual improvement in the quality, performance and reliability of vehicles. At the same time, competitive forces demand shorter product cycle times and new organizational approaches to the design process. The introduction of new technology and increased reliance on suppliers demand better methods of evaluating designs and materials. All of these factors lead to increased opportunities for the introduction of improved tribological design methods as well as the introduction of improved designs and materials.

SESSION II (Paper (iv)) - WEDNESDAY 7th SEPTEMBER 1988

TRIBOLOGICAL DESIGN - THE PROCESS INDUSTRY

by

J D Summers-Smith

(Consultant, Guisborough U K)

SYNOPSIS

The chemical process industry does not normally design its own machines, but has to purchase what is available in the market place. Such equipment will have been proved on the manufacturer's test bed, but this is a somewhat idealised situation well removed from the real operational environment where the machine will be subject to the full process conditions, seldom possible to realise on the test bed, as well as to process upsets, operational malpractice, gradual deterioration in service and other factors, probably unforeseen, outside those specified in the original purchase enquiry.

If failures are to be remedied, and in the context of this Symposium we are concerned with those affecting tribological components, the user must have a full understanding of the design and operation of such components in order that the true failure mechanism can be identified. Full cooperation with the original designer is necessary to obtain a feasible solution; however, before this is forthcoming it may even be necessary to convince the manufacturer by a suitable analysis and presentation of the facts that there is a genuine design fault and that failure is not merely the result of the maloperation of his machine.

Examples are given in the full paper of actual machine problems that have occurred in the chemical industry. These examples are concerned with boundary lubrication, load calculation, chemical attack of tribological components and bearing influenced rotor dynamics and have been chosen specifically both to highlight different tribological mechanisms and to illustrate the depth of analysis necessary to identify the cause of failure and obtain a satisfactory solution. These case studies show the need for a full understanding of the machine and the functioning of the machine elements that is crucial in developing the necessary degree of cooperation between the user and designer and show the role of the machine user in this process.

Ways are discussed in which the knowledge gained from the analysis of such operating experience can be disseminated and used to influence new designs in order to achieve enhanced reliability and predictability of performance of tribological machine elements. A brief look is given at future problem areas in tribology that are likely to become of significance in machines for the process industries.

SESSION III (Paper (i) - WEDNESDAY 7th SEPTEMBER 1988

DESIGN OF CONTROLLABLE MECHANICAL SEALS

by

R F Silant (Georgia Institute of Technology, U S A)

O Giles, W E Key (BW/IP International Inc., U S A)

SYNOPSIS

Modern noncontacting mechanical seals operate with a thin lubricating film of fluid between the seal faces. Conventional seals are designed such that this film is of optimum thickness at a single steady state design point. However, since most seals must operate over a range of steady state conditions and a variety of transients, they experience frequent periods during which the film thickness is too small, and frequent periods during which it is too large. The former lead to mechanical contact between the faces resulting in face damage, excessive wear, and decreased reliability, while the latter lead to periods of excessive leakage.

Basic Concept

The above problems can be alleviated with a seal in which the thickness of the lubricating film is electronically controlled. A microcomputer-based control system and actuator continuously adjust the film thickness, based on information received from a sensor which monitors conditions in the film. The control system sets the film thickness at an optimum value and responds to changes in operating and environmental conditions so that the film thickness is kept at an optimum value, and both face contact and excessive leakage are prevented.

The film thickness is adjusted by an electromechanical actuator which exerts a force on the backside of the nonrotating seal face. This causes the face to deform, and the sealing surface to cone in the radial direction (on the order of microns).

The shape of the pressure distribution in the fluid film is strongly dependent on the amount of coning, and that pressure distribution produces the "opening force" which keeps the film intact and determines film thickness. The larger the amount of coning, the more convex the pressure distribution, the larger the instantaneous opening force, and the larger the steady state film thickness.

Configuration

A controllable seal, as described above, is shown in figure 1. The rotating seal face is fixed in the axial direction, while the non-rotating face floats axially. A piezoelectric actuator mounted within the floating assembly exerts an axial force on the backside of the nonrotating face, near the ID, while the OD is constrained from axial movement (relative to the assembly) by the holder. Thus, the actuator causes the nonrotating face to deform and cone; the larger the voltage applied to the actuator, the larger the amount of coning, the larger the opening force, and the larger the steady state film thickness. Conditions within the nonrotating face, and those within the sealed cavity by a second thermocouple. The outputs of these thermocouples, and that of a shaft rotation sensor, are fed into an adaptive control system, which determines the level of voltage to be applied to the actuator for optimum seal operation.

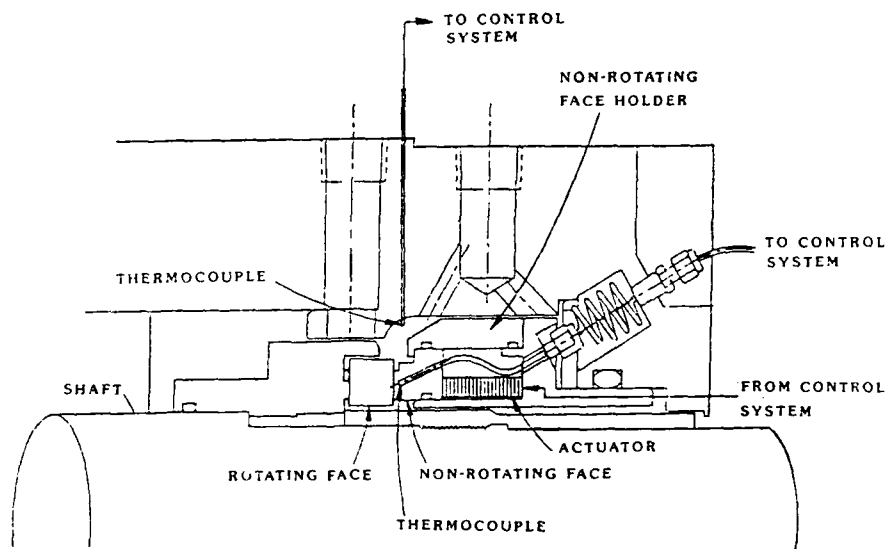


Figure 1

Testing

The above seal has been extensively tested in the laboratory and in the field. A 200 hour accelerated duty cycle laboratory test (simulating 300 weeks of normal operation), in which face temperature and other operating variables were monitored, indicated good performance. Examination of the faces following the test showed no observable face damage. An 800 hour field test on the feedwater pump for the steam generator of a nuclear power plant, also resulted in good performance. This was evidenced by the condition of the seal faces following the test, as well as histories of the important variables (e.g. face temperature) during the test.

MICRO-ELASTOHYDRODYNAMIC LUBRICANT FILM FORMATION
IN ROTARY LIP SEAL CONTACTS

by

A Gabelli

(SKF Engineering & Research Center B V, Nieuwegein, The Netherlands)

SYNOPSIS

1. Introduction

This paper examines the characteristics of the lubricant film developed under rotary lip seals. It has recently been shown experimentally (1) that these types of seals may operate with different regimes of lubrication varying from simple boundary conditions to full film formation. The mechanics of the lubricant film built up between apparently parallel surfaces is still controversial (2). There are however strong experimental indications (1) supporting the idea of film formation arising from the EHD action of colliding asperities at the sealing interface.

In the present study a theoretical understanding of rotary lip seals lubrication is attempted by analyzing the EHD contribution of the asperities in virtual contact. In addition also the positive hydrodynamic pressure originated by the wavy morphology of the sealing surfaces is evaluated.

2. Model of the Sealing Surfaces and Fluid Film Analysis

The mating surfaces forming the junction of the sealing ring, Fig. 1, are modelled as two rough surfaces having ideally flat and parallel mean plane, Fig. 2. The real pressure and area of the micro-EHD contacts is investigated by applying the Greenwood & Tripp (3) stochastic model for rough surfaces in contact. While the hydrodynamic contribution to the load support of the seal is directly computed from a simplified functional representation of the roughness texture of the sealing contact.

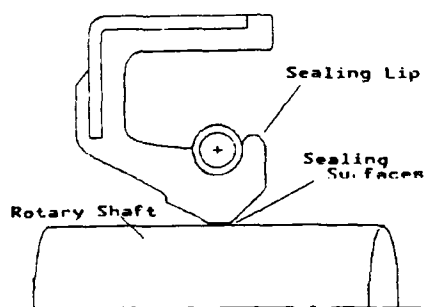


Figure 1

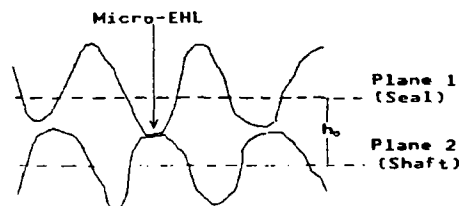


Figure 2

3. Results

The load support developed between the mating surfaces is analyzed on its elastic and hydrodynamic part. Typical sets of results for the average fluid film, i.e. surfaces separation, vs. the EHD pressure and hydrodynamic pressure are shown in Fig. 3 and 4.

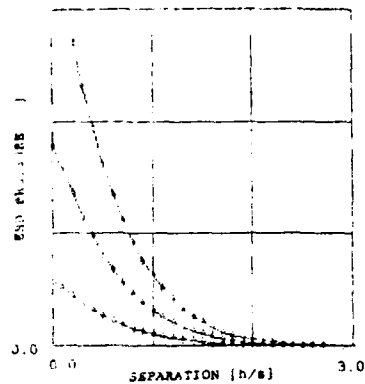


Figure 3

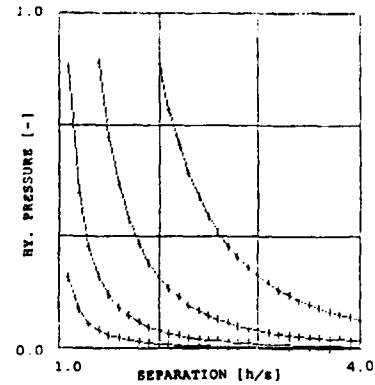


Figure 4

The first graph shows the influence of the stiffness of the asperities on the load carrying capability of the surface texture. Variations of the elastic modulus, as found in the different type of rubbers used in today's seals manufacturing, have a significant effect on the share of load supported by micro-EHD lubrication.

The influence of the variation of the topographic characteristics of the surface in contact is outlined in Fig. 4. The graph shows the nominal hydrodynamic pressure generated at the sealing interface for different values of root mean square of the surface height distribution calculated for the equivalent composed roughness of the two meshing surfaces.

References

- (1) OGATA, M., FUJII, T., SHIMOTSUMA, Y., "Study on Fundamental Characteristics of Rotating Lip-type Oil Seals" Proceedings of the 14th Leeds-Lyon Symposium of Tribology, pp 553-560, 1987.
- (2) LEBECK, A.O., "Parallel Sliding Load Support in the Mixed Friction Regime. Part 2 - Evaluation of the Mechanisms." ASME Journal of Tribology, Vol. 109, pp.196-204, 1987.
- (3) GREENWOOD, J.A., TRIPP, J.H., "The Contact of Two Nominally Flat Rough Surfaces." Proc. Instn. Mech. Engrs., Vol. 185, pp.525-533, 1970.

SESSION III (Paper (iii)) - WEDNESDAY 7th SEPTEMBER 1988

LUBRICATION OF RECIPROCATING SEALS: EXPERIMENTS ON THE INFLUENCE OF
SURFACE ROUGHNESS ON FRICTION AND LEAKAGE

by

A F C Kanters and M Visscher

(Eindhoven University of Technology, The Netherlands)

SYNOPSIS

Introduction

The literature on reciprocating elastomeric seals includes much experimental data on their frictional behaviour. Regarding the dependency of the friction force on the velocity or on the product of viscosity and velocity at constant fluid pressure, it appears that reciprocating seals exhibit the characteristic behaviour depicted in fig.1. This curve is like a Stribeck curve. For constant viscosity it appears that with increasing speed the lubrication mode of the seal changes from boundary lubrication, via mixed lubrication, to full film lubrication. Most theoretical work on reciprocating seals has been devoted to the solution of the smooth elasto-hydrodynamic lubrication problem.

Yet in the early seventies Field and Nau obtained results, which makes one reflect on the lubrication of the seal contact [1,2,3]. From experiments on annular rubber rings of rectangular cross-section they found that friction was of other than hydrodynamic origin. Nevertheless full lubricant films were observed, which would by viscous shear give rise to friction values at least an order of magnitude smaller. Their results imply the simultaneous occurrence of high friction and high leakage. It is rather amazing that no further work has been reported on this matter.

We believe that further investigation into the lubrication of the seal contact is desirable. As a first step friction and leakage measurements on a polyurethane rod seal with a rectangular cross-section have been performed. To study the influence of the surface roughness of the seal and of the rod two different rods have been used, one being very smooth, the other having a commonly used surface finish.

Experimental apparatus / measuring techniques

The essential parts of the test rig used for the measurements, are illustrated in fig.2. The seal housing, holding a seal and a clearance bush pressurised by a separate hydraulic system, is moved over the stationary rod by a hydraulic servo drive unit and is externally guided by a high precision linear motion bearing. At one side the rod is in axial direction freely suspended, so that a force transducer between the other end of the rod and the frame enables the measurement of friction.

Leakage measurements are performed by extracting the leaked fluid film from the rod over a defined length between two bands of gummed tape by solution in pure hexane. The hexane and oil are next separated by vacuum evapo-

ration and the oil is weighed, so that the average thickness of the leaked film can be determined.

Test program

An identical test program has been performed for both rods. The first part of this program consisted solely of friction measurements in dependence of pressure and velocity to establish friction curves as depicted in fig.1. The second part of the test program consisted of simultaneous measurements of friction and leakage. The results enabled some conclusions to be drawn on the lubrication of the seal contact.

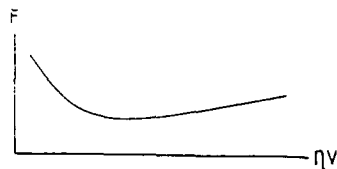


fig.1 characteristic friction curve

- 1 SEAL HOUSING
- 2 ROD
- 3 LINEAR MOTION BEARING
- 4 FRAME
- 5 RADIAL SUSPENSION WITH FORCE TRANSDUCER
- 6 RADIAL SUSPENSION
- 7 CYLINDER OF HYDRAULIC SERVO DRIVE UNIT

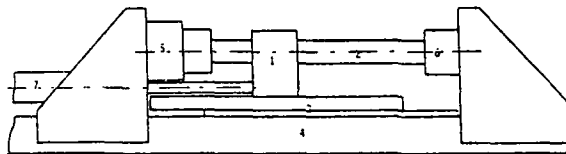


fig.2 essential parts of the test rig

References

- [1] Field, C.J., Nau, B.S., 'An experimental study of reciprocating seals', proceedings conference on elastohydrodynamic lubrication, organised by Inst. Mech. Engrs., 1972, paper C5, 29-36
- [2] Field, C.J., Nau, B.S., 'Film thickness and friction measurements during reciprocation of a rectangular section rubber seal ring', 6th Int. Conf. on Fluid Sealing, organised by BHRA, 1973, paper C5, 45-56
- [3] Field, C.J., Nau, B.S., 'The effects of design parameters on the lubrication of reciprocating rubber seals', 7th Int. Conf. on Fluid Sealing, organised by BHRA, 1975, paper C1, 1-13

SESSION III (Paper iv)) - WEDNESDAY 7th SEPTEMBER 1988

RADIAL LIP SEALS, THERMAL ASPECTS

by

M J L Stakenborg and R A J van Ostayen

(Eindhoven University of Technology, The Netherlands)

SYNOPSIS.

In studying the sealing and lubrication mechanism of radial lip seals it is important to know the influence of the seal-shaft contact temperature on the contact conditions such as the contact force, the contact width and the contact stress distribution. The influence of the contact temperature is studied by a coupled temperature stress analysis employing the finite element method (FEM).

The contact temperature resulting from dissipated friction heat was calculated using the thermal network method (TNM).

The contact temperatures were measured on a test rig using 3 different measurement techniques.

FEM ANALYSIS.

Using a coupled temperature-stress FEM analysis, the following temperature effects on the static seal-shaft contact conditions were studied : (1) change in seal material stiffness, (2) change in garter spring stiffness, (3) expansion of the seal material and (4) expansion of the shaft.

TNM ANALYSIS.

The seal-shaft contact temperature which results from a certain dissipated friction heat depends on the heat balance in the entire machine. The thermal network method is an appropriate method to calculate the (contact) temperatures which will occur in seal applications in practice. In the thermal network method a machine is divided into a network of thermal components such as heat resistors, capacitors and sources. The TNM is an easy to conceive and flexible method, which does not demand expensive software and hardware like the FEM.

EXPERIMENTS.

Because of the small dimensions of the contact width b (in practice $0.05 < b < 0.5$ mm) it is difficult to measure the temperatures inside the contact. Three different experimental techniques (NTC thermistors, thin film transducers and infra-red measurements) were employed to measure the seal-shaft contact temperatures on a test rig.

5

RESULTS.

- (1) The contact temperature T_c has only a minor influence on the static contact conditions of a rubber lip seal for $0 < T_c < 100$ °C.
- (2) Good correspondence was found between the contact temperatures calculated using the TNM and the temperatures measured on a test-rig for both transient and steady-state situations.

REFERENCES.

- [1] Upper, G. 'Dichtlippentemperatur von Radial-Wellen Dichtringen.' Ph.D. Thesis, Univ. of Karlsruhe, Germany, July 21, 1967. (In German)
- [2] Stakenborg, M.J.L. 'On the sealing and lubrication mechanism of radial lip seals.' Ph.D. Thesis, Eindhoven Univ. of Technology, Sept. 20, 1988.

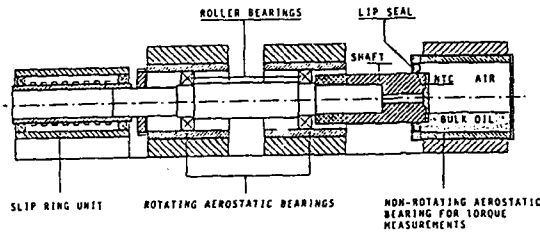


Fig. 1 : Test-rig.

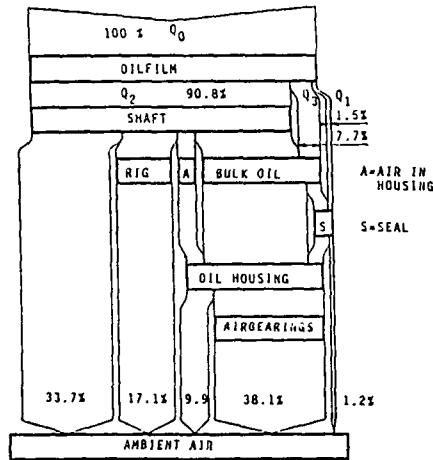


Fig 2 : Sankey diagram of heat flows in test-rig.

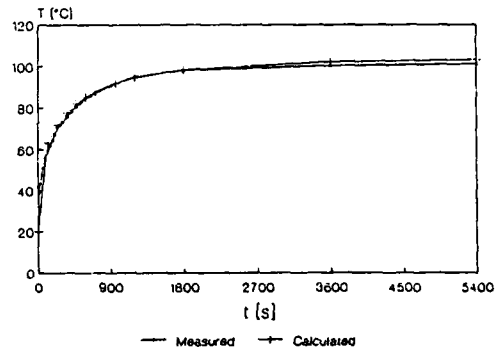


Fig 3 : Transient contact temperatures.

6

LUBRICATION AND FATIGUE ANALYSIS OF A CAM AND ROLLER FOLLOWER

by

B A Gecim

(General Motors Research Laboratories, Michigan, U S A)

SYNOPSIS

The lubrication characteristics of a cam and roller follower interface are investigated. The governing kinematic and geometrical relationships are incorporated with elastohydrodynamic lubrication analysis of concentrated contacts. The loads at the interface are determined by the dynamic analysis of the overall valve train.

The specific topics analyzed in this study are: the lubricant film thickness including thermal and squeeze-film effects; maximum Hertzian pressures and possibility of plastic flow; traction forces and possibility of gross slip; cam torque and valve train energy loss; fatigue life of several rolling surfaces; parametric studies to improve film thickness, contact pressures, and fatigue life.

Sample Results

Figure 1 shows the lubricant film thickness around the cam circumference for two speeds. The representative composite-RMS-roughness value for the cam/follower pair is also indicated.

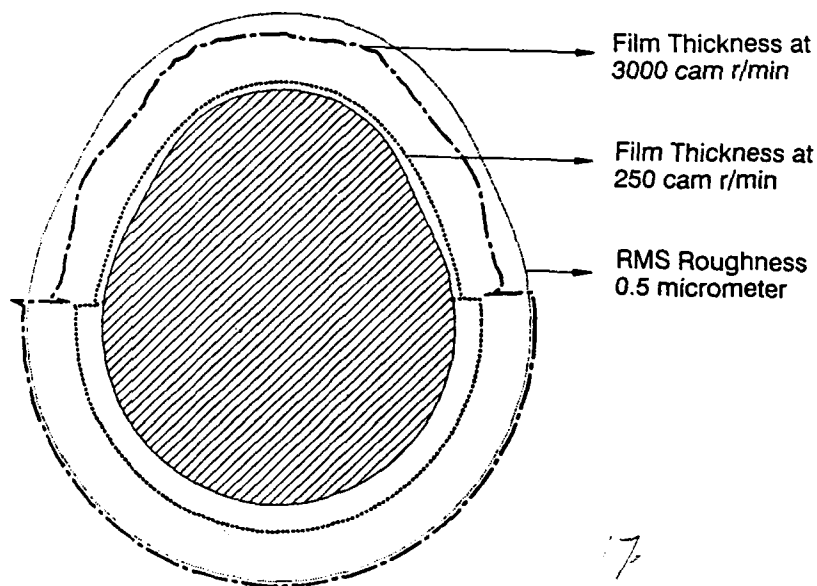


FIGURE 1

The specific film thickness is much smaller than unity at low speeds, even on the base circle, indicating boundary lubrication mode. At higher speeds, especially on the base circle, conditions are closer to the mixed lubrication mode.

Figure 2 shows the traction coefficient at the cam/follower interface for a no-slip condition. The traction force provides the required acceleration to the roller and overcomes the bearing friction. At low rotational speeds, inertia of the roller is negligible and the only traction required is to overcome the needle bearing friction. At high rotational speeds, the roller inertia becomes important. In either case, because of operating in boundary and mixed lubrication modes, gross slip at the interface seems unlikely.

Figure 3 shows the lubrication regimes at the cam/roller interface over one complete camshaft rotation at 3000 cam r/min. The operating conditions are in the elastohydrodynamic regime associated with heavily loaded contacts. At lower speeds, the elastic deformations become even more pronounced.

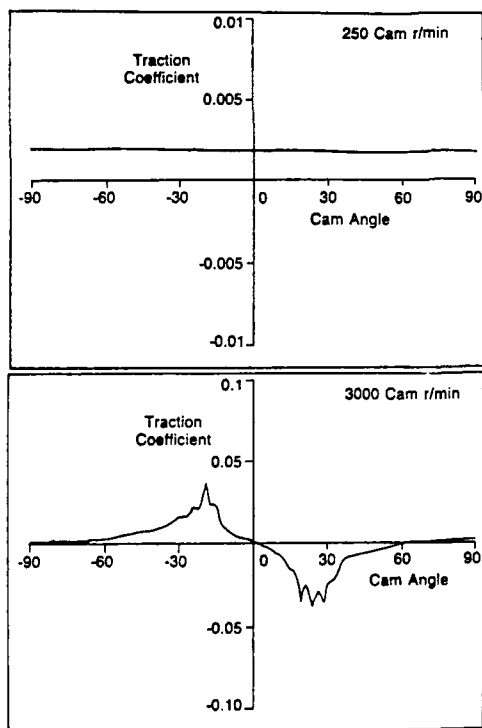


FIGURE 2

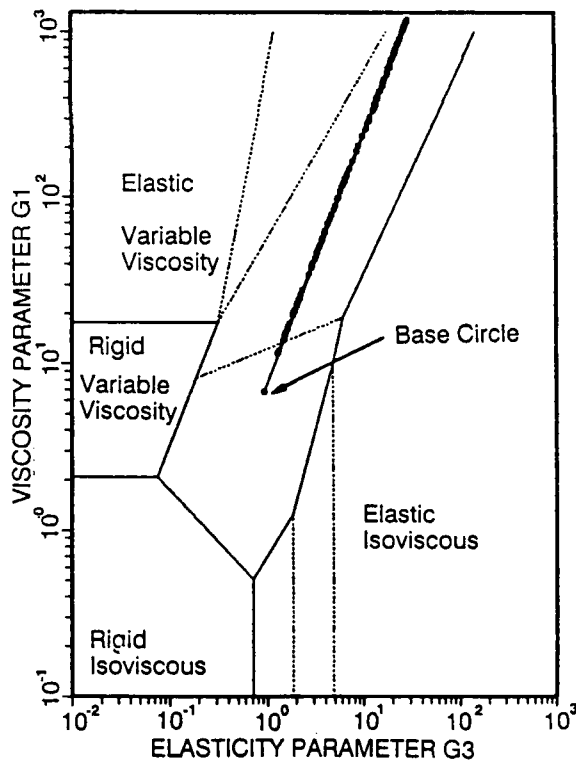


FIGURE 3

SESSION IV (Paper (ii)) - WEDNESDAY 7th SEPTEMBER

PREDICTIONS OF CAM WEAR PROFILES

by

R H Fries and C A Rogers

(Virginia Polytechnic Institute and State University, U S A)

Synopsis

This paper describes a computational method for predicting the profiles into which cams and followers wear in service. The method is conceptually simple. The first step is to solve the kinematic constraint problem for the cam and follower. This step determines the locations of the contact patch center on the cam and follower for all cam rotation angles. From these results, the follower displacement, velocity, and acceleration are determined. The next step is to solve the cam dynamics problem to obtain the normal forces at the contact patch. The tangential contact forces are determined assuming Coulomb or other friction conditions that may exist in the contact region. A simple wear model is then employed to estimate the localized wear as a function of the cam angle.

The cam and follower profiles are modified according to the amount of wear estimated, and new cam and follower profiles are obtained. The process is repeated sequentially so that the continuous wear process is approximated by a number of discrete wear steps. The process is nonlinear because the cam dynamics depend upon the cam and follower profiles.

This method has potential for predicting the shapes into which cams and followers will wear in service. The method is applicable to other mechanical components as well, and it has been applied to the wear process of rail vehicle wheels.

Cam Kinematics

When cams possess profiles that are described by simple analytical curves, cycloids, harmonics, and polynomials, for example, it is a straightforward matter to determine the follower motion. A number of undergraduate texts describe analytical methods to solve the cam kinematics problem. See Mabie and Reinholtz (1987) for example. When wear occurs on a cam and its follower, then the solution of the cam kinematics problem is not so easy because the profiles are no longer described by simple curves.

For wear predictions, it is convenient to describe cams and followers by sets of points located on their contacting surfaces. We developed a method of solving the kinematics problem for cams and followers so described. For a given cam position, the cam and follower profile points are fit with splines, and the contact point is found by determining the intersection of the splines. Follower displacements are then obtained for one revolution of the cam. To obtain follower velocity, we least squares fit the displacement curve and differentiate. Then we smooth the results. To obtain accelerations, we least squares fit the velocity results, and differentiate. We also smooth the accelerations results. Our method was adapted from the work of Cooperrider et al. (1976), who solved the kinematic constraint problem for railway wheels on rails.

9

1

For a given cam angular velocity, the above method provides follower displacement, velocity, and acceleration, and the location of the contact point on the cam and follower for any cam position.

We verified our kinematic solutions by comparing positions, smoothed velocities, and smoothed accelerations obtained numerically to those obtained analytically for simple cam profiles. The results of our numerical method were quite good.

Cam Dynamics

In this work we have thus far assumed that a flat follower with a given mass is spring loaded against the cam. The cam dynamics are therefore simple, and the normal contact force can be computed easily once the cam kinematics solution is obtained. More complex cam dynamics can be accommodated with an increase in computation time.

We have also assumed Coulomb friction conditions to exist at the contact patch. The presence of a lubricating film at the contact interface would influence the dynamics. This effect can also be accounted for, but it has not been included in the initial work.

Wear Model

We have assumed the wear process to be described by a simple wear model of the Archard (1953) type wherein wear is postulated to be proportional to normal load and sliding distance. The general method admits the use of essentially any wear model, and the Archard model was used in this work for its simplicity.

For each increment of cam rotation, a wear volume is computed according to the wear model. The points describing the cam and follower profiles are then changed in proportion to the wear volume. The process is repeated sequentially to simulate the continuous wear process.

Results

The paper contains results of wear predictions for the simplified conditions discussed above. As expected, wear rates are higher at cam positions corresponding to higher contact loads. These results are intended to be illustrative of the wear computation method. We have made no attempt in this initial work to compare predicted wear profiles to actual service worn profiles. These comparisons are the subject of future work.

References

- Archard, J. F., 1953, "Contact and Rubbing of Flat Surfaces," *Journal of Applied Physics*, Vol. 24, pp. 981-988.
- Cooperrider, N. K., et al., 1976, "Analytical and Experimental Determination of Non-linear Wheel Rail Geometric Constraints," *Symposium on Railroad Equipment Dynamics*, ASME, pp. 41-70.
- Mabie, H. H., and Reinholtz, C. F., 1987, *Mechanisms and Dynamics of Machinery*, John Wiley & Sons, New York.

20

SESSION IV (Paper (iii)) - WEDNESDAY 7th SEPTEMBER

CAM AND FOLLOWER DESIGN

by

A D Ball, D Dowson and C M Taylor

(The University of Leeds U K)

SYNOPSIS

Software has been developed within the Department of Mechanical Engineering at the University of Leeds which allows tribological studies to be carried out upon any of the cam and follower designs in common use in today's internal combustion engines. The program is written in such a manner that it can easily be used by any competent professional engineer.

The program uses analysis developed by Dyson and co-workers (1,2,3) to determine the kinematics of the contacting cam and follower pair. The loads at the cam/follower interface are determined by summing the force components arising due to the friction at the interface, the spring force and the inertia of the reciprocating parts. Throughout the analysis it is assumed that, apart from the spring, the valve train components are rigid. The frictional forces and moments at the valve guide and follower pivot point (or follower bore) are ignored, as is the load arising due to the gas pressure upon the head of the valve. Full details of the basis of the analyses involved will be presented.

The program allows studies to be made of the effects of changes in design parameters upon the tribological performance of the valve train. Parametric studies have been carried out on several different types of valve train layouts including those incorporating cams acting against end pivoted followers (eg. as employed in the Ford 2.0l Pinto engine currently used in the Sierra range) and cams acting against centrally pivoted followers (eg. as used in the Rover 2300 and 2600 engines). Table 1 shows some of the predicted benefits to be gained by making small, realistic changes (as shown in Table 2) to the valve trains mentioned above.

The software development has been accompanied by an experimental programme designed to validate the analytical model.

	Hertzian Stress at Cam Nose	Frictional Power Loss	Lubricant Film Thickness at Cam Nose
Rover 2300/ 2600	-20%	-14%	+12%
Ford 2.0l Pinto	-19%	-3%	+17%

Table 1 Predicted Benefits of Small Changes In Design For Two Types of Valve Train.

	Base Circle Radius	Follower Radius of Curvature	Valve Spring Stiffness
Rover 2300/ 2600	+10%	-8%	-10%
Ford 2.0l Pinto	+20%	+12%	-10%

Table 2 Small Changes Made to the Valve Trains.

References

- 1 Dyson, A. and Naylor, H. Application of the Flash Temperature Concept to Cam and Tappet Wear Problems. Proc. I. Mech. E. (A.D), No 3 1960-61, pp 255-280.
- 2 Dyson, A. Elastohydrodynamic Lubrication and Wear of Cams Bearing Against Cylindrical Tappets. SAE 770018.
- 3 Dyson, A. Kinematics and Wear Patterns of Cam and Finger Follower Automotive Valve Gear. Tribology International, June 1980, pp 121-132.

POWER TRANSMISSION BY FLAT, V AND TIMING BELTS

by

T H C Childs and I K Parker

(The University of Bradford, U K)

SYNOPSIS

This paper reviews aspects of current understanding of belt performance, relating for flat and V belts power loss and for timing belts tooth loading to belt tension and torque transmission, to belt mechanical and friction properties and to pulley radius and angle of wrap.

Belt Construction

Modern belts are composite constructions, transmitting load through a stiff tension member and traction through an elastomeric facing. Flat belts are made in two main ways: either a strip tension member, usually cold drawn nylon, is bonded to a fabric previously roll coated with elastomer, and made into a loop by a welded lap joint; or a truly endless belt is made by winding a nylon, polyester or glass fibre cord on to a cylindrical mandrel and moulding a rubber carcass round it. V and timing belts are always made by moulding a rubber carcass round a mandrel-supported cord; the driving faces of timing belts are reinforced by a textile cover but V belt faces are not always so protected.

The ratio c of belt extension force to strain for a 2mm thick strip tension member flat belt is typically 1 kN per mm of belt width while for typical automotive V and timing belts c is 5 to 10 kN/mm. Youngs modulus of belt elastomer carcasses is of the order of 10 MPa but can be anisotropic. Friction coefficients between textile faced belts and dry pulleys are about 0.2 to 0.35 and for belts without a textile cover are between 0.4 and 0.9.

Power Loss Preliminaries - Flat and V Belts

Figure 1 shows clockwise rotating pulleys, a driving pulley of radius R_1 , angular speed ω_1 and torque T_1 and a driven pulley with R_2 , ω_2 and T_2 . F_E and F_r , V_E and V_r are belt tensions and speeds as shown. In an ideal, no power loss system

$$\omega_1 R_1 = V_E = V_r = \omega_2 R_2 \quad \text{and} \quad T_1 = (F_E - F_r) R_1, \quad T_2 = (F_E - F_r) R_2$$

but in fact belt extension leads to $V_E > V_r$ when torque transmission makes $F_E > F_r$. The speed difference is accommodated by slip over part of the contact arc as shown. Further, compliance of the belt carcass enables a speed difference ΔV_E to occur between V_E and $\omega_1 R_1$ on the driving pulley and similarly on the driven pulley. Torque differences ΔT can arise between T and $(F_E - F_r)R$.

It can be shown that the fractional power transmission loss $\Delta P/P$ is made up of fractional speed and torque loss terms:

$$\frac{\Delta P}{P} = \left. \begin{aligned} & \frac{V_E - V_r}{V_E} + \frac{\Delta V_E}{V_E} + \frac{\Delta V_r}{V_r} \\ & + \frac{\Delta T_1}{T_1} + \frac{\Delta T_2}{T_2} \end{aligned} \right\} (1)$$

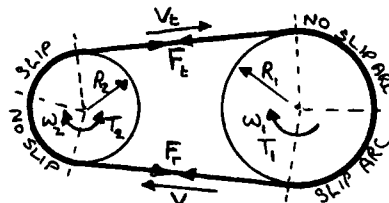


FIGURE 1

3

24

Flat Belt Power Losses

Classical theory¹ considers only losses due to extension creep, the first term of equation 1, and shows that

$$(V_E - V_r)/V_E = (F_E - F_r)/C \quad (2)$$

As $(F_E - F_r)$ increases, the no slip arc reduces until, by the capstan formula, when $F_E/F_r = \exp(\mu\theta)$, it disappears and then a sudden transition to skidding occurs. θ is the angle of wrap between belt and pulley.

Subsequently² it has been shown that shear of the belt carcass in the no slip arc gives rise to $\Delta V/V$ loss terms. These are only significant when $R\theta_2 A < 1$. $R\theta_2$ is the length of the no slip arc and A is $\sqrt{(G/c)(d/t)}$. G is the carcass shear modulus, t the carcass thickness and d the belt width. As $R\theta_2 A$ reduces to zero, $\Delta V/V$ increases steadily to infinity. With increasing torque there is thus a steady transition from equation 2 losses to skidding.

Experiments³ show that thick flat belts can also experience speed losses due to radial compression of the carcass. They also show torque losses, in the same way as V belts, considered next, but not yet properly analysed.

V Belt Power Losses

Belt carcass compliance in the pulley groove of a V belt transmission results in radial motion of the belt as its tension changes round the arc of contact. This can significantly increase the length of the slip arc for a given torque and also results in speed loss terms: for two equal pulleys

$$\Delta V_E/V_E + \Delta V_r/V_r = (F_E - F_r)(g/R^2) \quad (3)$$

where g is the belt's radial compliance, typically 0.02 to 0.05 mm²/N.

Hysteresis in V-belt bending at entry to and exit from a pulley causes torque losses. Further torque losses are caused by differences in sliding of the belt in the pulley groove at entry and exit: experiments with two equal radii pulleys show

$$\Delta T = 0.75(F_E + F_r)R (gEI/R^4)^{1/2} \quad (4)$$

where EI is belt bending stiffness; current analyses^{3,5} underestimate this.

Carcass shear, known to be important for flat belt losses, has not yet been considered in the context of V belt losses; equations 2 and 3 predict no dependence of speed loss on angle of wrap. Experiments will be reported that show that speed losses increase as angle of wrap, and belt tension too, decrease. Empirical equations exist for relating the efficiency of a V belt drive to the pulley layout.

Power Transmission by Timing Belts

Meshing between timing belt and pulley teeth enables torque transmission above the capstan formula limits for flat and V belts, without any speed loss. Torque loss occurs due to sliding at entry and exit. However the main interest of mechanical analyses⁶ has been to relate tooth loading to tension member and belt tooth stiffness, to pitch differences between belt and pulley teeth and to drive geometry, because tooth loading determines belt life, either limited by tooth fatigue or by cover wear.

1. SWIFT H.W., Proc I Mech E, 1928, 2, 659-699.
2. FIRBANK T.C., Int J Mech Sci, 1970, 12, 1053-1064.
3. CHILDS T.H.C. and COWBURN D., Proc I Mech E, 1987, 201 pt D, 33-53.
4. GERBERT G.B., Acta Polytechnica Scandinavica, 1972, Mech Eng Series No 67
5. GERBERT G.B., Trans ASME Jnl Engng Ind, 1974, 96, 877-885.
6. NAJI M.R. and MARSHEK K.M., Trans ASME Jnl Mechanisms, 1983, 105, 339-347

SESSION V (Paper (ii) - WEDNESDAY 7th SEPTEMBER

POWER RATING OF FLAT BELTS - A WEAR APPROACH

by

G Gerbert

(Chalmers University of Technology, Göteborg, Sweden)

SYNOPSIS

Modern flat belts consists of a kernel of fiber reinforced elastomeric material which takes up belt tension. One or both of the flat surfaces are covered with a thin layer of high friction material.

The power rating procedure of flat belt drives described in manufactures catalogues is based on testing and experience. It appears that the procedure might be adopted to a linear wear model of the surface layer.

Background

In most textbooks on machine elements the failure mechanism of a flat belt is assumed to be tensile stress fatigue. The tensile stress σ is a combination of belt tension and bending stresses

$$\sigma = F_2 / (b h) + E h / D$$

Application of the coefficient of traction $\lambda = (F_2 - F_1) / (F_2 + F_1)$ transforms tight side tension F_2 to effective pull $F'_u = F_2 / (1+\lambda)$. The specific effective pull is $F'_u = F_u / b$ or with stresses

$$F'_u = (\sigma - E h / D) h / (1 + \lambda)$$

A principal graph is shown in fig. 1. Failure is based on a certain stress σ .

Catalogue procedure

According to a catalogue a certain type of flat belt is capable to transmit specific effective pull proportional to minimum pulley diameter i.e.

$$F'_u = k D$$

A principal graph is shown in fig. 1. It appears that the procedure is equivalent of specifying a maximum pressure

$$p_{\max} = 2 (1 + \lambda) F'_u / D$$

between the belt and pulley. We identify

$$p_{\max} = 2 (1 + \lambda) k$$

There is no failure mechanism directly related to the maximum pressure.

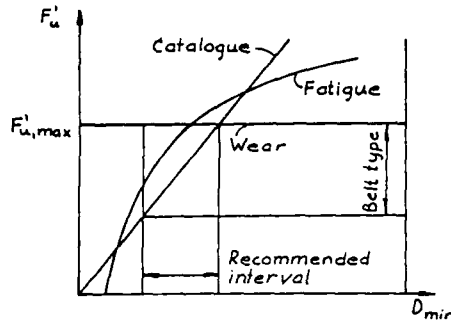


Figure 1. Competing failure mechanisms

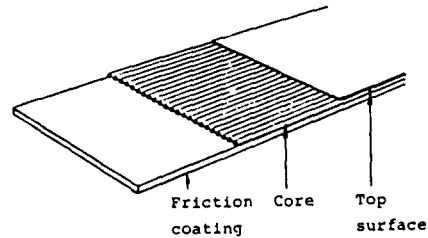


Figure 2. Cross section of flat belt

Wear concept

A cross section of a flat belt is shown in figure 2. Wear out of the friction layer leads to malfunction and failure of the drive. The linear wear rate law reads

$$w = p v / W \quad (W = \text{wear strength})$$

There are mainly two factors contributing to the sliding velocity v viz. belt elongation (creep) and pulley crowning.

Belt elongation

The sliding velocity due to stretching of the belt is $v = V (F - F_0) / (bc')$ where $c' = hE = \text{specific strain stiffness}$. Simple flat belt mechanics gives

$$p = F / (b R) \quad ; \quad dF = \mu F d\phi$$

The wear during one passage of a pulley then becomes

$$s_S = (F'_U)^2 / (2 \mu W c')$$

Pulley crowning

The pulley has a slight curvature in the axial direction the height of which is Δ . The sliding velocity on top of the pulley is $v = V \Delta / D$. Again application of p and dF gives the wear contribution during one passage to

$$s_C = F'_U \Delta / (\mu W D)$$

It is recommended that $\Delta / D \approx 0.003 \approx \text{const.}$

Total wear

By summing the two contributions we get

$$(F'_U)^2 / (2 c') + F'_U \Delta / D = \mu W s$$

Failure is based on a certain wear s . A permissible F'_U can be calculated which is independent of pulley diameter as shown in fig.1.

Power rating

Wear of the friction layer of a flat belt leads to a gradual decrease of the function of the belt and that is to be preferred compared to belt breakage. Power rating can be based on the derived equation so the situation shown in figure 1 will occur.

SESSION VI (Paper (i) - WEDNESDAY 7th SEPTEMBER

THE RELATIONSHIP BETWEEN UNEVEN TOOTH CONTACT LOADING
AND SURFACE DURABILITY IN FLEXIBLE GEAR DESIGNS

by

J F Harrop and A Tam

(Pratt and Whitney, Canada)

SYNOPSIS

Aero engine gearboxes must be compact, light-weight, durable, easy to maintain and low cost in order to meet the demands of a highly competitive gas turbine market.

To minimize weight, material is removed from the rim, web and barrel of the gear shaft and pinion. Unfortunately, this contributes to non-parallel flexing and distortion between the loaded pinion and gear (Figure 1), which then leads to uneven load distribution in the tooth mesh.

Traditional methods of analysis do not accurately predict tooth contact load distribution, especially when the gear body is flexible. An analytical procedure (1) has been developed at Pratt & Whitney Canada using the finite element method with 3D representation of the complete gear stage (Figure 2) to better assess the gear tooth contact load distribution. Highly localized loads and high scoring probabilities were predicted by this method on a high contact ratio helical gear set of a development engine. The prediction was supported by evidence of tooth damage experienced during early engine testing. By stiffening the gear web, rim and changing the tooth design from high contact ratio to low contact ratio, a significant improvement in tooth contact load distribution and reduction in scoring probability was demonstrated analytically.

This paper discusses the analytical procedures for predicting gear tooth contact load distribution and assessing tooth surface durability using pitting, scoring and spalling criteria. These criteria relate to local tooth contact loading, friction, sliding velocity, oil film thickness, contact temperatures, surface finish and case hardness. The effects on tooth contact loading due to misalignment, lead correction and bearing support stiffness are also evaluated.

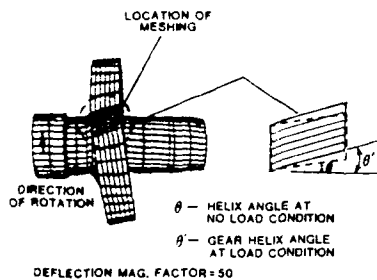


FIG. 1: HCR GEAR DEFLECTION

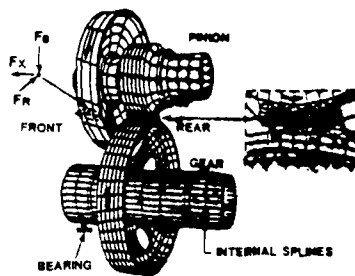


FIG. 2: HCR GEAR SET

SOME RESULTS

Table 1, figures 3 and 4 summarise the effects on tooth contact load distributions due to misalignment, lead correction and bearing support stiffness for the high contact ratio gear set.

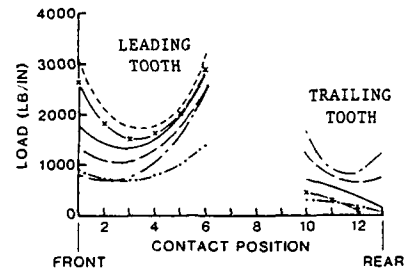


FIG. 3: HCR GEAR TOOTH CONTACT LOAD INTENSITIES

CASE	DESCRIPTION	SYMBOLS
1	Original (flexible) casing, no lead correction.	- x - x -
2	Stiffened casing, no lead correction.	_____
3	Original (flexible) casing, .002 rad. lead correction.	-----
4	Stiffened casing, .002 rad. lead correction.	-----
5	Stiffened casing, .002 rad. misalignment.	-----
6	50% input load, stiffened casing, no lead correction	-----

TABLE 1: LOAD CASES

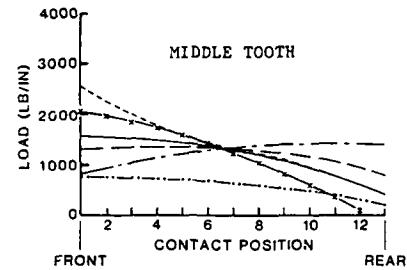


FIG. 4: HCR GEAR TOOTH CONTACT LOAD INTENSITIES

REFERENCE

- (1) Sundararajan, S. and Young, B. "Finite Element Analysis of Large Spur and Helical Gear Systems", AIAA/SAE/ASME/ASEE, 23rd Joint Propulsion Conference 1987, San Diego, California. AIAA-87-2047.

SESSION VI (Paper (ii) - WEDNESDAY 7th SEPTEMBER

TEMPERATURE - AND PRESSURE-MEASUREMENTS IN GEAR CONTACTS

WITH THIN-FILM-TRANSDUCERS

by

H Peeken and P Ayanoglu

(Institut Fuer Maschinenelemente und Maschinengestaltung,
RWTH Aachen, West Germany)

SYNOPSIS

The project has the aim of investigating the temperature- and pressure distributions in the elastohydrodynamic lubricating film in gear contacts, using sputtered thin-film transducers, which can be applied in various positions on the tooth surface.

Test Gear and Thin-Film Transducers

The experiments are carried out on a purpose-built gear rig. The gears are loaded by means of a belt-drive with a continuously variable ratio.

A specially designed gear wheel with offset teeth was necessary to enable the coating of the tooth surface in the sputtering apparatus.

Thin-film transducers function as Ohm-resistances, which change under temperature and pressure influence. They are produced in a sputtering apparatus. The first process is that of coating the tooth flank with an isolating alumina-film. The transducer is sputtered onto this layer, using a mask. The transducer material is manganin for pressure- and titanium for temperature-transducers. Finally, a second, protecting layer of alumina is applied onto the transducer.

The transducers are then calibrated, to determine their pressure- and temperature-coefficients.

Results

Experiments were carried out so far with three manganin- and one titanium transducer, all positioned above the pitch-point.

The pressure curves show typical elastohydrodynamic pressure distributions, with a gradually increasing gradient in the inlet zone. Elliptical distribution is seen in the parallel gap, followed by an abrupt fall in the outlet region (Fig.1).

There were noticeable differences between values measured under the same conditions, but with different teeth of the opposing gear, with peak pressures sometimes more than twice as high as the calculated values. This can be explained with the unequal load distribution over the tooth width, a result of the directional errors of the tooth profiles. The peak pressure doesn't increase in the same rate as the load, as

the contact-width gets larger with increasing load.

Quite high temperature increases were registered in the tooth contact (Fig. 2). The slip was 0,33 at the point where the transducer was positioned. The contact temperature increases with load, speed and lubricant viscosity.

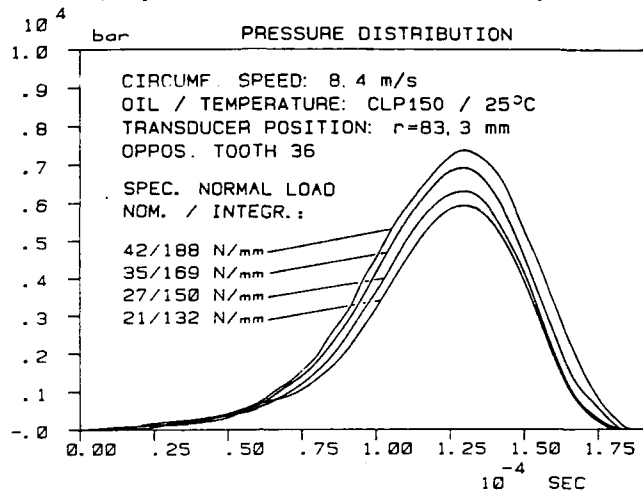


Fig. 1

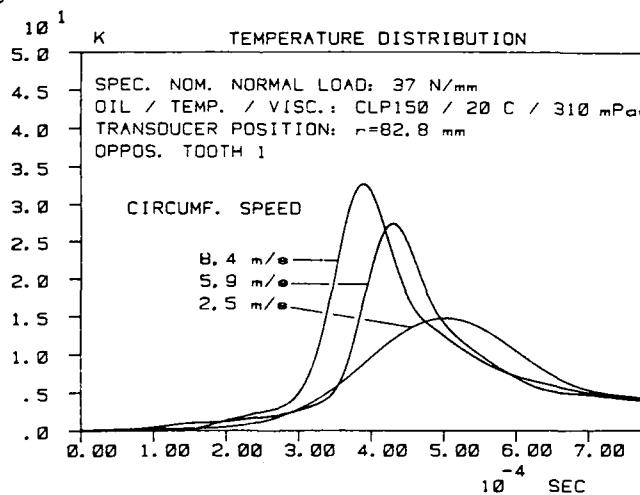


Fig. 2

References

DOWSON, D., HIGGINSON, G.R. Elasto-Hydrodynamic Lubrication, SI-Edition, Pergamon Press Ltd, 1977

RODERMUND, H. 'Beitrag zur elasto-hydrodynamischen Schmierung von Evolventenzahnrädern', Dissertation TU Clausthal, 1975

SIMON, M. 'Messung von elasto-hydrodynamischen Parametern und ihre Auswirkungen auf die Grübchenträgfähigkeit vergüteter Scheiben und Zahnräder', Dissertation TU München, 1984

SESSION VI - (Paper (iii)) - WEDNESDAY 7th SEPTEMBER

A STATIC AND DYNAMIC ANALYSIS OF MISALIGNED GEARS
WITH PARTIAL CONTACT AREAS

by

Ph Sainsot Ph Velez and D Berthe

(Institut National Des Sciences Appliquees de Lyon France)

SYNOPSIS

This paper presents an evaluation of the influence of misalignments on tooth load distribution in gear systems.

Static and dynamic analyses are conducted using a normal contact algorithm including local and global effects.

This algorithm is shown to be well adapted to determine the pressure field between surfaces with any manufacturing errors, inversely, profile modifications can be calculated to have a given load distribution.

The dynamic problem is treated on a simplified reduction unit model, some examples of instantaneous tooth loading, variations of contact stiffness, and critical rotation speeds are given.

Results show that contact conditions may strongly depend on the overall mechanical environment.

SESSION VII (Paper (i) - THURSDAY 8th SEPTEMBER

THE PALMGREN-MINER RULE DERIVED

by

J J Kauzlarich

(University of Virginia, U S A)

SYNOPSIS

The Palmgren-Miner linear damage rule predicts fatigue failure of the component when the summation of the cycles of reversed stress amplitude, N'_i , to the cycles of stress causing failure at each stress amplitude, N_i , equals unity, i.e., $\sum_i N'_i/N_i=1$. It is shown that the failure strength curve for a rolling element bearing represents an "energy of failure." As such it is possible to sum the total "energy of failure" for a variable loading duty cycle and derive the P-M Rule. It is shown that the Rule assumes the rated fatigue life curve exponent incorrectly, but that it is possible to revise the Rule to take into account the correct rated life exponent.

Theory

The AFEMA standard load rating for bearings is a probability equation in which the rated load at which 90% of a group of apparently identical bearings will give a life of at least 10^6 revolutions before the first evidence of failure by fatigue is detected, and is

$$L_{10} = 10^6 (C/P)^3 \quad [1]$$

where C is the rated dynamic load listed in tables of standards and P is the actual load.

The maximum orthogonal shearing stress strain energy density amplitude, W_S , for a roller bearing is given by

$$W_S = 0.0521 \frac{P' \Gamma E^*}{GZ} \quad [2]$$

where G is the shear modulus, Z is number of rollers, $P'=P/L$ where P is bearing load and L is roller length, the geometry factor $\Gamma=1/R_1+1/R_2$, and the reduced modulus $E^*=E/2(1-\mu^2)$ where μ is Poisson's ratio.

The most important aspect of the analysis is that the external load on the bearing, P ($P' = P/L$), is directly proportional to the subsurface strain energy density amplitude, W_S (Eq. 2), which is occurring in the raceway or rollers, so that $N P \equiv$ "Energy of Failure." Thus, the product of N times P on a fatigue strength plot is proportional to energy, and has all of the characteristics of a scalar function.

Palmgren-Miner Rule

Consider a simple duty cycle applied to a roller bearing where the load continually varies between P_1 for N'_1 revs and P_2 for N'_2 revs, where the number of revs to failure at the respective loads is N_1 and N_2 , and after some unknown number of revs, N , a detectable fatigue failure occurs. The energy of failure equation is

$$P_1 N'_1 + P_2 N'_2 = P_{avg} N \quad [3]$$

Defining $n_i = N'_i/N_i$ and making use of Eq. 1 where $L_{10} = N$, Eq. 3 becomes

$$n_1 (P_1/P_{avg})^{1-p} + n_2 (P_2/P_{avg})^{1-p} = 1 \quad [4]$$

If it is assumed that the value of the exponent p which comes from the equation of rated life, Eq. 1, was $p=1$, then Eq. 4 will become the Palmgren-Miner Rule, $\sum_i n_i = \sum_i N'_i/N_i = 1$.

It is seen that the Rule makes a drastic assumption about the slope of the rated life equation, as well as neglecting the effect of crack growth length during progressive fatigue crack extension.

In order to use the P-M Rule for rolling element bearing selection, we define $\alpha_i = N'_i/N$. Then, get

$$10^6 C^3/N_{P-M} = \sum_i \alpha_i P_i^3 \quad [5]$$

Applications of Eq. 5 are shown in modern machine design texts.

P-M Rule Revised

Now reconsider Eq. 4, where Eq. 1 shows that $p=3$. The unknown average load is

$$P_{avg} = \frac{1}{N} \sum_i P_i \alpha_i N = \sum_i \alpha_i P_i \quad [6]$$

Substituting Eq. 6 into 4 with $p=3$, and using Eq. 1 results in a new equation for rolling element bearing selection with a known duty cycle, of

$$10^6 C^3/N_{rev} = [\sum_i \alpha_i P_i]^3 \quad [7]$$

Discussion

The revised P-M Rule will predict a higher value for fatigue life of roller and ball (with conforming races) bearings depending upon the loads and cycle ratio encountered. A search of the literature did not result in any test data for variable loaded bearings, but all of the bearing manufacturers recommend that the P-M Rule be used when designing for variable load.

SESSION VII - (Paper (ii)) - THURSDAY 8th SEPTEMBER

PREDICTION OF ROLLING BEARING LIFE
UNDER PRACTICAL OPERATING CONDITIONS

by

E Ioannides, B Jacobson and J H Tripp

(SKF Engineering & research Centre B V, The Netherlands)

ABSTRACT

A previously developed fatigue life model for rolling contacts, Ref. [1], calculates the expected life of a stressed volume from the survival probabilities of those constituent volume elements exposed to a stress level above the local fatigue limit. The application of this model is extended in the present work by exploiting its ability to handle completely general stress distributions. Restriction to idealized Hertzian contact stresses is no longer necessary and a variety of realistic bearing situations can be investigated. This is necessary as with the advent of improved, cleaner, steels an increasing percentage of bearings suffer surface initiated fatigue as compared with the sub-surface initiated fatigue associated more with earlier "dirtier" steels. Important factors in such surface failures are higher surface stresses and stress concentrations around surface features like asperities or dents created by particulate debris in the lubricant. Moreover, the presence of residual or internal stresses, which can be either local around the above-mentioned surface features or more widespread within the races of the bearings, has to be considered in such detailed calculations. This is very important when such stresses become tensile, a status which, when combined with high shear stresses, is more likely to initiate fatigue.

For this purpose, multi-axial fatigue criteria are introduced into the life calculation in which the damaging effect of the shear stress is modified by the simultaneous prevailing hydrostatic pressure. Using these concepts, different practical aspects of the bearing operations have been examined and their effect on the bearing life is discussed.

Surface roughness has a large influence on the local stresses close to the bearing surfaces and the contact stresses of the ideally smooth bearing surfaces are significantly modified by the actual topography imposed by the manufacturing finishing processes - grinding, honing, polishing, etc. The gap formed by the roughness is obtained directly from surface profilometry, which provides a sampling of surface heights with the usual known limitations of random signal representation. Such a height sample is regarded as providing the

only available geometrical information, so that the need to interpolate between sampled points, i.e., to introduce an asperity model, is completely avoided. Corresponding to this step height representation of the surface, the normal contact stress is also computed as a step distribution. From such stresses, the sub-surface stress fields in the raceway and rolling element may be found and input to life calculations. Life predictions relative to the nominal smooth contact show the strong effect of the large stress fluctuations associated with regions of high slope near the more prominent surface features.

Finally, this work is being extended to study running-in effects. Preliminary results unexpectedly suggest that a run-in surface may show a life reduction relative to the unrun profile. The conditions under which this occurs will provide valuable information on possible extensions to the life model, going beyond purely elastic, geometrically determined stress distributions.

The modification of the stress field introduced by the EHL lubricant film is also discussed.

The original calculations by Lundberg and Palmgren assumed pressure distributions between the rolling elements equal to dry contact pressure distributions without friction between the surfaces. By using actual calculated pressure and shear stress distributions on the bearing surfaces, it is now possible to see the influence of the lubricant rheology not only on the film thickness and power loss (friction) but also on bearing life.

The most influential parameters for lubricants regarding stress distributions in the steel surfaces are viscosity, pressure viscosity and temperature viscosity coefficients, elasticity, compressibility, shear strength increase proportionality constant, and solidification pressure.

When the maximum pressure in the EHL contact is well below the solidification pressure for the lubricant at the local temperature, the shear velocity has to be high to induce high shear stresses in the oil. This means that rather high slip velocities can be accommodated in the oil without causing the shear stress to reach the shear strength of the oil. This can be seen when comparing a naphthenic oil with a polyalphaolefine oil, as a roller bearing working with a maximum contact pressure of, say, 1 GPa will get high shear forces in the oil film for very small slip velocities when it is lubricated with the naphthenic oil, but the polyalphaolefine oil, which is still liquid at 1 GPa, will easily deform and accommodate the slip velocity.

Next, when the effects of contamination are investigated, it is important to consider the residual stress field in the neighbourhood of debris-generated dents. In this case it is particularly important to account for the deleterious effects

of the tensile residual stresses which are generated during the formation of the dents. As explained above, for this situation new, multi-axial fatigue criteria are considered, and in the first instance a simple modification of the shear stress amplitude criterion, τ_a , as used in Ref.[1], is introduced in which a term proportional to the prevailing hydrostatic pressure is added, i.e.:

$$\sigma = a p_H + \tau_a \quad (1)$$

The value $a = 0.3$ is used which is in agreement with the findings in many combined experiments of compression and torsion. It is now possible to compare the L_{10} fatigue lives of a 6309 deep groove ball bearing under different radial loads using the two fatigue criteria, the one from Ref. [1] (the shear stress amplitude criterion, τ_a) and the one depicted in Eqn. (1) above. This comparison is given in Fig. 1 where it can be seen that there is reasonable agreement of the predictions using the two different criteria, especially at the high load range.

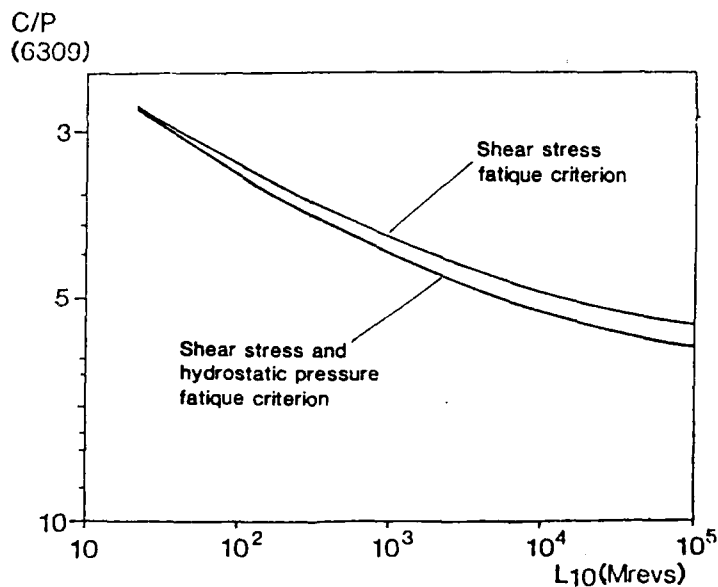


Fig. 1 L_{10} fatigue lives for 6309 deep groove ball bearings using two different fatigue criteria.

Next, the new criterion of Eqn. (1) was used to simulate the experimental results of Ref. [2]. In this work modified NU 209 roller bearing inner races were mechanically subjected to different tensile stresses and run in a four-contact

fatigue machine. The different relative fatigue lives obtained in these experiments, together with the predictions of the present model, are shown in Table 1 below. For the predictions in this table a low fatigue limit in shear of 70 MPa was used. This was obtained as the best agreement value of the experimental results and the predictions. The important feature of this comparison is the good agreement of the relative values of the L_{10} lives for three different levels of tensile hoop stresses.

TABLE 1: Experimental and predicted relative L_{10} lives of an NU 209 inner ring under different tensile stresses.

CLAMPING PRESSURE (MPa)	EXPERIMENTAL RELATIVE L_{10} LIVES	PREDICTED RELATIVE L_{10} LIVES
5	1	1
40	0.07	0.084
80	0.0125	0.00955

CONCLUSION

With the large computation facilities now available, it is possible to obtain very detailed stress fields associated with surface features as well as to combine them with residual stresses arising from plastic deformations or heat treatment. Moreover, these stresses can be combined with surface stresses coming from the pressure and shear stress in the lubricant. The present fatigue life model can also handle a detailed description of the local material properties. However, at present such exact knowledge of material behaviour is not available but has to be deduced by bearing experiments in the main. This is an ongoing process which today makes it possible to quantify the influence of surface and lubricant parameters combined with residual or other internal stresses on the endurance life of rolling bearings and, more generally, lubricated machine elements.

REFERENCES

- [1] IOANNIDES, E. and HARRIS, T.A. "A new fatigue life model for rolling bearings", Trans. ASME J. of Tribology 107, pp.367-378 (1985).
- [2] CZYZEWSKI, T. "Influence of a tension stress field introduced in the elastohydrodynamic contact zone on rolling contact fatigue", Wear 34 (1975), pp.201-214.

SURFACE DAMAGE ON ROLLING ELEMENTS AND ITS SUBSEQUENT EFFECTS ON PERFORMANCE AND LIFE

by
R S Sayles (Imperial College U K)
E Ioannides (SKF The Netherlands)
J C Hamer (Imperial College U K)
A A Lubrecht (Twente University of Technology The Netherlands)

Surface Damage on Rolling Elements and its Subsequent effects on Performance and Life

Abstract

Surface contamination and subsequent surface damage is increasingly recognised as having a significant effect on bearing fatigue lives which would not normally be predicted by the traditional Lundberg and Palmgren model. Ioannides and Harris (1) have published an important generalisation of the classical model. Essentially the new model is an extension of the classical analysis, where the probability of failure is calculated for a small volume of material from a known stress distribution within it. Webster and Ioannides (2) used a structural contact model coupled to a finite element analysis to determine the state of stress in a bearing raceway in the presence of debris initiated dents. The stress information was used in conjunction with the modified fatigue model to determine the reduction in fatigue life.

To obtain a complete picture of the subsurface stress distribution, a knowledge is required of both the stress field generated in an indentation Hertz contact and the plasticity induced from the high pressure indentation. As a first step, in this model the stress distribution in the dry contact of an indented surface is superimposed upon the residual stress distribution resulting from the high pressure indentation of an elastic half space. A two dimensional plane strain approach is used to determine the appropriate contact stress used to estimate the residual stresses. For simplicity the profile of the dent was made to form an arc of a circle and could be considered as a roughness running perpendicular to the direction of motion. A typical dent had a width of 10 micrometers and height of 5 microns although these could be varied with respect to the Hertz contact size.

So that the full stress history could be used in the life calculations, the pressure distribution under dry line contact conditions was calculated for a series of positions during the overrolling of the surface defect. This problem is usually solved by a direct method (Newton Raphson), resulting in long computing times for large problems. To solve the dry contact problem with many points an iterative solution method was used with the application of multilevel techniques to accelerate convergence as developed by Lubrecht (3). A surface pressure and film thickness map for the overrolling of a dent at the centre of the contact and a subsurface shear stress contour map are shown in figures 1 and 2 respectively.

The smooth surface profile of many surface defects appears to be the result of high pressure extrusion of a ductile debris particle. The effective forging of these particles causes a combined high normal and tangential force to be applied to the surface, frequently resulting in permanent deformation of the bearing surface. The forged particle is modelled by a rigid die impressing a rigid plastic half space coupled with a traction force extending from the centreline. The slipline field is virtually identical to that developed by Olver (4) for a shearing asperity except in this case the whole field is reflected around the centreline. The residual stresses can be calculated by adding the plastic stresses to the elastic stresses produced during unloading. A typical residual shear stress contour map is shown in figure 3. A map of the combined residual shear stresses and elastic shear stresses from the overrolling of the dent at the centre of the contact is shown in figure 4.

Results are presented for the life reduction factors for indented contacts of differing size and depth. The calculations are repeated with the addition of the approximate residual stresses resulting

from forging particles of varied interface friction coefficients. Preliminary results suggest that the modified elastic stress distribution significantly reduces the predicted fatigue life. The effect of superimposing the residual stresses is less marked, possibly because the effect of the increased tensile stresses around the edge of the dent is counteracted by the large residual compressive stresses under the bulk of the dent.

References

- (1) Ioannides. E. and Harris. T. A., "A new fatigue life model for rolling bearings.", ASME Trans., 1984, J. Trib.
- (2) Webster. M. N., Ioannides. E. and Sayles. R. S., "The effect of topographical defects on the contact stress and fatigue life in rolling element bearings." Leeds-Lyon 1988.
- (3) Lubrecht. A.A., "The numerical solution of the elastohydrodynamically lubricated line and point contact problem, using multigrid techniques", Phd thesis, Twente University, 1988, The Netherlands.
- (4) Olver. A. V. , "Wear of hard steel in lubricared rolling contact", Phd thesis, Imperial College, 1986.

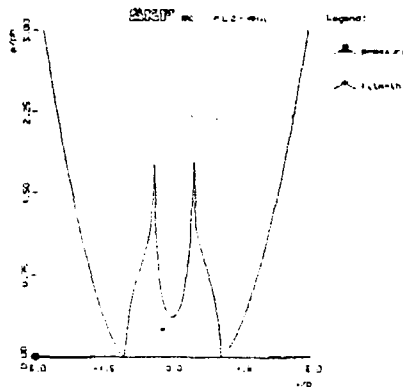


Figure 1

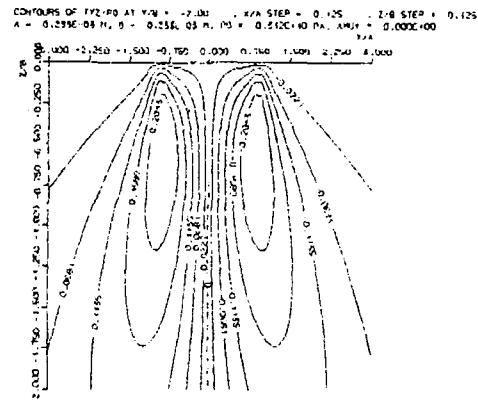


Figure 2

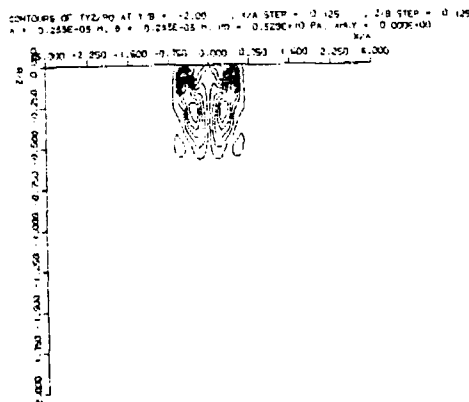


Figure 3

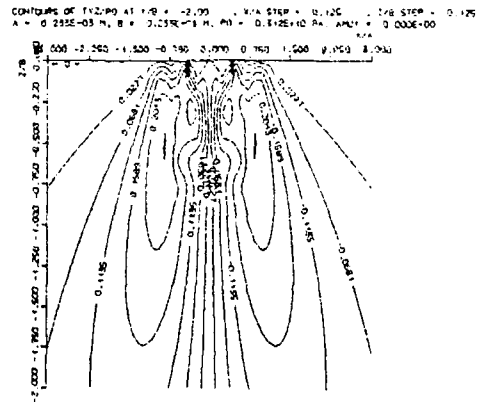


Figure 4

37

SESSION VII - (Paper (iv)) - THURSDAY 8th SEPTEMBER

DEBRIS DENTING - THE ASSOCIATED RESIDUAL STRESSES
AND THEIR EFFECT ON THE FATIGUE LIFE OF ROLLING
BEARINGS: AN FEM ANALYSIS

by

C N Ko and E Ioannides

(SKF Engineering & Research Centre B V, The Netherlands)

ABSTRACT

During overrolling of debris in lubricated contacts, plastic flow takes place both in the debris particles and the raceways and rolling elements of the bearings. The outcome of this overrolling is a dent combined with a local residual stress field surrounding the dent. Elastic-plastic calculations were performed for typical bearing-debris configurations using the FEM program ABAQUS, and such residual stress fields, as well as the resulting dent shapes, were obtained. These have been subsequently used to predict the fatigue life reduction of rolling bearings in the way described in Ref.[1].

This follows on from the work reported recently in Ref.[2] and the effects of strain rate hardening, debris and rolling bearing component hardness on the fatigue life of bearings are discussed and assessed.

REFERENCE S

- [1] HAMER, J.C., SAYLES, R.S. and IOANNIDES, E.
"Deformation mechanism and stresses created by 3rd body debris contact and their effect on rolling bearing fatigue"
14th Leeds-Lyon Symposium on Tribology, INSA, Lyon, France, September 1987.
- [2] WEBSTER, M.M., IOANNIDES, E. and SAYLES, R.S.
"The effect of topographical effects on the contact stress and fatigue life in rolling element bearings",
12th Leeds-Lyon Symposium on Tribology, INSA, Lyon, France, September 1985.
- [3] HAMER, J.C., SAYLES, R.S. and IOANNIDES, E.
"Particle deformation and counterface damage when relatively soft particles are squashed between hard anvils"
(to appear on the Journal of Tribology, ASME)

SESSION VIII (Paper (i) - THURSDAY 8th SEPTEMBER

AXIALLY PROFILED CIRCULAR BEARINGS AND THEIR POTENTIAL APPLICATION
IN HIGH SPEED LUBRICATION

by

D T Gethin

(D T Gethin, University College of Swansea, U K)

Summary

The isothermal and thermal characteristics of an axially profiled circular bore bearing are determined using the finite element technique. These are compared with the predicted performance characteristic of a cylindrical bearing operating over the same range of conditions. The results obtained lead to the conclusion that the present analysis may be used to obtain general design data for an axially profiled bore bearing operating at high sliding speed. Axial profiling reduces the bulk operating film temperature by a small amount and it decreases the load carrying ability of the film and frictional losses also.

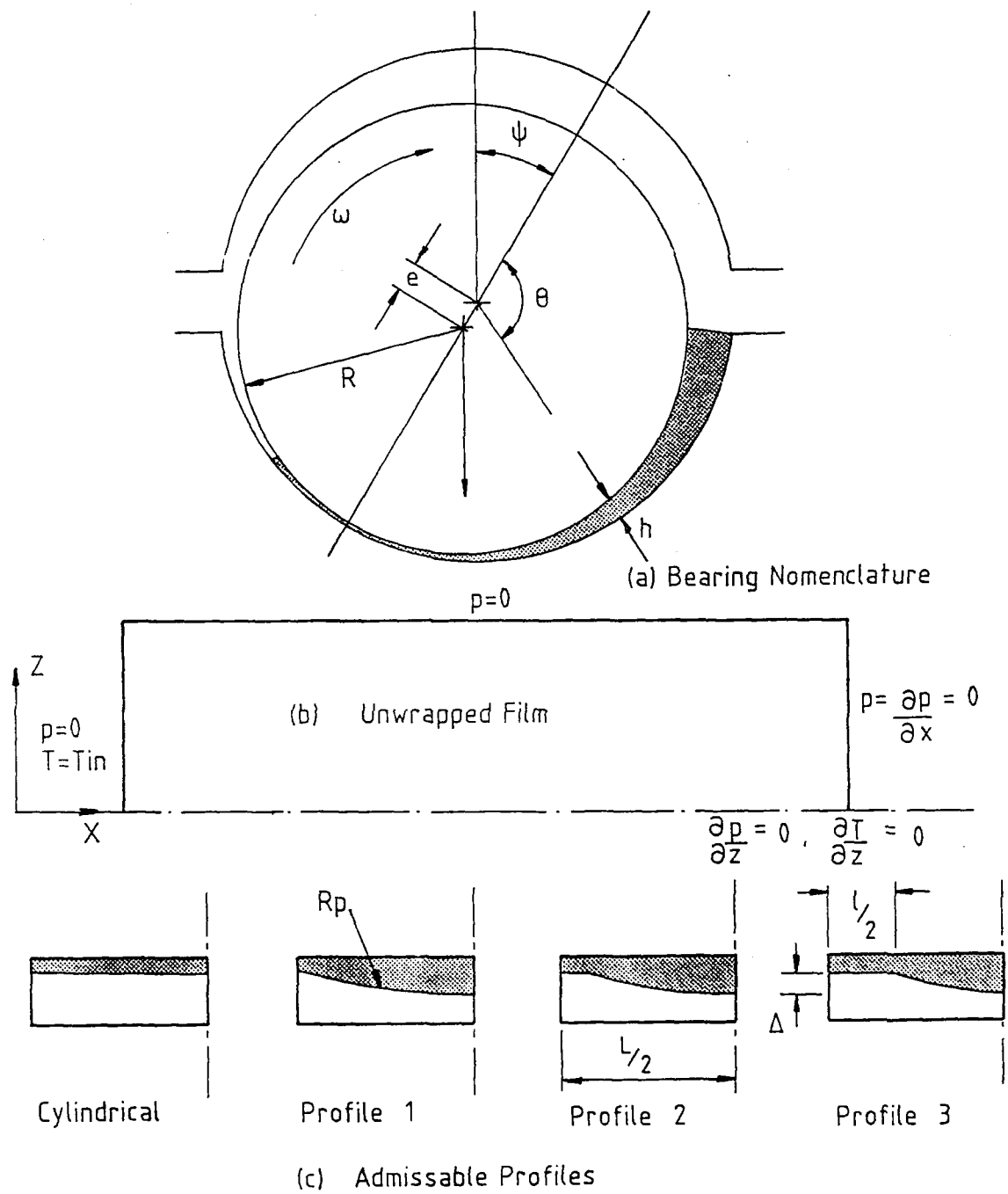


FIGURE 1. BEARING NOMENCLATURE AND AXIAL PROFILES CONSIDERED.

SESSION VIII (Paper (ii) - THURSDAY 8th SEPTEMBER

ANALYSIS OF PARTIAL ARC JOURNAL BEARINGS

by

E W Cowking

(GEC Engineering Research Centre, Leicester, U K)

SYNOPSIS

This paper is concerned with the validation of computer programs for the thermohydrodynamic analysis of journal bearings. The aim is to demonstrate the correctness of the programs mainly by external checks on the results rather than by checking the computer code.

The Computer Programs

Two computer programs are considered which analyse journal bearings with a variable number of partial arcs. A range of temperature calculations is provided from isothermal up to full thermohydrodynamic solutions. The inlet pockets are treated as lumped systems, each at a single temperature which is determined by a heat balance. The two programs produce two and three-dimensional solutions to the problem. The pressures are calculated by an optimum variational method in the two-dimensional program and by relaxation methods in the three-dimensional program. The two dimensional program is described in (1).

Validation Procedure

Results are compared with isothermal solutions published by Lund and Thomsen (2) which provide accurate dynamic coefficients, obtained by direct differentiation of Reynolds equation.

The programs include a simple thermal analysis which predicts the average temperature across the fluid film. Results obtained by this method for a single arc are compared with those published by Hakansson (3) in tabular form.

The thermohydrodynamic analysis of the fluid film cannot so easily be compared with published results. It is shown, however, that if the journal position is fixed the average temperature across the film agrees closely with the average temperature predicted by the simple thermal analysis. Overall mass flow and heat flow balances also provide useful checks on the validity (and accuracy) of results.

Thermohydrodynamic Results

There is clearly a need for results which can be used as benchmarks for thermohydrodynamic analyses. As an attempt to improve this situation, a table of results are provided for a 160° arc. An adiabatic analysis is carried out for a specified lubricant and operating conditions and for a range of loads.

References

- 1) Cowking, E.W.
"Thermohydrodynamic analysis of multi-arc journal bearings."
Tribology International, August 1981, p 217.
- 2) Lund, J.W. and Thomsen, K.K.
"A calculation method for the dynamic coefficients of oil
lubricated journal bearings."
Topics in Fluid Film Bearing and Rotor Bearing System Design and
Optimisation, ASME, 1978, pp 1-28.
- 3) Hakansson, B.
"The journal bearing considering variable viscosity."
Transactions of Chalmers University of Technology, Nr 298, 1965.

SESSION VIII - (Paper (iii)) - THURSDAY 8th SEPTEMBER

ELAPSED TIME FOR THE DECAY OF THERMAL TRANSIENTS
IN FLUID FILM BEARING ASSEMBLES

by

C M M Ettles (Rensselaer Polytechnic Institute New York U S A)
H Heshmat (Mechanical Technology Incorporated New York U S A)
R Brockwell (National Research Council Canada)

SYNOPSIS

When the operating conditions of a fluid film bearing are changed a finite time must elapse before thermal equilibrium becomes re-established. This paper concerns two aspects of the thermal response of a bearing: the time required for some proportion of the temperature change (e.g., 50%, 70%, 90%) and the effect of thermoelastic deformation. An attempt is made to correlate the results of six thrust bearings and two journal bearings, to give a unified method that characterises response time.

A Simplified Approach Using Classical Solutions

When applying the equation of transient heat conduction to a plate, journal or bush, a single parameter appears when the equation is set in nondimensional form. This is nondimensional time, known as the Fourier number F, given by

$$F = \frac{k}{\rho c} \cdot \frac{t}{H^2} \quad (1)$$

where k, ρ , c are the thermal properties, t is time and H is the thickness of the plate or radius of the journal.

The classical solutions could be characterized by a Fourier number in the form

$$\frac{\Delta T}{\Delta T_F} = 1 - e^{-aF} \quad (2)$$

where ΔT is the time varying temperature, ΔT_F is the final temperature change and a is a constant of the order 1.5 - 5.

A Numerical Solution of the Complete Assembly

The use of classical solutions allows a simplified, general approach, but difficulties arise in choosing the dominant thermal mass. A numerical solution is described that considers the coupled system of pads, rotor, and film in elevation, as in [1]. The complete temperature distribution is obtained in a series of time intervals, consequent to some change such as an increase of speed or load.

Figure 1 shows the subsequent temperature rise of a thrust bearing in which the load is doubled at zero time. After the initial rise, the growth (or decay) is approximately exponential. In [1] it is shown that the behavior of a unit eight times the size was similar, which led to the use of Eq.(2) to characterize experimental results as well as model solutions.

Correlation of Experimental Data

Figure 2 shows the 50% rise time for six thrust bearing units, plotted against pad thickness H. The line has the characteristic $t \propto H^2$, which gives for these bearings:

$$\frac{\Delta T}{\Delta T_F} = 1 - e^{-1.6 F} \quad (3)$$

One feature of Eqs.(2), (3) is that individual bearing assemblies should have a characteristic "time constant," so that the same time elapses for (say) a 50% change, regardless of the final temperature change being large or small. This is a common feature of experimental results.

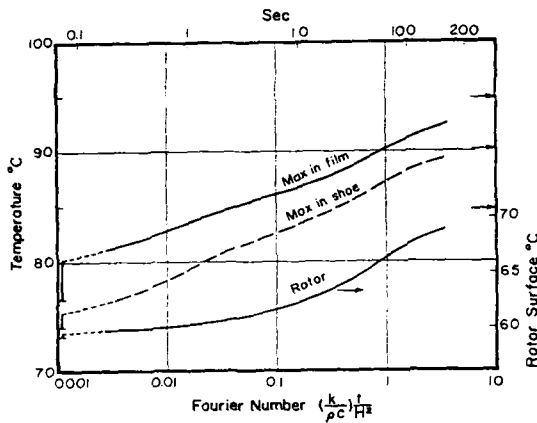


Fig.1 Changes in Temperature in a Thrust Bearing when the Load is Doubled at Zero Time

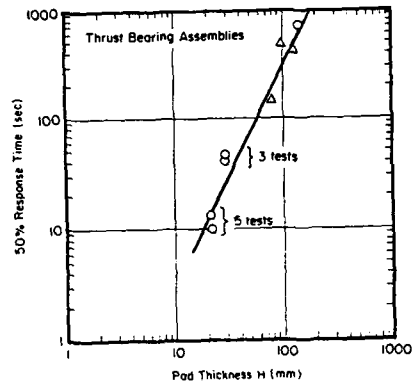


Fig.2 The 50% Rise Time for Six Thrust Bearing Units Subject to a Sudden Change of Conditions

Reference

1. Ettles, C.M.M., "Transient Thermoelastic Effects in Fluid Film Bearings," *Wear*, 79, 53-71 (1982).

16

SESSION VIII (Paper (iv) - THURSDAY 8th SEPTEMBER

DESIGN PROCEDURES IN HYDRODYNAMIC LUBRICATION
BASED ON NUMERICAL METHODS

by

J O Medwell

(University College of Swansea U K)

This paper presents a review of numerical schemes for analysing the thermohydrodynamic behaviour of journal bearings. The schemes are based on the finite element and finite difference methods which are used to solve the momentum and energy equations simultaneously. Off bearing design operation such as lubricant starvation and misalignment are featured in the procedures. The effect of bush conduction and the recirculation of heat therein is included and the effect of various types of boundary conditions considered.

Some comparisons with experimental data are also presented

THE EFFECT OF RESIDUAL STRESS AND TEMPERATURE

ON THE FRETTING OF BEARING STEEL

by

(M Kuno, NTN Toyo Bearing Co. Ltd., Japan)

and

(R B Waterhouse, University of Nottingham U K)

SYNOPSIS

The fretting arrangement consisted of a high carbon chromium steel ball in contact with a flat of the same material. In order to investigate the effect of residual stress and temperature on the fretting of high carbon chromium bearing steel, the test was carried out at room temperature and 200°C (specimen temperature) under unlubricated conditions. The normal load was varied between 135N and 437N, the slip amplitude between 8µm and 45µm and the frequency was 50Hz.

Tensile stresses of +400MPa and +600MPa were applied to the stationary flat specimen during the fretting tests. The relationship between the maximum Hertzian contact stress, the slip amplitude and the number of cycle was investigated.

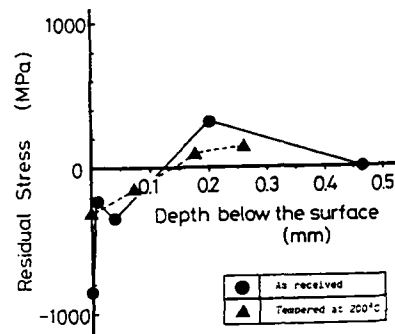


Fig. 1

The residual stress distribution in the specimen is shown in Fig. 1.

Fig. 2 shows the relation between the slip amplitude, the maximum contact stress and the number of cycles to failure when the specimen is subjected to an applied tensile stress of +400MPa at room temperature.

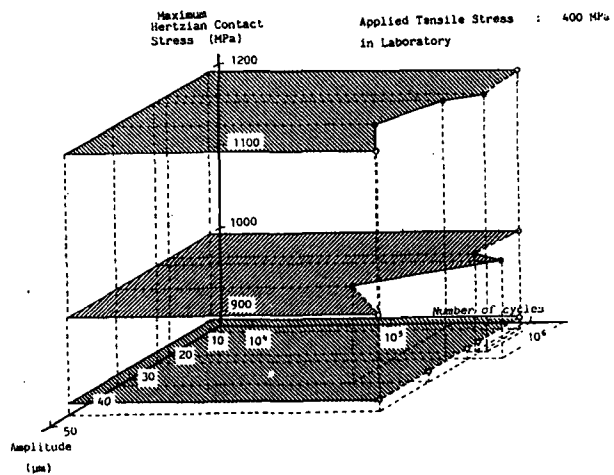


Fig. 2

The shortest time to failure at room temperature was associated with a critical amplitude of 35 μ m which corresponded to the maximum value of the coefficient of friction, 0.72, as shown in Table 1. On the other hand, no specimen fractured in the tests at 200°C. A "glaze type oxide film" reduced the coefficient of friction, and no cracks were generated in this case.

Table 1

Amplitude	10 μ m	20 μ m	25 μ m	35 μ m	45 μ m
Coefficient of Friction	0.50	0.44	0.49	0.72	0.49

normal load : 437N (Pmax = 1200MPa)
frequency : 50Hz
applied tensile stress : 400MPa
coefficient of friction measured at 10⁵ cycles

The residual stress in the specimen surface is still compressive even when the specimen is subjected to a tensile applied stress of +600MPa. This result suggests that the presence of a residual compressive stress in the surface appears to have very little influence on the initiation of cracks by fretting. However, the changeover from compressive to tensile residual stress is brought to within 10 μ m of the surface, which has a profound influence on the propagation of the cracks once they are initiated.

57
SESSION IX (Paper (ii) - THURSDAY 8th SEPTEMBER

WEAR MAPS AND THEIR USE IN DESIGN

by

T S Eyre

(Brunel University, U K)

The transfer of technology from tribology research to designers is very slow, particularly in wear of materials and there appears to be as many industrial problems seeking solutions today as there were twenty years ago. In recent years there has been considerable attention focussed upon wear testing particularly using the pin on disc machine to measure absolute wear rates and compare interlaboratory repeatability etc. This type of information particularly based on single load/speed tests does not, however, help the designer in his search for optimisation of the material variables or in the search for new materials or surface technology for wear resistance in engineering systems.

In this investigation a pin on disc machine is used, with some modifications, in particular to vary the operating conditions over a wide range of load, speed and environmental conditions. Well known engineering metals and alloys, particularly cast iron, steel and aluminium alloys have been characterised in terms of their composition and microstructure and then their sliding wear resistance have been determined. A wide variety of techniques have been used to measure or assess wear and also to characterise the main features of the surfaces and wear debris. Wear information is expressed in the form of running-in, steady state wear rates and also transitional behaviour, which has then been compiled into wear maps. These wear maps not only show how optimisation of the metal or alloy itself brings about significant improvements in wear behaviour but also for specific materials how wear changes with both load and sliding speed. The main emphasis is on safe regions of wear and their boundaries relative to operating conditions rather than single figure wear rates or wear factors. These maps are based upon known wear types and how transitions from one form of wear i.e. "mild" to another "severe" may cause catastrophic wear behaviour.

Intelligent interpretation of wear behaviour over a wide range of conditions based upon a "standard" wear test, will enable designers to choose their materials for construction with greater efficiency and with care in simulation in the wear tests of service behaviour this information can be related to specific industrial problem areas. Specific classes of materials can be optimised on the basis of their known and measured characteristics i.e. microstructure and wear.

SESSION IX (Paper (iii) - THURSDAY 8th SEPTEMBER
THE WEAR OF HOT WORKING TOOLS APPLICATION TO FORGING
AND ROLLING OF STEEL

by

E Felder

(CEMEF, Ecole de Mines de Paris, Valbonne, France)

1 - Mechanical analysis of working processes and damage maps of hot working tools

Two main damage types occur in hot working : thermal fatigue and along the interfaces where the metal slides on the tool abrasive wear. The sliding velocity Δu and the contact pressure are the mechanical factors of wear and can be estimated by the calculation of the plastic flow of the workpiece : so fig. 1 provides the damage map of the rolling cylinders according to the Tresca's friction coefficient \bar{m} and the aspect ratio A of the workzone. In forging the friction conditions are often dissymetrical and an increase in friction on the upper die reduces Δu on the upper die and increases Δu on the lower die (fig. 2.a)

2 - Mechanical model of abrasive wear

From Archard's law, we derive the wear depth of a point M of the tool surface :

$$\Delta z = k \int p |\Delta u| dt \quad (1)$$

History of contact in M.

Where t is the time. For a stationary process as the rolling of a strip of length L (fig. 1), integration of (1) provides, ($\bar{m} < 0.66$; $A > 3$) :

$$\Delta z = 0.057 k \sigma_0 \frac{(H_1 - H_2)^{1.5}}{H_2 R^{0.5}} \left(1 + \frac{\bar{m} A}{4} \right) L \quad (2)$$

where σ_0 is the yield stress of the strip

For upsetting of cylinders the integration of (1) provides the theoretical wear depth profile designed on fig 2, in qualitative agreement with the experimental one.

3 - The factors of the wear rate coefficient k

We write
$$k = K_F K_W H_V^{-2.1} \quad (3)$$

With H_V the Vickers hardness of the tool material. ($H_V < 6$ GPa) and K_W a function of the chemical composition of the tool material :

$$\begin{cases} K_W = 1 + 5.1 e^{-0.085 Weq} \\ Weq = (\% W) + 2(\% Mo) + 4(\% V) + 0.5(\% Cr) \end{cases}$$

The factor K_F varies with the superficial films : lubricant film, composition and temperature of the scale of the workpiece ... and is deduced from experiments. This model (3) describes very well the wear of flat dies without surface treatments. The nitrated layer avoids abrasion, but promotes thermal fatigue (fig. 2c).

References :

[1] THORE Y., Etude théorique et expérimentale du frottement et de l'usure par abrasion des matrices en forgeage des aciers. Influence d'une nitruration. Thèse Dr Ing. (Ecole des Mines de Paris) 25 Juin 1984.

[2] FELDER E., Interactions métal - cylindres en laminage, Cessid - IRSID. (Maizières les Metz) 85-171 (1985) 166 p.

SESSION IX (Paper (iv) - THURSDAY 8th SEPTEMBER

DEBRIS INCLUSION IN POLYMERIC BALL VALVE SEALS

by

B J Briscoe and P J Tweedale

(Imperial College, London, U K)

SYNOPSIS

This paper describes the results of an experimental study and an associated analysis of the particle debris inclusion processes which occur in certain polymer-metal contacts. The work has been designed as a means of evaluating certain facets of the operation of ball valves, which contain polymeric seals, when they are used in environments which contain small hard solid particles. The particles are progressively included onto the polymer surface and as a result the torque required to activate the valve increases. A simulation of this process is described and data are given for a range of organic polymers. These data are analysed using a simple but apparently effective model which introduces a debris inclusion rate parameter. This parameter expresses the sensitivity of the polymer to debris inclusion.

The data are briefly compared with field test results and the important material characteristics which influence the debris inclusion rate are discussed.

Apparatus

The apparatus to be described induces debris inclusion by a rolling action where a steel roller is traversed over a small polymeric sample. Periodically the roller is locked and the frictional force is measured. These studies have used a range of debris laden media but the work to be reported deals with aqueous silica suspensions. The polymers investigated include PTFE, PEEK, polyethersulphone, and a number of special composites. The latter materials will be described in detail in the full paper.

Experimental Data and Analyses

Typically we observe that the frictional force required to slide the contact between the polymer and the steel progressively increases as more debris is introduced into the contact. Most of the systems have a common limiting friction value corresponding to a fully silica encrusted surface. The initial frictions are different; PTFE is low and PEEK is high. What is more interesting, however, is the rate at which the frictional force changes as the debris inclusion cycles are increased. For PTFE this is rapid whilst for PEEK it is comparatively slow under similar operating conditions.

The analysis to be described assumes that a certain fixed fraction of the surface is impregnated with particles during each rolling traverse for each polymeric system. The data when analysed on this basis produce a parameter which describes the relative sensitivity of the polymers to debris inclusion. PTFE for example incorporates debris quite rapidly whilst PEEK does so much more slowly.

The inclusion sensitive is an inverse function of the polymer's hardness.

Conclusions

We demonstrate that a simple simulation and analysis is capable of predicting some of the operational features of polymeric contacts in ball valves. An important material characteristic is the hardness of the polymer.

TRIBOLOGICAL CHARACTERISTICS OF NEEDLE BEARINGS

by

S Bair and W O Winer

(Georgia Institute of Technology, Atlanta, U S A)

SYNOPSIS

A Needle Bearing Test Rig has been constructed which allows the measurement of frictional torque, axial thrust, needle axial skew angle, and needle complement velocity for an applied radial load of up to 3500 N and a speed of up to 7000 rpm. Either shaft rotation or cup rotation can be accommodated. Two fiber optic probes transmit light to and receive reflected light from both ends of the needles. The needle skew angle changes the phase relationship of the optical probe signals as shown in Figure 1.

Preliminary data indicate that frictional torque is greater for full-complement bearings than caged bearings, that torque is higher for cup rotation than shaft rotation, and that torque is minimized when the needles (full-complement) are axially aligned with the shaft in the load zone. Full complement bearings tend to operate with a preferred needle skew direction and attending thrust direction with occasional spontaneous reversals. Operation without thrust and needle skew is not stable. A change in needle skew is captured in Figure 2. A correlation was found between needle skew angle and axial thrust (See Figure 3). Less than one degree change of needle skew is required to go from no thrust to the maximum thrust developed (about 5% of the radial load).

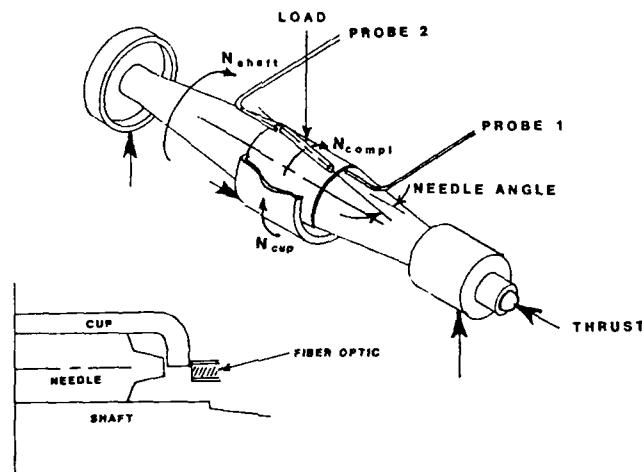


Figure 1. Definitions of Rotation Directions, Load, Thrust and Needle Angle and Optical Probe Detail

53

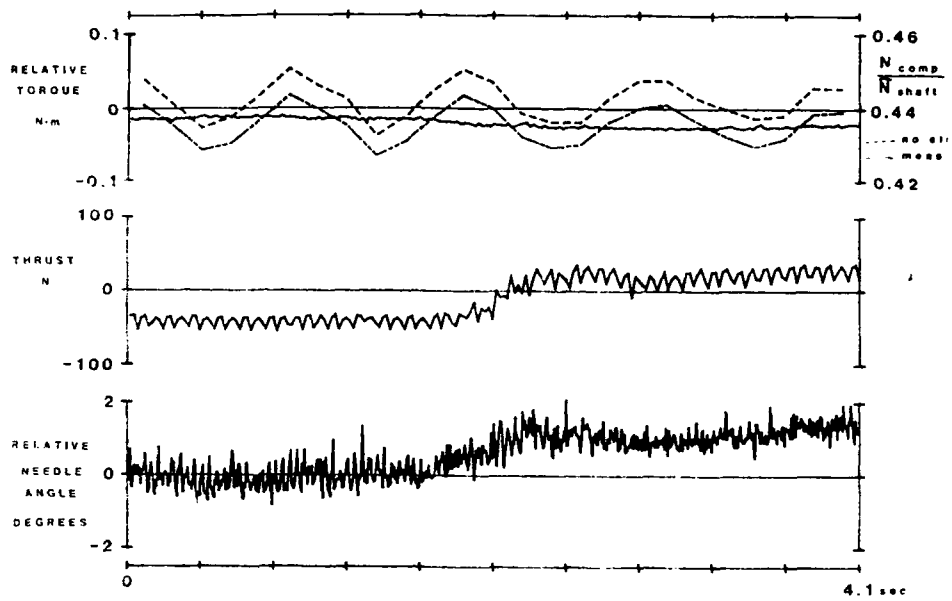


Figure 2. Run D, $\bar{N}_{shaft} = 841$ rpm, 860 N load, grease

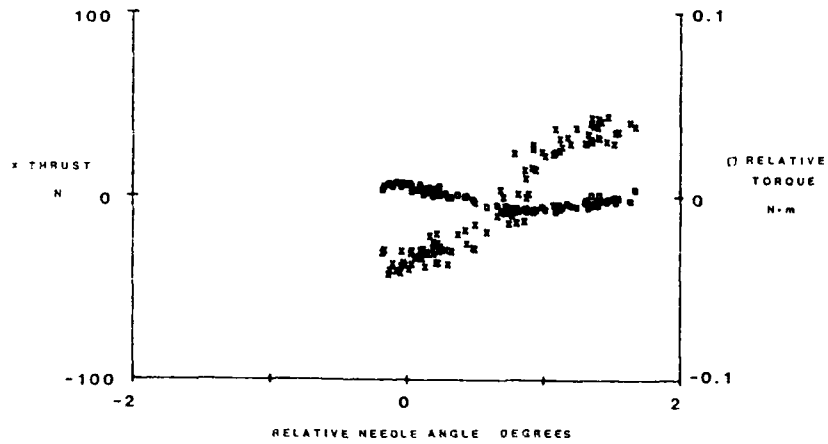


Figure 3. Run E, $\bar{N}_{shaft} = 850$ rpm, 860 N load, grease

POWER LOSS PREDICTION IN BALL BEARINGS

by

R J Chittenden, D Dowson and C M Taylor

(The University of Leeds U K)

SYNOPSIS

A deep groove ball bearing subject to a principal load in the axial direction and operating towards its maximum allowable rotational speed presents a complex problem for a full lubrication analysis. The dynamic analysis of such bearings has been studied by several workers, (Gentle and Boness (1) and Pasdari and Gentle (2)) but such theoretical work required the use of several experimentally derived relationships.

The work described in this paper brings together results from a bearing dynamics analysis and computed elastohydrodynamic film and pressure profiles. In this way a purely theoretical model is built up which allows reasonable estimates of power loss to be calculated for single conjunctions as well as whole bearings. This approach requires several broad assumptions to be made since the computation of a complete elastohydrodynamic solution for each contact within a bearing is impractical due to the amount of c.p.u. time required. The analysis allows a representation of Non-Newtonian effects to be introduced into the analysis.

Analysis

The bearing dynamics analysis followed was that of a high speed ball bearing presented by Jones (3,4), as set out by Harris (5). This analysis provided information on the operating conditions at each contact within the bearing and was used together with a previously computed elastohydrodynamic solution to enable extrapolated film thickness and pressure profiles to be determined for each conjunction. The extrapolations were made in the following ways:-

Pressure

$$P_{i,j} = \frac{\sum_{x,y} P_{i,j} \delta_x \delta_y}{P_{Ball}} P_{i,j}$$

Film Thickness

$$H_{i,j} = C_1 H_{i,j}^2 + C_2 H_{i,j} + C_3$$

Once these profiles had been determined local values of the shear stresses acting upon the two surfaces were calculated according to Newtonian theory. The assumption that the extrapolated profiles would not be significantly altered by a Non-Newtonian fluid allowed a further set of local shear stresses to be evaluated according to a Non-Newtonian stress-strain relationship, which for the work described in this paper was that presented by Johnson and Tevaarwerk (6):-

$$\dot{\gamma} = \frac{1}{G} \frac{d\tau}{dt} + \frac{\tau_0}{\tau_0 \eta} \sinh \left(\frac{\tau}{\tau_0} \right)$$

The resulting knowledge of the shear stresses on each surface then allowed the associated traction forces to be calculated, as well as the power loss at each conjunction and any power transfer across the contact.

Typical Results

Figure 1 illustrates the effect on power loss of a Non-Newtonian lubricant compared to a Newtonian fluid for a single ball, in a typical aero engine deep groove ball bearing, upon which different slip speeds have been imposed for a constant entraining velocity. It can be seen that even the pure rolling case is influenced by Non-Newtonian effects which reduce the spin power loss, and hence the total power loss for this condition.

Figure 2 shows the component power losses and total power loss for the inner-race/ball contacts of an entire bearing with a Non-Newtonian fluid model. As might be expected the major source of power loss is that attributed to sliding, even at the relatively small values of fractional slip calculated for such a bearing.

References

- (1) Gentle C R and Boness R J (1976) 'Prediction of Ball Motion in High Speed Thrust Loaded Ball Bearings', *J. Lub. Technol.*, 98(3), 463-471.
- (2) Pasdari M and Gentle C R (1986) 'Computer Modelling of a Deep Groove Ball Bearing with Hollow Balls', *Wear*, 111, 101-114.
- (3) Jones A B (1959) 'Ball Motion and Sliding Friction in Ball Bearings', *Trans. A.S.M.E., J. Basic Eng.* 1-12.
- (4) Jones A B (1960) 'A General Theory for Elastically Constrained Ball and Roller Bearings Under Arbitrary Load and Speed Conditions', *Trans. A.S.M.E., J. Basic Eng.*, 309-320.
- (5) Harris T A (1984) 'Rolling Bearing Analysis', John Wiley and Sons, New York.
- (6) Johnson K L and Tevaarwerk J L (1977) 'Shear Behaviour of Elasto-hydrodynamic Oil Films.' *Proc. R. Soc. Lond.*, A356, 215-236.

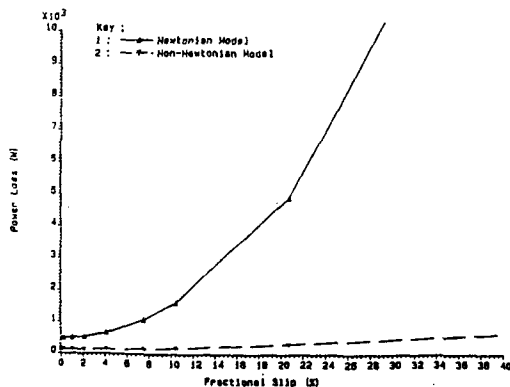


Figure 1 Total Power Loss for a Single Conjunction

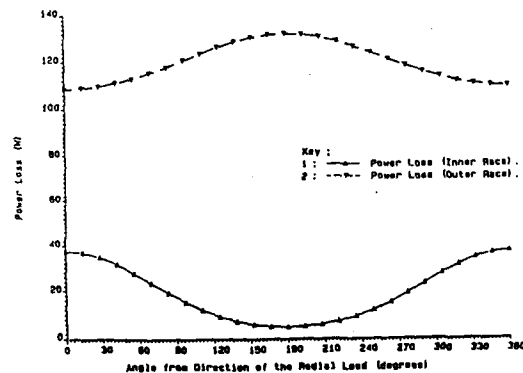


Figure 2 Predicted Power Loss from the Bearing. Non-Newtonian, Barus Pressure Viscosity Expression.

SESSION X (Paper (iii) THURSDAY 8th SEPTEMBER

THE EFFECT OF ROLLER-END FLANGE CONTACT SHAPE UPON
FRICTIONAL LOSSES AND AXIAL LOAD OF THE RADIAL CYLINDRICAL
ROLLER BEARINGS

by

H Krzminski-Freda and B Warda

(Technical University of Lodz, Poland)

SYNOPSIS

The subject of the considerations is the radial cylindrical roller bearing of the NJ type with conical flanges and spherical ends rollers. The paper comprises an analysis of the roller balance conditions in the bearing subjected to combined load, the aim of which is creating theoretical bases for selection of the most advantageous - from the viewpoint of friction losses in the bearing - values of the angle of inclination of the flange (β) and the roller end radius (R_w) (Fig. 1).

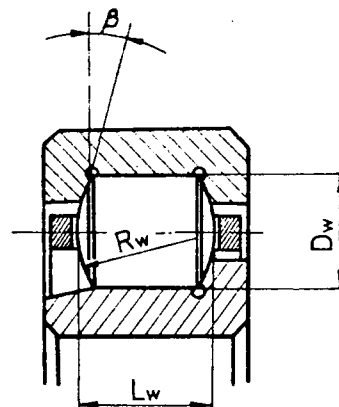


Figure 1

Theory

In the analysis of the balance conditions, friction forces and friction moments acting on the roller were taken into consideration. The coefficient of friction was presented in the function of a relative slide and a maximum pressure at the contact. The directions of friction forces were determined by making an analysis of the bearing kinematics. The roller tilt caused by the action of axial forces and its skew resulting from the friction occurring at the roller end - flange contact were taken into account. The pressure distributions at the roller end - flange contacts were determined according to hertzian formulae for the point contact, while the pressure distributions at the roller - main race contacts were determined using a dependence given by Lundberg. In the analysis of the balance conditions, continuous pressure distributions were substituted by concentrated forces. The system of equations of balance of the roller and the outer ring fragment was solved numerically, using Hook-Jeeves method.

Results

The solution of balance equations made it possible to determine a number of parameters describing the roller balance condition for the set values of radial and axial forces acting on one roller, and to make distributions of load on particular rollers. The analysis of the calculation results has shown that the angles of inclination of flanges $\beta = 0.4^\circ - 0.6^\circ$ ensure the most advantageous conditions of the bearing operation within a wide range of axial load. Small pressures at the roller end - flange contacts (~ 250 MPa), small skew angles of the rollers ($\sim 1'$) and as a result small friction losses in the bearing correspond to them. Fig. 2 presents the characteristics of the coefficient of the moment of friction resulting from the axial load (f_2) in the function of the F_a/F_r ratio and angle β . Smaller angles β may lead to a considerable reduction of the inlet zone or to its disappearance, which will render formation of an oil film at the roller end - flange contact difficult or impossible. Greater angles β are accompanied by greater friction losses in the bearing. Thus, the proposed range of the inclination angles allows one to achieve a compromise between an attempt to ensure the smallest possible friction losses and the necessity to guarantee an appropriate shape of the oil gap conducive to formation of an oil film at the roller end - flange contact.

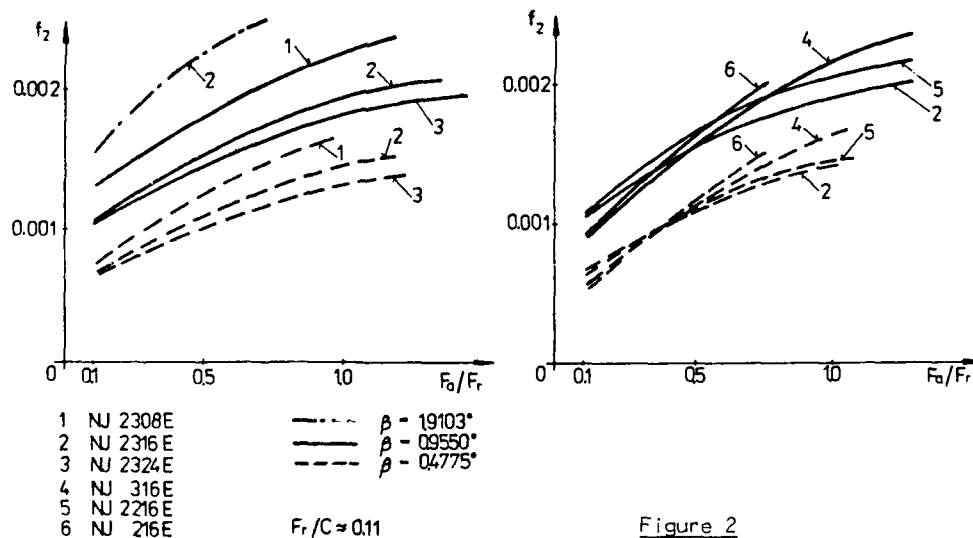


Figure 2

References

- (1) WARD A. B. "The effect of the roller end - flange contact shape of the radial cylindrical roller bearing upon the ability to transfer axial load" (doctoral thesis), Łódź: Technical University of Łódź, 1987.

SESSION X (Paper (iv) - THURSDAY 8th SEPTEMBER

THE STUDY OF ROLLER END AND
GUIDING SHOULDER CONSTRUCTION OF ROLLER BEARINGS

by

M Li and S Wen

(Tsinghua University, Beijing, China)

SYNOPSIS

This paper deals with the roller end and guiding shoulder construction of roller bearings on the basis of EHL theory and experimental analysis. An orthogonal test dealing with the main effect factors of friction torque and temperature increasing has been done in a wide scope. Optimized roller end and guiding shoulder construction which can improve the lubrication condition has been obtained, it is shown that the axial load carrying capacity of the new construction can be increased by 5-10 times, compared with the usual ones.

Theoretical and Experimental Analysis

For roller bearing, the axial loads are carried by roller ends and guiding shoulders. Usually, the roller ends and guiding shoulders of commercial products are flat in shape, EHL film can not exist in such a state, and thus the axial load carrying capacity of these bearings is very small. In order that the roller bearing can be used in a great radial load combined with a certain axial load case, theoretical and experimental analysis has been done to find the possible good construction of the roller ends and guiding shoulders.

In theoretical analysis, numerical solutions of the EHL film between conical-to-conical surfaces and spherical-to-conical surfaces of roller ends and guiding shoulders of roller bearings are obtained.

In experimental analysis, eight sets of bearing samples are designed and manufactured of which the roller ends and guiding shoulders are different in shape. The test bearings were running with 0-3000 rpm speed under different load conditions. The contact surface temperature on outer race guiding shoulder is measured with thermo-couples, the body temperature of outer ring is measured with four mercury thermometers which contact directly with the outer ring. The friction torque is measured with a torque transducer. In order to ensure the comparability of testing results, the testing conditions for any bearing sample are identical.

Results

The conical-to-conical construction of roller ends and guiding shoulders (Fig.1) is the best construction. The inclination angle of guiding shoulders is the key factor affecting axial load carrying capacity of this

construction. The optimum value of the inclination angle of guiding shoulders is 45'-55' for outer race shoulder and 40'-50' for inner race shoulder.

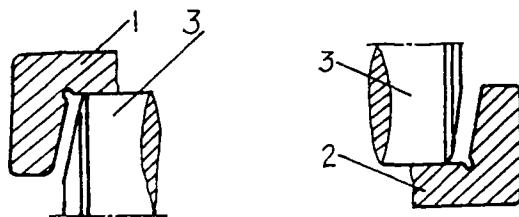


FIGURE 1 Conical-to-conical construction
1. outer ring, 2. inner ring, 3. roller

Using the best construction proposed in this paper, the axial load carrying capacity of roller bearings can be increased by 5-10 times, compared with usual commercial ones.

SESSION XI (Paper (i)) - THURSDAY 8th SEPTEMBER

DYNAMICALLY LOADED JOURNAL BEARINGS:
A MODAL APPROACH TO EHL DESIGN ANALYSIS

by

A Kumar (Cornell University New York U S A)
J F Booker (Cornell University New York U S A)
P K Goenka (General Motors Research Laboratories Michigan U S A)

SYNOPSIS

A new mathematical model, based on the finite element method, is presented for transient elastohydrodynamic lubrication analysis.

Relative (differential) displacement of lubricated surfaces is represented by a (truncated) linear combination of orthogonal modeshapes, which form the basis of both relative rigid body motion and relative elastic deformation.

The model combines hydrodynamic and elastostatic aspects in a coupled initial value problem of relatively low order.

Idealized case studies are carried out to validate the model, which is then applied to a practical automotive connecting rod to demonstrate its versatility.

Problem Formulation

Consider a finite element discretization of a lubricant film. Nodal film thickness, clearance, and relative displacement satisfy the n kinematic relations

$$h = c + d$$

and nodal pressures and forces satisfy the n equivalence relations

$$A p = r$$

Conventional 2-D finite element analysis of the lubricant film (for specified clearance, boundary conditions, and cavitation) gives the n hydrodynamic relations

$$C(d, t) \dot{d} + b(d, t) = -r$$

Conventional 3-D finite element analysis of the structure (for specified boundary conditions) under k external forces gives the n elastostatic relations

$$K d + B f = r$$

where the (relative) stiffness is both symmetric and singular.

The essential approximation of the present work is the replacement of n physical displacements by $m \ll n$ generalized displacements through the n transformation relations

$$\mathbf{d} = \Psi \mathbf{d}'$$

where the m columns of the modal transformation matrix are chosen arbitrarily to capture the essential features of both rigid body and elastic displacements.

The result is the m coupled equations of motion

$$\mathbf{C}'(\mathbf{d}', t) \dot{\mathbf{d}}' + \mathbf{K}' \mathbf{d}' + \mathbf{b}'(\mathbf{d}', t) = -\mathbf{B}' \mathbf{f}(t)$$

where

$$\mathbf{C}' = \Psi^T \mathbf{C} \Psi$$

$$\mathbf{K}' = \Psi^T \mathbf{K} \Psi$$

$$\mathbf{B}' = \Psi^T \mathbf{B}$$

$$\mathbf{b}' = \Psi^T \mathbf{b}$$

Specification of m appropriate initial (typically arbitrary) generalized displacement values completes the problem formulation.

Sample Results

A connecting rod bearing studied previously by Oh and Goenka [1985] is chosen to demonstrate the present more approximate approach.

Figure 1 compares instantaneous minimum film thickness predictions for present and previous approaches for both rigid and elastic bearings. (Such a local examination is a particularly rigorous test of a global approximation technique.) For the rigid case, results are (predictably) identical; for the elastic case, results are qualitatively similar but quantitatively different.

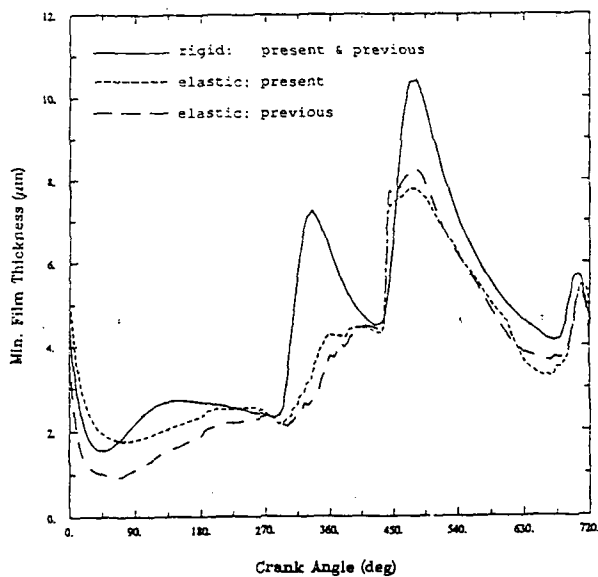


FIGURE 1

SESSION XI - (Paper (ii)) - THURSDAY 8th SEPTEMBER

SHAPE DEFECTS AND MISALIGNMENT EFFECTS
IN CONNECTING-ROD BEARINGS

by

P Maspeyrot and J Frene

(University of Poitiers France)

SYNOPSIS

Connecting-rod and crankshaft bearings in petrol or diesel engines are subjected to very important dynamic loading. The importance of the analysis of this problem is obvious by the number of papers published in this area.

In this paper, the effects of the radial clearance in a perfect bearing under dynamic loading is shown. Then the effects of shape defects of the journal bearing (journal with a taper or a parabolic axial profiles) or the misalignment of the journal are studied.

The misalignment introduces two supplementary parameters : β , the angle between the eccentricity direction and the journal centreline projection and δ , the non-dimensional magnitude of the projection of the complete journal centreline onto the mid-plane. The misalignment is constant and the journal is assumed to rotate about its own centreline.

THEORY

The film geometry equation for any axial and angular position can be written as follows :

$$h(\theta, z) = C + c_e \cos \theta + f(\theta, z)$$

where $f(\theta, z)$ is depending on the defect.

The Reynolds equation has been written using the mobility method of BOOKER (1) :

$$\frac{\partial}{\partial \theta} \left[H^3 \frac{\partial P}{\partial \theta} \right] + \left[\frac{R}{L} \right]^2 \frac{\partial}{\partial z} \left[H^3 \frac{\partial P}{\partial z} \right] = 12 \left[\cos(\theta + \alpha) - \frac{\delta z}{\epsilon_0} \sin \alpha \sin(\theta - \beta) \right]$$

Solution of this equation is obtained by an iterative method to determine α , the mobility angle, and by finite differences with the Gauss-Siedel method and the Reynolds boundary conditions to obtain the pressure field. Knowing the pressure field, numerical integrations give the friction torque and the axial flow.

RESULTS

Numerical results are obtained for the big-end connecting-rod bearing, without circumferential groove, of the RUSTON-HORNSBY 6 VER-X Mk III diesel engine.

The curve of the effect of the radial clearance on the minimum film thickness has a similar aspect than for a bearing under steady state conditions. In table 1 details of the influence of shape defects or misalignments on the minimum film thickness are given :

Minimum film thickness (μm)	
Perfect bearing	8.5
Tapered bearing	7.8
Parabolic bearing	7.8
Horizontal misalignment	3.6
Vertical misalignment	4.5

TABLE 1

REFERENCE

(1) BOOKER, J., F. "Dynamically Loaded Journal Bearings: Numerical Application of the Mobility Method ." JCLT-ASME, series F, Jan 1971.

The completion of problem formulation and the calculation of bearing duty cycle history rests with either of two distinct approaches (1):

Problem I: Crankangle θ is specified as a function of time t (kinematic specification); external torque T_{ext} must be determined.

Problem II: External torque T_{ext} is specified as a function of time t (dynamic specification); crankangle variation θ must be determined.

Connectingrod and main journal displacement responses (eccentricity "orbit" responses) to bearing duty cycle history are calculated by using the (short-bearing) mobility method (2).

Some Results

As an example of Problem II formulation, the external environment is modelled by an external torque formulation of the form

$$T_{ext} = -J_{ext} \ddot{\theta} - c_{ext} \dot{\theta} + T_g(t)$$

and by an aperiodic cylinder pressure history representing engine throttling. The external torque formulation and the aperiodic cylinder pressure history are applied to the engine model of Fig. 1.

The resulting transient duty cycle history is subsequently applied to the connectingrod and the two (identical) main engine bearings. Fig. 2 shows that the transient cyclically-minimum film thickness is significantly reduced when the cylinder pressure history jumps from "half-throttle" to "full-throttle".

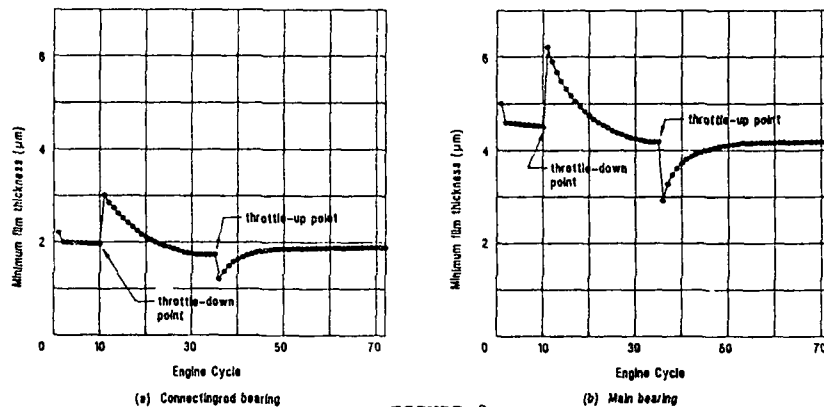


FIGURE 2

References

- (1) BOEDO, S. 'Dynamics of Engine Bearing Systems: Rigid Body Analysis', M.S. Thesis, Cornell University, Ithaca, New York, USA, 1986.
- (2) BOOKER, J.F. 'Dynamically-Loaded Journal Bearings: Numerical Application of the Mobility Method', Trans. ASME, J. Lub. Tech., v. 93, 1971, p. 168. Errata: n. 2, 1971, p. 315.

SESSION XI - (Paper (iv)) - THURSDAY 8th SEPTEMBER

THERMAL CONSIDERATIONS IN ENGINE BEARINGS

by

G A Clayton and C M Taylor
(The University of Leeds U K)

SYNOPSIS

In the analysis of dynamically loaded journal bearings, such as those occurring in the internal combustion engine, the prediction of shaft orbit and the cyclic minimum oil film thickness has attracted most attention. Relatively little effort has been expended in developing techniques to give a reliable estimation of the effective lubricant temperature through thermal analysis. One reason for this relates to the lack of precision of the determination of lubricant flow rate and heat dissipation to the oil, two factors which are important in thermal calculations.

The present study has been directed towards a thermal analysis of the Ruston and Hornsby 6VEB Mk III big-end bearing; this connecting rod bearing has become a standard test case for those concerned with engine bearing analysis. Straightforward predictions of flow rate and power loss based on the commonly adopted short bearing analysis have been undertaken leading to an iterative internal balance to predict the effective operating temperature and viscosity (1,2,3). In addition a more rigorous analysis based on considerations of oil film history has been undertaken (4).

The results of the simple approach were found to give good agreement with those obtained by the more complex analysis. It is proposed to undertake experimental work in the near future to provide a validation of the theoretical model adopted.

Theory

(a) For the rapid solution technique the journal orbit was determined from short bearing theory using an assumed effective oil temperature. The oil flow rate and power loss were calculated at 72 points in the orbit from the following expressions and numerical integration used to sum for one engine cycle.

$$Q_H = \frac{\bar{FM} (C_d/d)^2 C_d}{2\eta} \quad (1) \text{ Hydrodynamic Flow}$$

$$Q_P = \frac{0.0315 P_f C_d^3}{\eta} \left(\frac{d}{b} \right) (1.5 \epsilon^2 + 1) \quad (1) \text{ Pressure Flow}$$

$$H_{SH} = \frac{\eta d^3 b (\omega_j - \omega_b)^2 J_1}{4 C_d} \quad (3) \text{ Shear Power Loss}$$

$$H_{SQ} = FV \cos \beta$$

(4) Squeeze Power Loss

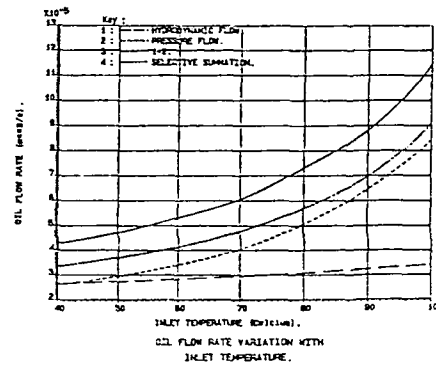
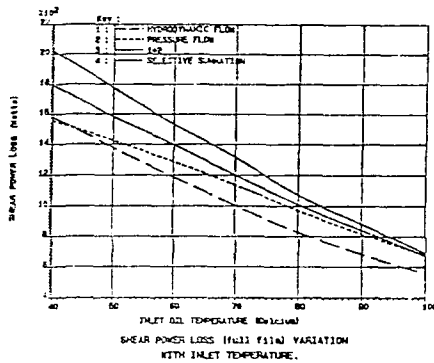
A new effective temperature was determined using the following expression and an iterative loop repeated until satisfactory convergence.

$$T_* = \frac{H}{\rho Q C_p} + T_{in} \quad (5)$$

(b) The analysis incorporating oil film testing effects involved complex considerations concerning the true extent of the cavitation region. This will be discussed in detail.

Results

Some typical results are shown below.



References

- (1) F A Martin and C S Lee, "Feed Pressure Flow in Plain Journal Bearings", Trans. A.S.L.E., Vol 23, 3, 1983, pp 381-392.
- (2) F A Martin, "Friction in Internal Combustion Engines", I.Mech.E., Conference - Combustion Engines-Reduction of Friction and Wear, Paper C67/85, 1985, pp 1-17.
- (3) F A Martin, "Developments in Engine Bearings", Proc. 9th Leeds-Lyon Symposium on Tribology - Tribology of Reciprocating Engines, 1983, pp 9-36.
- (4) G J Jones, "Crankshaft Bearings: Oil Film History", Ibid, pp 83-88.

SESSION XII (Paper (i) - THURSDAY 8th SEPTEMBER

DESIGN REQUIREMENTS OF CERAMIC SLIDING CONTACTS

by

R J Godzdawa (Advanced Bearing Technology, plc, Middlesex, U K)
and

T A Stolarski (Brunel University, Middlesex, U K)

SYNOPSIS

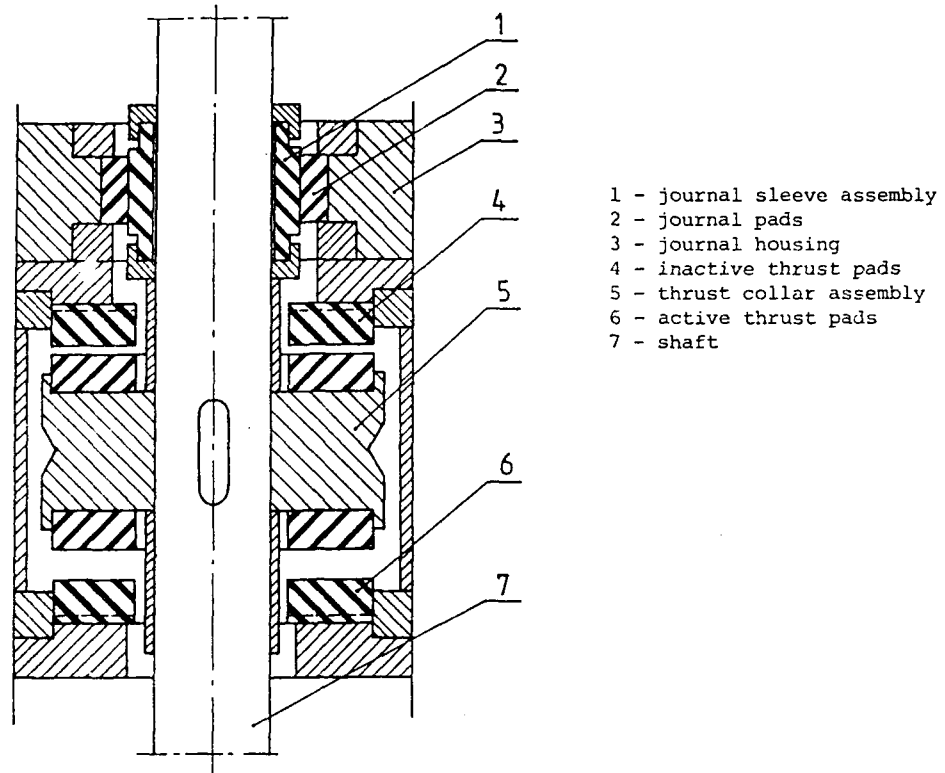
The main aim of this paper is to discuss, using design case study, factors controlling the performance and affecting the utilization of engineering ceramics, particularly silicon carbide, as a material for the components of a sliding bearing. The bearing system designed for Framo Engineering, was destined for the special pump used in North Sea oil exploration.

Introductory information

Current demands on bearings are leading to the developments in bearing technology aimed at running them at high speeds, hostile environments and increased unit loads. The design and manufacture of such bearings is at the limit of established technology. The most promising designs at present, able to cope with such demands, are believed to be in the area of ceramic/ceramic material combinations. The design brief required that the bearing system, supporting vertically positioned shaft of the pump, should be lubricated by the working fluid which consists of a mixture of an oil used for cooling purposes and hard, abrasive particles coming from the drilling operation. This requirement excluded a number of traditional bearing materials and put ceramics at the top of the list. Additional requirements of specific load up to 13 MPa, rotational speed of 6000 rpm and the temperature of the working fluid of up to 130°C provided further support for ceramics as the only suitable type of material.

Bearing system design and testing

The bearing system designed for Framo Engineering, Norway, consisted of radial and thrust tilting pad bearings combined together and shown schematically in Fig.1. A full scale prototype was tested in a specially designed test rig in order to establish the limits of operating conditions. During the course of testing, two failures occurred. First failure of the thrust bearing pad took place under specific load of 12.75 MPa and speed of 6000 rpm. The lubricant was a diesel oil. The silicon carbide face of the rotating thrust collar was also damaged, mainly in the form of deep scratches, by loose particles generated by the brittle fracture of the silicon carbide pad at the pivot point. The failure was attributed to excessive loading. The second failure occurred at much less load of 8 MPa and after a relatively short period of time of around 4.5 hours. A hydraulic oil (Shell Tellus T-37) was used this time as a lubricating medium. The test programme leading to the failure consisted in the progressive oil inlet temperature increase of 10°C every 60 minutes starting from 80°C. At 120°C oil inlet temperature, the bearing was run for only 30 minutes when the failure occurred. During testing, load on the bearing and speed were kept constant and the oil flow rate was at 38 l/min. On investigation it was found that the pad failed in fracture mode again. As in the previous case, loose particles produced by fracture process damaged the surface



- 1 - journal sleeve assembly
- 2 - journal pads
- 3 - journal housing
- 4 - inactive thrust pads
- 5 - thrust collar assembly
- 6 - active thrust pads
- 7 - shaft

Fig.1 Bearing system

of rotating thrust collar. This second failure is thought to be due to high oil inlet temperature and hence thin lubricating film. Predominant mode of lubrication was probably mixed lubrication leading to high temperatures at the interface. Visual inspection of the bearing after the second failure suggested that the load was not shared equally by all the pads and was probably caused by the variations in pad thicknesses. This points to the importance of precision during the manufacture of ceramic elements as they do not deform sufficiently to absorb any eventual inaccuracies.

Temperature rise in the bearing, monitored by means of thermocouples fixed to pads, was consistent with oil inlet temperature. For the oil inlet temperature from 80 to 120°C, corresponding temperature rise in the radial bearing, run at the speed of 6000 rpm and the load of 1000 N, was in the range of 20 to 30°C respectively. Temperature rise in the thrust bearing, however, was rather constant and equal to approximately 34°C regardless the oil inlet temperature.

The main conclusion to be drawn from data accumulated during prototype testing is that silicon carbide tilting pad radial/thrust bearing system seems to offer a good solution for this particular application. It is now quite clear that to ensure long service life of the bearing with ceramic components, unit loads can be significantly higher than that for conventional materials provided that the effective lubrication is secured.

SESSION XII (Paper (ii) - THURSDAY 8th SEPTEMBER

UNLUBRICATED WEAR AND FRICTION BEHAVIOUR
OF ALUMINA AND SILICON CARBIDE CERAMICS

by

G Kapelski, F Platon and P Boch

(Ecole National Supérieure de Céramique Industrielle, Limoges, France)

SYNOPSIS

Ceramics behave as brittle materials at low and medium temperatures. Fracture suddenly develops when the stress field reaches a critical state. This critical state depends on many parameters. It also depends on whether the stress field is uniaxial or multiaxial. Therefore, it is difficult to correlate the damage which is observed in tribological studies of ceramics - which corresponds to a multiaxial stress state - with macroscopic data. In particular, the "tribological strength", understood as the yield point beyond which local cracks develop, is generally higher than the macroscopic strength (as can be determined using, for instance, a uniaxial bending test).

In the case of wear and friction tests with high contact pressures, cracking of the friction track can develop during the very beginning of the test. The extent of damage of the contact surfaces and the production of wear debris are very sensitive to such cracking. This means that the entire life of a tribological couple can be affected by the first few seconds, and that the wear and friction behaviour of a ceramic-to-ceramic couple is very dependent on an eventual overload.

This work was thus focused on the study of the damage which can occur during the first few instants of the life of a ceramic-to-ceramic couple, tested using a ball-on-disc configuration. Several ceramic materials were studied, in particular silicon carbide and alumina. The friction tests, called "dynamic" because they involve the displacement of the ball on the disc, were completed by indentation tests, called "static" because they simply correspond to loading the disc by the ball.

For the static indentation tests, and assuming that the material behaves in a perfectly elastic manner, the maximum of the principal tensile stress at the surface is (1) :

$$\sigma_{1s} = (1-2\nu)/(2\pi)(0.75 k R/E)^{-2/3} F^{1/3}$$

where F is the normal load, E and ν are Young's modulus and Poisson's ratio of the disc material, R is the ball radius, and k is a parameter which is a function of the elastic constants of both the disc and the ball materials. Fracture develops when σ_{1s} reaches a critical value : σ_{1sF} . This value was found to be about 1200 MPa for alumina as well as for silicon carbide, which corresponds to loads of 1250 N (for Al_2O_3) and 430 N (for SiC). The respective macroscopic strengths were 285 MPa and 450 MPa, i.e. about one third only of the "tribological strengths". For the dynamic friction tests, the maximum value of the principal tensile

stress (σ_{1d}) becomes a function of the coefficient of friction (f). At the rear of the friction contact, this maximum is (2,3) :

$$\sigma_{1d} = (\sigma_{1s})(1+k_v f)$$

where k_v is a function of Poisson's ratio of the disc material. Fracture develops when σ_{1d} reaches a critical value, σ_{1df} , which was found to be approximately equal to σ_{1sf} . It was verified that when the load on the ball is sufficient to give $\sigma_{1d} = \sigma_{1df}$, a crack array develops during the first revolution of the ball on the disc. Data are discussed, and the evolution of the crack array as the test proceeds is described.

References

- (1) JOHNSON K.L. 'Hertz Theory of Elastic Contact', 90-104, 'Pressure Applied to a Circular Region', 56-53, in Contact Mechanics, the Press Syndicate of the University of Cambridge Publ., (1985).
- (2) HAMILTON G.M. and GOODMAN L.E., 'The Stress Field Created by a Circular Sliding Contact', in J. Appl. Mech., 371-374, (1966).
- (3) LAWN B.R., 'Partial Cone Crack Deformation in Brittle Material Loaded with a Spherical Indenter', in Proc. Roy. Soc., A299, 307-316, (1967).

THE EFFECT OF SURROUNDING ATMOSPHERE ON THE FRICTION AND WEAR OF CERAMICS

by

S Sasaki

(Mechanical Engineering Laboratory, Japan)

SYNOPSIS

The effect of surrounding atmosphere on the friction and wear of the ceramics, Si_3N_4 , SiC , Al_2O_3 , $\text{ZrO}_2(\text{PSZ})$, have been studied under the following conditions;

1. Lubricating conditions in water and in some organic liquids.
2. Dry conditions in nitrogen gas atmosphere containing water vapour and some organic compounds vapours.
3. Vacuum conditions at pressures ranging from 10^5Pa to 10^{-6}Pa .

The experiments were conducted with the combinations of pin and disk of the same ceramics at room temperature.

In order to investigate wearing behaviour, damage on the sliding surface and wear debris were observed and analysed using a scanning electron microscope (SEM) with an energy dispersion x-ray (EDX) spectroscopy attachment, electron spectroscopy for chemical analysis (ESCA) and other analytical tools.

Based on the experimental results, the mechanisms of the atmospheric effects were considered as the following;

At first, the molecules, which constitute the surrounding atmosphere, adsorb on the sliding surface and form adsorption layers. The adsorption layers obstruct the solid-to-solid contacts and protect the sliding surfaces.

At the same time, the adsorption decrease the surface energy of ceramics. In brittle materials, surface energy is closely related to mechanical strength. Especially the adsorption of water, which has a lone-pair electron orbital, causes stress corrosion. Furthermore, in PSZ, stress corrosion induces phase transformation from the tetragonal phase ZrO_2 to monoclinic structure. The phase transformation brings about microcracks on the surface and results in an increase in wear rate.

Moreover, tribochemical reaction occurs on the sliding surface. The tribochemical reaction products on sliding surfaces are softer than base-materials, so they perform like solids lubricants and decrease the friction. On the other hand, owing to the leaving of the soft products from the sliding surfaces, tribochemical corrosion wear occurs. The wear rate due to tribochemical corrosion is, however, much smaller than that of fracture wear.

Some Results

1. The effects of atmospheric pressure

Figure 1 shows the effects of atmospheric pressure on the coefficient of friction of SiC at a sliding velocity of 0.1 m/s and a load of 3 N .

The difference between in N_2 and in O_2 was caused by tribochemical reaction. SiC undergoes a tribochemical reaction with O_2 to form SiO_2 . On the sliding surface, SiO_2 performs like solids lubricant and decrease the friction.

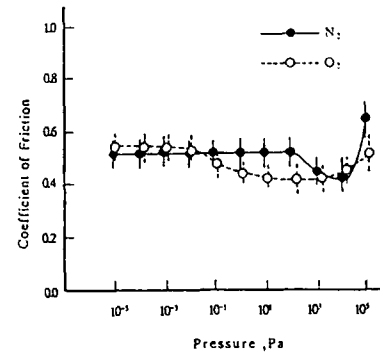


Fig.1

2. The effects of some organic compounds vapors

Figure 2 shows the effects of some organic compounds vapours on the friction and wear of Al_2O_3 and Si_3N_4 at a sliding velocity of 0.4 m/s and a load of 10 N.

The friction and wear behaviours vary with combinations of organic compounds and ceramics. Tribochemical reaction products, which looked like friction polymers, were observed on the sliding surfaces.

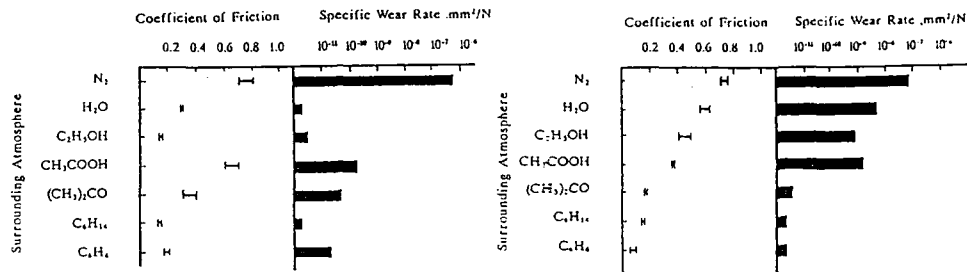


Fig.2(a)

Fig.2(b)

3. The effects of water

Figure 3 shows the effects of humidity at a sliding velocity of 0.4 mm/s and a load of 10 N.

The coefficient of friction decreased with an increase in humidity.

Figure 4 shows the effects of sliding velocity at a load of 50 N in water.

In Si_3N_4 and SiC, the coefficient of friction was as low as 0.01. This was caused by additive effect combining the tribochemical reaction and the hydrodynamic lubrication (1).

Reference

- (1) H.TOMIZAWA and T.E.FISCHER, 'Friction and Wear of Silicon Nitride and Silicon Carbide in Water: Hydrodynamic Lubrication at Low Sliding Speed Obtained by Tribochemical wear', ASLE TRANS., 1987, 30, 1, 41-46.

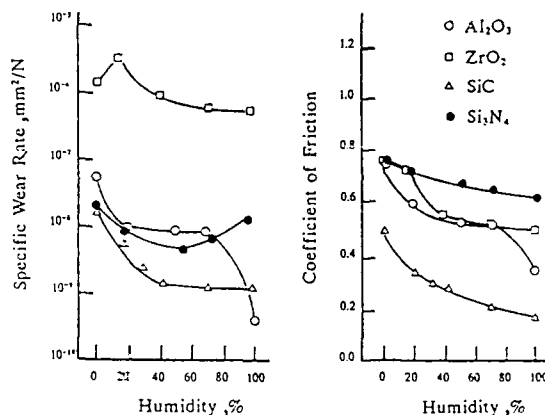


Fig.3

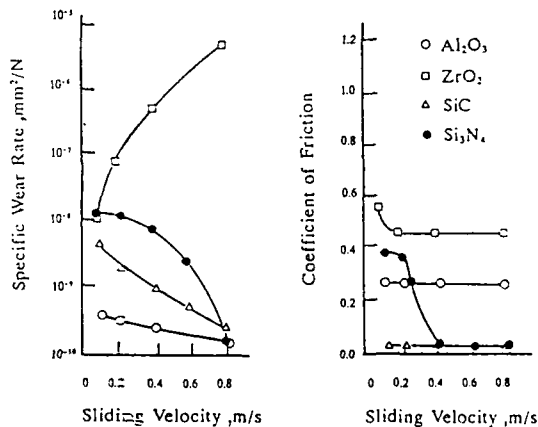


Fig.4

WEAR PERFORMANCE OF MATERIALS FOR BALL SCREW AND SPLINE
APPLICATIONS IN CANDU REACTOR FUELLING MACHINES

by

P E Dale (Ontario Hydro Research Division, Canada)
and
R M Tristani, McMaster University, Canada)

Synopsis.

Background.

In the Candu nuclear reactor, fuel bundles are moved into the channel by means of a ram connected to a ball screw. The screw is driven by a recirculating ball nut and constrained to axial movement by a low friction ball spline. The splines and screws are manufactured from both AISI S17400 (17-4 PH) and AISI S45500 (Custom 455) while the balls are cast Stellite No. 6 alloy with 59.4% Cobalt. Wear of these heavy water lubricated ball splines and screws leads to high maintenance costs and radiation exposure for maintenance personnel. Cobalt wear debris is also thought to contribute to high radiation fields in the heat transport system due to Cobalt's long half-life.

Examination of used Stellite balls from in-service fuelling machines and splines from out of reactor fuelling simulations have indicated three failure mechanisms; ball sliding causing wear, corrosion and fatigue. This experimental effort has been concerned with ball sliding. Ball sliding occurs under a number of circumstances including interaction between adjacent balls, debris contamination of the rolling contact and ball "piling" due to resistance of the balls to enter the highly loaded contact zone from the ball recirculation channel (Fig. 1).

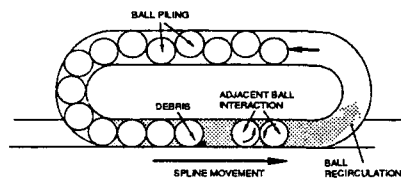


Figure 1. Mechanisms of ball sliding in ball spline.

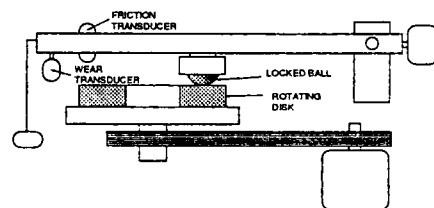


Figure 2. Ball on disk wear test schematic.

Test Procedure.

Simulation tests have been performed using a locked ball on a rotating disk (Fig. 2) to compare the sliding wear resistance of a number of candidate replacement materials with that of Stellite 6. These included Silicon Nitride, Alumina and partially stabilized Zirconia in addition to a non-cobalt containing metallic ball, Cenium ZNZ. These first screening tests were performed at ambient temperature and in air. Although test load (152N), speed ($5.25 \times 10^{-2} \text{ ms}^{-1}$) and sliding distance (756 m) were selected to represent service conditions.

Results.

All the balls tested, with the exception of alumina, gave similar ball wear rates although there were large differences in disk wear rates (Fig. 3).

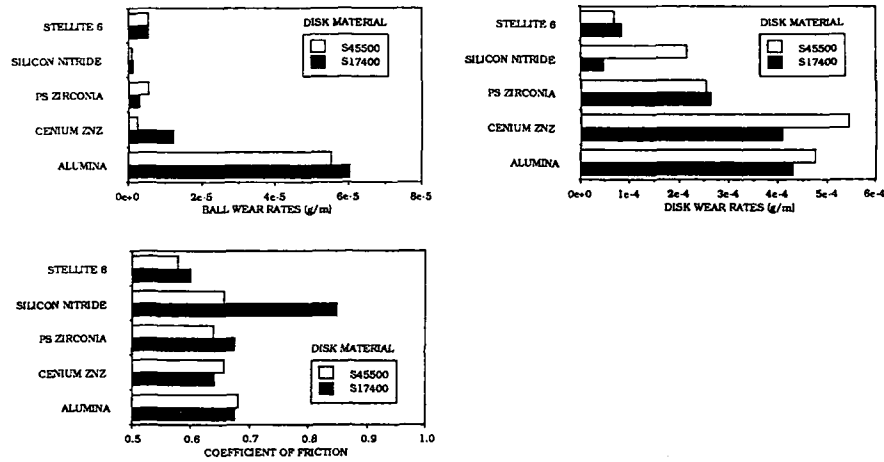


Figure 3. Wear rates and friction coefficients for various ball materials sliding against S17400 and S45500 disk materials in air.

Results indicate that Silicon Nitride balls sliding against S45500 give significantly better wear performance than the traditional cast Stellite balls, although they exhibit higher friction coefficients. In addition to the large difference in wear rates for the two disk materials sliding against Silicon Nitride balls, the friction coefficient for Silicon Nitride and S17400 is significantly higher than for S45500. Work is continuing in an effort to understand the implications of these effects on ball screw performance.

SESSION XIII - (Paper (i)) - FRIDAY 9th SEPTEMBER

TRIBOLOGICAL DESIGN - THE POWER GENERATION INDUSTRY

by

P G Morton

(G E C Stafford U K)

SYNOPSIS

Many machines and components used in the power generation field are common to a wide range of plant. What is unique in this field is associated with the main power line-out, i.e. the combination of prime mover and electrical generator usually on a single shafting system. Individual machines have their rotors solidly coupled and their stators are also structurally coupled.

Power plant is distinguished in the field by its size, mass and power output all of which have affected the design of machine elements. Problems emerging over the past 30 years have been almost entirely associated with increases in size and power. The paper deals with design problems in three types of power plant viz steam turbosets, hydroelectric generators and gas turbine plant. The subject areas are as follows.

Journal Bearings

Journal bearings have increased in duty over the years and the treatment of their steady state characteristics has become more sophisticated over the years. Thermohydrodynamic theory has improved from the earlier work of Christopheron to include now the effect of non-laminar flow, oil recirculation, boundary reformation, cavitation, conduction into shaft and bush, angular and tranverse misalignment and more recently thermoelastic and elastic distortion. The dynamic characteristics and their influence on system stability have also benefited from much theoretical and experimental research so that it is possible to predict the contributions of the bearings to the system dynamics with reasonable accuracy, in some cases making allowance for non-linear effects. The history is briefly examined and also the various attempts to adjust oil film profiles to improve both steady and dynamic characteristics.

Seals and Glands

Seals and glands affect rotating systems in two ways. First they add to the system instability by 'negative damping' mechanisms. Second, by shaft rubbing they produce 'synchronous instability' in an unstable spiral vibration vector.

The approach of various authors to designing away from these problems is reviewed.

Thrust Bearings

The largest and most heavily loaded thrust bearings are those supporting vertical hydroelastic shafts. In contradistinction to journal bearings, thrust bearing analyses have included the thermoelastic effect for many years. Some of the problems in thrust bearing design dealt with in the literature are reviewed, including the opposing effects of elastic and thermoelastic pad distortion the influence of water cooling and transient effects.

Movement of Turbine Supports

Due to changes in operating conditions at the turbine end of the steam turbo set allowance has to be made for expansion in all directions. Relative movement has to be allowed for internally in the HP and IP turbines and externally on both turbine and generator supports. Comment is made on publications on the attendant wear problem arising from movements at the interfaces and the choice of materials to ensure the maintenance of good alignment and reduction in internal stresses.

Effects of Internal Friction in Rotors

Papers relating to movements in the windings of generator rotors leading to insulation wear and fretting fatigue are commented on. Instability arising from rotating friction is also covered.

Effects of Friction in Laminated Electrical Machines

Several publications have dealt with frictional effects on the laminations of generator stators and certain laminated rotors resulting from relative conductor/stack movements. These are briefly discussed.

SESSION XIII (Paper (ii) - FRIDAY 9th SEPTEMBER

TRIBOLOGICAL DESIGN AND ASSESSMENT -

The Nuclear Industry

by

T C Chivers

(CEGB, Berkeley Nuclear Laboratories, U K)

SYNOPSIS

The Operational requirements and/or environmental considerations within the Nuclear Industry frequently invalidate those design codes that deal with the tribology of mechanism elements. As a consequence, the Industry has had to evolve its own methods. Frequently these have to be iterative, ie a design is produced and then assessed. In some instances it will be necessary to redesign or modify the operational/maintenance/monitoring strategy to deal with uncertainties.

Within most areas of nuclear reactors the use of conventional lubricants is prohibited and hence design to cope with unlubricated wear is a major interest. In the paper the current assessment strategies will be outlined. For some components the assessment is based on a simplified "Archardian" approach, viz:-

$$\text{Wear Volume} = K.L.S.$$

Where K is a specific wear rate, L is the interfacial load and S the total sliding distance.

However, the high power densities encountered within nuclear reactors frequently results in flow or noise induced relative movements of components. This complicates the determination of loading and sliding distance information, and these parameters influence specific wear rates. Hence wear volume determination can be very uncertain. To determine these input parameters requires close collaboration between various specialists. In general the strategy adopted is to determine acceptable bounds and the positive identification of the appropriate limiting criterion. Examples will be given where these approaches are employed.

Assessments as outlined above relate to individual contact geometries. However, in some instances, such as control mechanisms or valves, component tests are conducted to validate design. In these tests the full duty cycle and environmental conditions are simulated. Examples will be given where this approach has identified the need for plant modifications, and the way that the proposed changes have in turn been evaluated.

An important input into assessment procedures are the consequences of failure. Outage costs associated with loss of availability are high; reactor safety is of paramount importance. A high level of quality assurance is, therefore, necessary in formulating recommendations. Peer review and method/data endorsement is part of this process. Data relating to a design or component tests are considered by an industry wide committee of experts. Following agreement, recommendations will be made to a parent body which includes design representatives. At this level the usefulness of the advice is considered, and it is endorsed for use if appropriate.

SESSION XIII (Paper (iii) - FRIDAY 9th SEPTEMBER

TRIBOLOGICAL DESIGN - THE SPACECRAFT INDUSTRY

by

R A Rowntree, E W Roberts and M J Todd

(National Centre of Tribology, UKAEA, U K)

Abstract

Modern spacecraft abound with mechanisms where relative movement between contacting surfaces occur. Failure or abnormal performance of such mechanisms can rapidly lead to loss of an experiment or mechanism function; for critical items this can lead to complete failure of the spacecraft mission.

The designer of spacecraft mechanisms faces several 'hostile' conditions in which hardware must operate without any possibility of repair, with extreme reliability, minimum mass and minimum power consumption. The environmental design drivers include the high vacuum of space, temperature extremes of -269°C to $+150^{\circ}\text{C}$, temperature differentials across rotating components of typically $\pm 55^{\circ}\text{C}$, the launch vibration, the effect of zero (or near-zero) gravity, rapid depressurisation and particle radiation. Dependent on mission type satellite life is currently in the range 7 to 10 years and even longer lives will soon be required.

This paper will examine the characteristics of the main types of electro-mechanical mechanisms used in spacecraft and their tribological requirements. To give low friction and avoid severe adhesive wear in the space environment, specialised lubricants are used. The techniques, properties and types of suitable solid and liquid lubricants will be described. Problematic areas and new developments in space tribology will be highlighted. To illustrate the fundamental role of tribology in spacecraft mechanism design, examples will be drawn from operating and current designs of satellite. The paper stresses the need to consider tribology as a fundamental part of the spacecraft mechanism design process and not something to be left in the specification as 'TBD' (to be decided).

SESSION XIII (Paper (iv) - FRIDAY 9th SEPTEMBER

TRIBOLOGICAL DESIGN - THE ELECTRONICS INDUSTRY

by

E A Muijderman, F Bremer, P L Holster, A v Montfoort and A G Tangena

**(Philips Research Laboratories and Philips Centre for Manufacturing Technology)
(The Netherlands)**

SYNOPSIS

The paper provides an impression of tribological research and development within Philips. We will first introduce Philips, then summarize the different tribological research areas and the existing design procedures and finally give a short description of desirable future research work.

Philips is a multinational company with national organizations in more than 60 countries. It has a turnover of 22 billion ECU and employs 340,000 people.

Tribological research and development work is mainly performed in the Philips Research Labs. and at the Philips Centre for Manufacturing Technology (CMT). This work is largely concentrated in Eindhoven, the Netherlands.

For a description of the tribological activities and design procedures at Philips we prefer to use the classifications: full-film lubrication, mixed & boundary lubrication and dry-running systems.

Full-film lubrication

Externally pressurized air and oil bearings:

In the research attention is focussed on the dynamic behaviour and on the construction of optimal (infinitely) stiff bearings. In the company numerous bearings for widely varying applications are in use.

Spiral Groove Bearings (SGBs)

Grease-lubricated SGBs for the scanner motor of video recorders have been used in mass production since 1978. Air-lubricated SGBs are used in the design of laser scanners, whereas oil-lubricated SGBs for flywheels have shown a lifetime of more than 20 years.

Foil bearings

This research investigates the tape-scanner system of video recorders, where the tape acts as an air-lubricated foil.

Mixed & boundary lubrication

For the selection of lubrication fluids we have a well-established routine. Problems in this field are solved by functional tests. An important research topic is precision machining, which includes the machining process itself, machine dynamics, measurement and control and their interactions.

Dry-running systems

In this field studies are made of material characterization, contact mechanics (for use in wear models like the zero-wear model and Archards model), coatings and magnetic recording. The purpose of this work is twofold. Part of it has the nature of research, while other parts are more development-oriented.

The network for transfer and acquisition of tribological knowledge within Philips will be mentioned.

There is an enormous amount of tribological R&D work which is of interest to Philips. Here we limit ourselves to the following:

- a universal, reliable, user-friendly programme package to design full-film bearings (like FEM packages for mechanical calculations)
- dynamic analysis of (aerostatic) bearing behaviour
- analysis of the fundamentals of the failure of coatings
- development and characterization of new (tribo)materials
- analysis of boundary lubrication (transition diagrams), so that research results can be transferred to practical applications
- conditions for zero wear.

OPTIMUM DESIGN AND AUTOMATIC DRAWING
OF RECESSED HYDROSTATIC BEARINGS

by

Xu Shangxian and Chen Baosheng

(Southwest University, Nanjing, China)

SYNOPSIS

The optimum design and automatic drawing of the hydrostatic bearing with any number of recesses are studied. For analysis and calculation of the dynamic effects on the lands, the Reynolds' equation is directly solved by the finite difference method with unequal steps or finite element method.

In the optimum design of the bearing, there are some optimization methods and several objective functions to be offered to the users. Because several technical approaches are employed, it becomes practicable to do the optimization of bearings by solving the Reynolds' equation directly.

To draw the bearing draught automatically, the interface between the standard graphic software AUTO-CAD and the programming language is worked out.

THEORY

1. The mathematical model of the optimum design [1]

(1). The design variables in optimization are considered as:

$$X = \{L/D, La/L, Lt/D, \beta, K\}^T$$

(2). There are several objective functions in the system, such as load capacity, stiffness, flow rate, total power loss and total power loss/load capacity.

(3). It has to subject to these following constraints:

- | | |
|---|--|
| (a). $1.2 \geq L/D \geq 0.5$ | (b). $0.5 \geq La/L \geq 0.1$ |
| (c). $\pi/(2 \cdot No) \geq Lt/D \geq 0.$ | (d). $0.9 \geq \beta \geq 0.$ |
| (e). $12. \geq K \geq 0.$ | (f). $WNO \geq W_0$ |
| (g). $p_s \max \geq p_s \geq p_s \min$ | (h). $\zeta \max \geq \zeta \geq \zeta \min$ |

2. The selection of optimization method

Because the above mathematic model is a nonlinear problem and it is difficult to describe the bearing performances (e.g. load capacity) and their derivatives by analytical functions, the direct optimization method seems to be more suitable for this kind of problem.

In order to make the optimum design available for use, a series of technical approaches are applied to save computer time, such as the reasonable selection of the initial values, the automatical modification of the superrelaxation factors and the higher and/or lower accuracy iteration technique.

3. The finite difference solution

In the hydrostatic and hybrid bearings, a dimensionless form of the Reynolds' equation can be stated as follows: [2]

$$\frac{\partial}{\partial X} (H^3 \frac{\partial P}{\partial X}) + (D/L)^2 \frac{\partial}{\partial Z} (H^3 \frac{\partial P}{\partial Z}) = 24\pi S_H \frac{\partial H}{\partial X}$$

The solution domain of the bearing is divided into the differential mesh lines with inequal steps and the pressures at all nodal points of the bearing mesh can be obtained by solving both the Reynolds' equation and the flow continuity equation simultaneously .

4. The automatic drawing

The standard graphic software package Auto-CAD is employed in this module. To apply to the computer-aided design ,it is very important to endow it with the capacity of "parametric drawing", therefore, the interface between Auto-CAD and programming language has been carried out. Now, we can generate the drawing of bearings by the software written in FORTRAN and modify the parameters of drawing freely according to the design parameters. Finally, all the files are transmitted to Auto-CAD to draft the desired drawing.

EXAMPLE

Using this software system, the design of a concrete bearing has been carried out.

The specifications of the bearing are as follows:

Bearing type: Recessed bearing without axial grooves

Type of restrictor: Orifice restrictor

Number of recesses: No = 4

Bearing Diameter D = 50.0 mm

Bearing Length : L = 50.0 mm

Eccentricity Ep= 0.30

All the data above are stored in a data file, then to run the program, some results are given in Tab.1.

The drawing of the bearing has been generated simultanuously. (see Fig. 1)

Table 1. Comparison of the Parameters

	Unit	Optimal Design Parameters	Original Design
Supply pressure	MPa	0.20	0.167
Flow rate	L/min	0.552	0.676
Total power	W	0.056	0.041
Bearing diameter	mm	50.00	50.00
Bearing length	mm	50.00	50.00
Orifice diameter	mm	0.20	0.20
Orifice length	mm	0.20	0.20
Pressure ratio		2.546	1.63
Power ratio		2.364	1.64

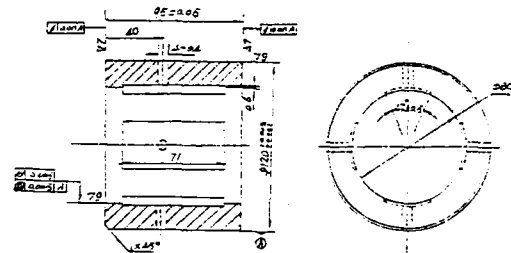


Fig. 1. The Recessed Hydrostatic Bearing Without Axial Grooves

References

- (1). Xu Shangxian, Chen Baosheng, 'The Optimum Design of The Hydrostatic and Hybrid Bearings' (in Chinese) Machine Tool & Hydraulics, No.5, 1986
- (2). W.B.Rowe, Xu Shangxian, F.S.Chong, W.Weston, 'Hybrid Bearings --- with particular reference to hole-entry configuration' Tribology Int. Dec. 1982

SESSION XIV (Paper (ii) - FRIDAY 9th SEPTEMBER

COMPUTER AIDED DESIGN OF EXTERNALLY PRESSURIZED BEARINGS

by

G J J van Heijningen and C M Kalker-Kalkman

(Delft University of Technology, The Netherlands)

SYNOPSIS

The selection and calculation of suitable bearings for a given mechanical application is a significant problem for a mechanical engineer. He meets the difficulty to compare different types of bearings and to make the best choice for his problem out of the most promising types. The designer would need to be an expert on all competing types to make a meaningful comparison. Such levels of knowledge are rare amongst specialists. There is, however, scope for making the necessary information available via a computer, which in effect acts as the expert and operates in an interactive consultation mode.

A research programme has been instigated at the Delft University of Technology which aims to introduce such a computer-aided technique into the bearing selection process. As a first stage of the development the bearing type: "externally pressurized bearing" is chosen.

We managed to reduce the selection criteria down to 8 basic factors depending on what kind of design function is involved. When all data describing an application have been used as input to the system, the desired properties are compared with those in a database system.

The proposed bearing type is not only presented by its name but also by a simple drawing on a second screen. If the designer is satisfied with the proposed bearing the remaining general properties of the chosen bearing are collected from the database. Further output includes the detailed analysis of specific properties by means of a spreadsheet program.

Expert knowledge for other bearing types might be implemented using the same system architecture.

SESSION XIV (Paper (iii)) - FRIDAY 9th SEPTEMBER

A THEORETICAL INVESTIGATION OF HYBRID JOURNAL BEARINGS

APPLIED TO HIGH SPEED HEAVILY LOADED CONDITIONS

REQUIRING JACKING CAPABILITIES

by

D Ives, (Liverpool Polytechnic, U K)

W Weston (Huddersfield Polytechnic, U K)

P G Morton (GEC Engineering Research Centre, Stafford, U K)

W B Rowe (Liverpool Polytechnic, U K)

SYNOPSIS

This paper presents the results of a theoretical investigation of a commonly used generator bearing geometry and an alternative slot entry configuration. The work attempts to show the improvements in performance that are possible by paying particular attention to the type and positioning of the high pressure jacking sources within the bearing. The work also shows that optimisation using laminar or superlaminar theory produces the same optimum bearing geometry.

Theory

A dimensionless form of the Reynolds equation capable of accounting for superlaminar flow was used in the analysis.

$$\frac{\partial}{\partial X} \left(\frac{H^3}{k_x} \frac{\partial P}{\partial X} \right) + \left(\frac{D}{L} \right)^2 \frac{\partial}{\partial Z} \left(\frac{H^3}{k_z} \frac{\partial P}{\partial Z} \right) = 2\pi S_h \frac{\partial H}{\partial X} + S$$

The terms k_x , k_z were used to take account of turbulence effects and were derived from the work of Elrod and Ng [1]. The term S is a source term for the slot entry bearing. The transition region between laminar and fully developed turbulent flow was accounted for using the techniques developed by Constantinescu et al [2].

Comparisons between bearing types were conducted using load/total power and a coefficient of merit scheme. [3].

Results

Optimisation studies conducted for both laminar and superlaminar theory showed that the load capacity of conventional generator bearings could be enhanced by correct positioning of the jacking pockets. Further improvements in load capacity were possible by adopting the slot entry configuration (fig.1). As a result of these increases in load capacity, it was shown that reductions in power consumption were possible.

The optimisation studies also showed that the optimum geometry indicated by superlaminar theory was identical to that indicated by laminar theory.

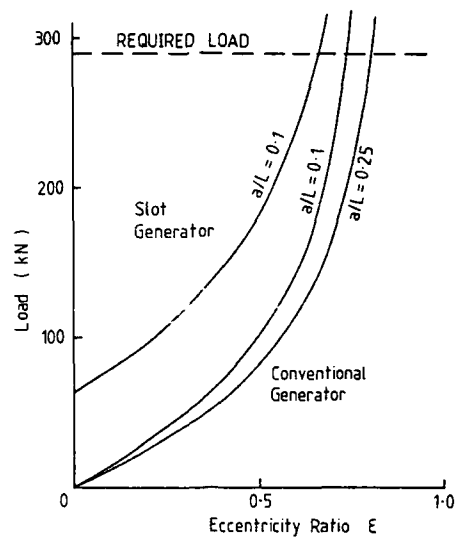


FIGURE 1

References

- (1) ELROD, H.G. and NG, C.W. 'A theory for turbulent films and its application to bearings', Trans. A.S.M.E., J.Lub.Tech., 1967, 346-362.
- (2) CONSTANTINESCU, V.N., PAN, C.H.T. and HSING, F.C. 'A procedure for the analysis of bearings operating in the transition region between laminar and fully developed turbulent flow', Rev.Roum.Sci. Tech-Mech.Appl., 1971, 16(5), 945-982.
- (3) ROWE, W.B. and KOSHAL, D. 'A new basis for the optimisation of hybrid journal bearings', Wear, 1980, 64, 115-131.

SESSION XIV (Paper (iv) - FRIDAY 9th SEPTEMBER

BEHAVIOUR OF A HIGH-SPEED HYDROSTATIC THRUST
BEARING WITH RECESS INSERTS AND GROOVED LANDS

by

D Ashman (Lucas Aerospace Ltd., Birmingham, U K)
E W Parker (Wolverhampton Polytechnic, U K)
A Cowley (U.M.I.S.T., Manchester, U K)

SYNOPSIS

The programme of research reported in this paper was undertaken with the aim of improving the high-speed performance of a multi-recessed hydrostatic thrust bearing. The effects of high peripheral speeds are discussed and how recently proposed bearing modifications, in the form of orthogonal grooved lands and changes in recess geometry (by the use of recess inserts), are used to reduce the frictional power consumption, lower operating temperatures, and reduce unwanted hydrodynamic pressure variations. The results from a comprehensive experimental programme confirmed the important merits of the new bearing design under high-speed conditions.

Operation of a Hydrostatic bearing under speed conditions

Fig. 1 shows the operation of a plain hydrostatic thrust bearing recess under speed conditions (1). It can be seen that the lands act as barriers to lubricant flow in the pockets. In order to ensure flow continuity a pressure difference is built up between the trailing and leading edges, the higher the velocity of the moving member the larger the pressure difference. If this velocity increases a point is reached where the pressure drops below ambient causing aeration and possible bearing failure. Also, for a given speed the induced pressure difference increases the rate of shear of the fluid adjacent to the moving member, which results in a corresponding increase in drag and frictional power consumption.

Much work has been undertaken by Mohsin and Sharratt (2) on the use of grooved lands instead of conventional flat lands. It has been shown that grooved lands reduce considerably the frictional power consumption compared with a flat land of equal hydraulic resistance. It has also been shown that they produce a negligible level of hydrodynamic action thus eliminating cavitation, aeration and whirl and were less sensitive to tilt, manufacturing tolerances and shaft bending.

Fig. 2 shows a hydrostatic bearing recess incorporating an External Recess Flow System or ERFS (3). Preliminary analytical work by Mohsin and Sharratt (3) has shown that the ERFS reduces the frictional power consumption and the pressure difference between the leading and trailing edges by allowing the fluid to circulate around the system and not in the pocket. In order to verify the theoretical results obtained by Mohsin and Sharratt, an experimental rig, which had the facility to vary the land and pocket geometries, was manufactured and tested. A detailed description of the test bearing is given in reference 5.

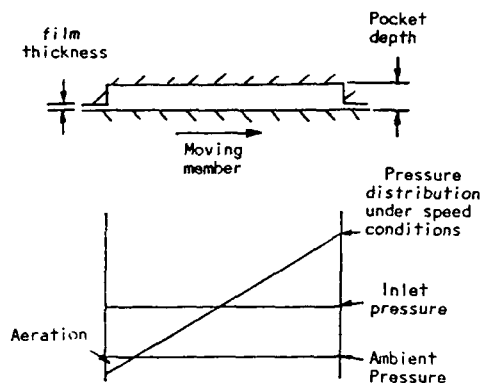


Fig. 1 Operation of a plain recess under speed conditions

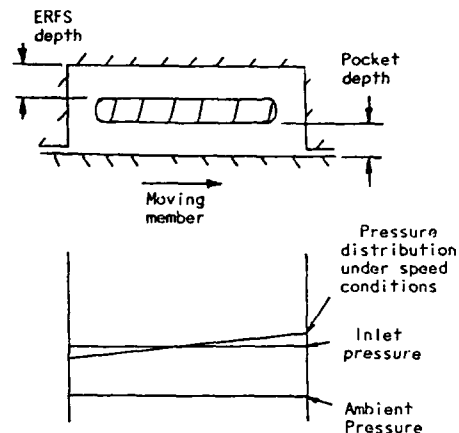


Fig. 2 Operation of an ERFS under speed conditions

Experimental Results

The benefits of a bearing with an ERFS using recess inserts have been confirmed, namely, lowering frictional power consumption and reducing the hydrodynamic pressure variations in the deep recesses. In Table 1 details of the frictional power consumption and the maximum pressure difference between the leading and trailing edges are given for two bearing geometries under identical operating conditions, i.e., speed = 3000 rpm, film thickness = 0.05mm and oil temperature of 50°C. Further tests confirmed the experimental results published by Mohsin and Sharratt (3) with regard to the loading, flow rate and frictional power consumption of grooved lands.

Pocket Depth (mm)	ERFS Depth (mm)	Land Type	Frictional Power Consumption (Watts)	Maximum ΔP between Leading and Trailing Edges (bar)
1.5	-	Grooved	2700	1.3
1.5	4	Grooved	2450	0.25

Table 1 The effects of an ERFS on bearing performance

References

- (1) SHINKLE, J.N. and HORNUNG, K.G. 'Frictional Characteristics of Liquid Hydrostatic Journal Bearings', ASME Trans., J. Basic Eng., Series D, V87, N1, March, Pages 163-169 (1965).
- (2) MOHSIN, M.E. and SHARRATT, A.H. 'The Behaviour of Hydrostatic Pads with Grooved Lands', Tribology, V14, N1, February, Pages 33-45 (1981).
- (3) MOHSIN, M.E. and SHARRATT, A.H. 'The Behaviour of a Total Cross Flow Hydrostatic Journal Bearing', Proc. 23rd Int. M.T.D.R. Conf., Manchester, 14-15 September, Pages 13-24 (1982).
- (4) MOHSIN, M.E. and SHARRATT, A.H. 'The Behaviour of a Total Cross Flow Hydrostatic Thrust Bearing', Proc. 21th Int. M.T.D.R. Conf., Swansea, Pages 449-459 (1980).
- (5) ASHMAN, D. 'High-speed Performance of a Hydrostatic Thrust Bearing', Ph.D. Thesis, Wolverhampton Poly. (1987).

TRIBOLOGICAL DESIGN - INFORMATION STORAGE AND RETRIEVAL

by

B Bhushan

(IBM Research Division San Jose U S A)

This paper presents the status of our current understanding of the tribology of head-medium interfaces in magnetic storage devices. To start out, designs and materials used in the construction of heads and media for tape, floppy, and rigid disk drives are presented. Theories of conventional friction, stiction, interface temperatures, wear, liquid/solid lubrication, and compressible hydrodynamic lubrication relevant to magnetic media are presented. Whenever necessary, experimental data are presented.

1.0 INTRODUCTION

Magnetic recording process is accomplished by relative motion between magnetic media against a stationary (audio and data processing) or rotating (video) read/write magnetic head. Under steady operating conditions, a load carrying air film is formed. There is a physical contact between the media and the head during starting and stopping. In modern high-end computer tape and rigid disk drives, the head-to-media separation ranges from about 0.1 to 0.4 μm . In floppy disk drives, head-to-media separation is even less ($<0.2 \mu\text{m}$) and physical contact generally occurs (Bhushan, 1989).

Need for higher and higher recording densities requires that surfaces be as smooth as possible and flying heights be as low as possible. Smoother surfaces lead to an increase in friction and interface temperatures and closer flying heights lead to occasional rubbing of high asperities and increased wear. Since interface failure even on a microscopic scale can lead to loss of valuable magnetic data recorded on a media, high interface reliability through the life of a magnetic storage becomes extremely important. A fundamental understanding of the tribology of magnetic storage systems is, therefore, crucial for the continued growth of the magnetic storage industry.

This paper presents the status of our understanding of tribology of head-medium interfaces.

2.0 MAGNETIC STORAGE DEVICES

Magnetic storage systems used for information storage and retrieval are: tape, floppy disk, and rigid disk drives. Magnetic media fall into two categories: particulate media, where magnetic particles are dispersed in a polymeric matrix and coated onto the polymeric substrate for flexible media (tape and floppy disks) or onto the rigid substrate, typically aluminum for rigid disks; thin-film media, where continuous films of magnetic material are deposited onto the substrate by vacuum techniques. Typical materials used for various magnetic media and operating conditions in computer applications are shown in Table 1 (Klaus and Bhushan, 1985).

Magnetic heads used to date are either conventional inductive or thin-film inductive and magnetoresistive (MR) heads. Conventional heads are combination of a body

forming the air bearing surface and a magnetic core carrying the wound coil with a read-write gap. In the film heads, the core and coils or MR stripes are deposited by thin-film technology. The air-bearing surfaces of most heads are made of hard ceramic materials - Ni-Zn ferrite, Mn-Zn ferrite, calcium titanate, and $\text{Al}_2\text{O}_3\text{-TiC}$ (Klaus and Bhushan, 1985).

Schematic of head-medium interfaces for tape, floppy, and rigid disk drives are shown in Fig. 1.

SESSION XV (Paper (iii) - FRIDAY 9th SEPTEMBER

ACTIVE MAGNETIC BEARING DESIGN METHODOLOGY -
A CONVENTIONAL ROTORDYNAMICS APPROACH

by

H Ming Chen

(Mechanical Technology Inc., New York U S A)

Synopsis

The recent advance of Active Magnetic Bearing (AMB) technology opens a new challenge to rotor-bearing design methodology.(1) Although rotor-bearing design is a well developed field in mechanical engineering, these new bearings involve electromagnetics and system control, areas which traditionally fall outside the rotor-bearing field. Mathematical modeling of AMBs is generally performed in electrical engineering and control language, in which the mechanical engineer is less fluent. To bridge the communication gap, the author promotes the features of the AMB from a rotor dynamist's point of view: (a) The AMB should be treated as a locally controlled device similar to other types of bearings, not actuators. (b) Like other bearings, the main functions of the AMB are to provide load capacity, stiffness and damping for supporting rotors.(2) Specific AMB characteristics are described below:

- A radial AMB consists of four quadrants of north-south poles (see Fig. 1). Each pair of opposite quadrants is stabilized independently by current control - similar to controlling a vertical rod at its base.
 - AMB size is dictated by the saturation flux density of the ferromagnetic material. More stator poles can save radial space.
 - The current slew rate, coil inductance and bias current of the power amplifiers/electromagnets limit the AMB frequency response and can cause instability in high frequency range.
 - A PID controller with three adjustable parallel circuit elements is used to achieve desired static and dynamic stiffnesses and damping. Only the journal displacement is measured. Analog circuit elements, such as the differentiator, phase-lead network or Velocity Observer can be used in the controller to obtain a pseudo velocity for generating damping.
- The AMB dynamics are represented by a set of first-order differential equations (see Fig. 2). The conventional rotor model state vector is extended to include the AMB states; thus an electromechanical dynamic model is formed for rigorous stability and unbalance response analyses.
- The control guidelines for rotor bending modes are described through use of an example. Bending modes below the operating speed must be well damped. The next one should be 15 to 20% in frequency above the operating speed and reasonably damped. Other unstable, high frequency modes, if they exist, can be detuned using band-reject filters implanted in the feedback control loop.

Because this presentation of AMBs uses a technical language that is more acceptable to mechanical engineers, it can accelerate the development of AMB

technology. It provides a methodology consistent with the conventional rotor-bearing design approach for specifying and implementing rotor-AMB systems.

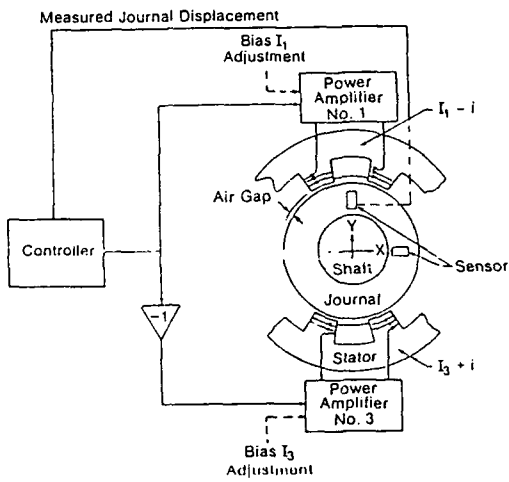


Figure 1

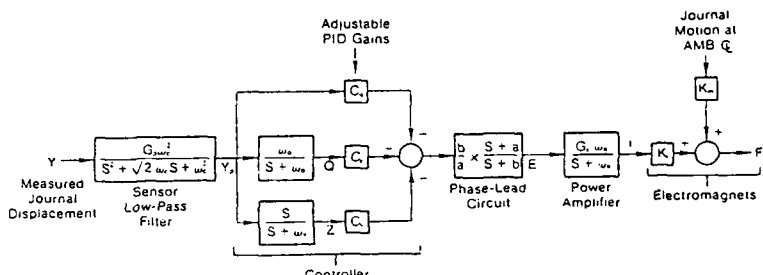


Figure 2

Rotor/AMB Force Coupling Equation

$$F = K_c i + K_m Y$$

AMB State Equations

$$i' + \omega_a i = G_s \omega_a E$$

$$E' + b E = -b/a [C_1 Q' + C_2 Z' + a(C_3 + C_2 Q + C_1 Z)]$$

$$Q' + \omega_a Q = \omega_a Y_p$$

$$Z' + \omega_a Z = V_p$$

$$Y_p' = V_p$$

$$V_p' + \sqrt{2} \omega_c V_p + \omega_c^2 Y_p = G_{sens} Y$$

References

1. Habermann, H. & Liard, G., "An Active Magnetic Bearing System", Tribology International, pp. 85-89, April 1980.
2. Hustak, J. F., Kirk R. G., & Schoeneck, K. A., "Analysis and Test Results of Turbocompressors Using Active Magnetic Bearings", Journal of ASLE, Lubrication Engineering, Vol. 43, pp 356-362, May 1987.

**THE INCORPORATION OF ARTIFICIAL INTELLIGENCE
IN THE
DESIGN OF HERRINGBONE JOURNAL BEARINGS**

by

K Ishii, B J Hamrock and J Klinger

(The Ohio State University, U S A)

SYNOPSIS

The objective of this research is to develop an intelligent computer program to aid in tribological design. Our focus is to integrate Artificial Intelligence and conventional numerical design techniques. As a vehicle for our effort, we focus on an example problem: the optimal design of herringbone journal bearings.

BACKGROUND

A fixed-geometry journal bearing that has demonstrated good load capacity and stability characteristics for both incompressible and compressible lubrication is a herringbone journal bearing. It consists of a circular journal and bearing sleeve with shallow, herringbone-shaped grooves cut into either member. Figure 1 illustrates a partially grooved herringbone journal bearing. Figure 2 indicates the groove and bearing parameters. Hamrock and Fleming (1971) reported a study on the optimization of self-acting herringbone journal bearings. They developed a program that, given the bearing parameters λ and Λ (design requirements), finds the groove parameters (design variables) such that the radial load capacity of the bearing is maximized.

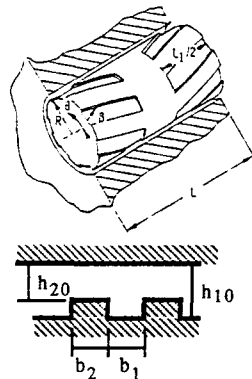


Fig. 1 Bearing Parameters

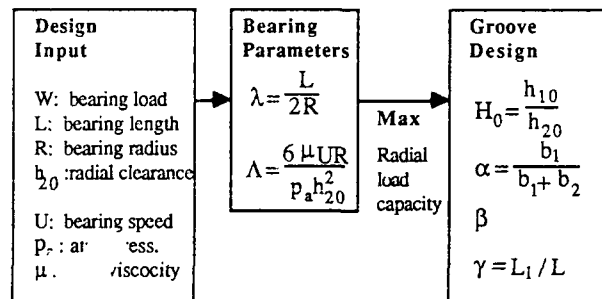


Fig. 2 Optimization of the groove parameters

Knowledge-based techniques can add another level of computer-aid to the above mentioned design synthesis program. Such techniques could identify incompatibilities between the design solution and factors not considered in the optimization program: bearing load requirement, the method of surface finish, constraints on speed, etc. A knowledge-based program could also catch obvious over design, such as an unnecessarily large bearing envelope. Another important task for our program is to make intelligent suggestions to remedy the incompatibilities: e.g., consider the use of different lubricant, modifying speed, radial clearance, or bearing envelope. The suggestions should also take into account effectiveness (sensitivity) of each remedy and its implications to other design constraints.

Ishii and Barkan (1987) developed a framework for knowledge-based design called Design Compatibility Analysis (DCA) that accommodates the features described above. DCA focuses on the compatibility, both qualitative and quantitative, between design requirements and design solutions (Fig. 3). DCA matches a given requirement and solution with compatibility knowledge (good and bad templates of design), combines the matching compatibility knowledge, and gives a total evaluation. In addition, DCA provides justifications for the evaluation and suggestion for improvement that applies not only to the design solution, but also to the design specification.

CURRENT WORK

This paper reports the use of DCA as a knowledge-based design loop that applies to the optimization program developed by Hamrock and Fleming (1977). Fig. 4 shows the flow of the design process which uses the numerical optimization as an inner design loop and DCA as an outer loop. The user of the program first enters the design requirements: bearing envelope (L and R), lubricant viscosity μ , bearing speed U, radial clearance h_{20} , and the bearing load W. The optimization program calculates the value of the groove parameters, H_0 , α , β , γ , i.e., for the design solution. Then, DCA asks additional questions (e.g., surface finish) and evaluates the compatibility of the design solution. If the design solution is unacceptable or is obviously an over design, the user can seek suggestions from DCA. DCA could suggest changes in bearing envelope, the lubricant, bearing speed, or radial clearance. The overall program helps the designers to consider manufacturing concerns in their design and thus helps them make a tradeoff between performance and cost.

Some specific performance checks that are made for each consideration are:

- 1) suitability of a hydrodynamic bearing
- 2) safe minimum film thickness
- 3) adequacy of load capacity and stiffness
- 4) effect of shaft angular deflection and assembly misalignment on h_{20} at the edge of bearing
- 5) transition speed between laminar and Taylor vortex flow
- 6) self-excited whirl instability ratio
- 7) flow rate, power loss, and attitude angle.

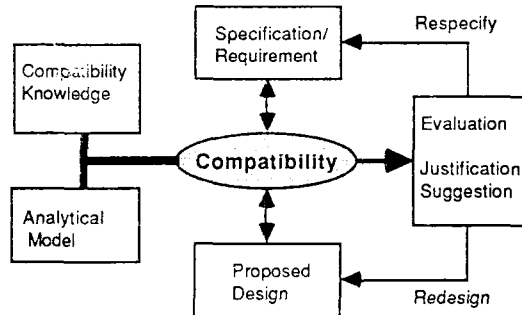


Fig. 3 Schematics of DCA

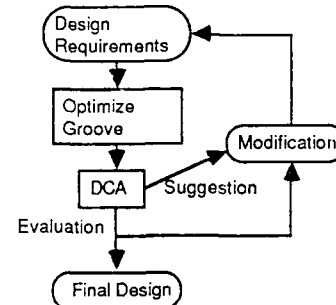


Fig. 4 Flow of intelligent bearing design

We implemented both the numerical and AI programs on an IBM PC. The program uses Turbo-PROLOG for DCA and FORTRAN for numerical optimization. The overall program generates an executable object file which the users can run without compilers or loaders.

In summary, this paper shows an example of how one can combine numerical techniques and AI-based methods to aid in the design of herringbone bearings. We hope to extend our methodology to other tribological design examples.

REFERENCES

- Hamrock, B.J. and Fleming, D.P. (1971) Optimization of Self-acting Herringbone Journal Bearings for Maximum Radial Load Capacity. NASA Technical Note, NASA TN D-6351.
- Ishii, K. and Barkan, P. (1987) Design Compatibility Analysis--a framework for expert systems in mechanical design. ASME Computers in Engineering 1987. Vol. one, pp.95-102.

SESSION XVI (Paper (ii)) - FRIDAY 9th SEPTEMBER

BEARING SELECTION USING A KNOWLEDGE BASED SYSTEM

by

R T Griffin, M J Winfield (Birmingham Polytechnic, U K)

S S Douglas (Liverpool Polytechnic, U K)

SYNOPSIS

It is recognised that there is a considerable difference in the levels of tribological knowledge typically found in academia and other research establishments compared to that frequently encountered in industry. If this difference is to be addressed, technology transfer mechanisms need to be developed, which can act as a conduit through which knowledge can flow. One technology transfer mechanism currently receiving wide attention is the development of tribological databases.

This paper reports upon a different technology transfer strategy which utilises knowledge based systems. These systems differ from a database approach in that they comprise both a knowledge base coupled with a search mechanism. These two components interact with the user to establish a solution to a specific problem, using the expert knowledge represented within the system. Two prototype systems have been developed to illustrate technology transfer for the selection of rotary rolling-element bearings. In particular the practicalities of acquiring knowledge and its subsequent representation within a system are discussed.

A block diagram representing the major stages of the system operation is shown in figure 1:

1) FORM FILLING SESSION - data is interactively entered into the system at the beginning of a session by filling in forms. Once entered, data is checked against a set of constraints. If any data items conflict, the system reports them to the user and requests the user to alter one of the conflicting data items.

2) PROBLEM SOLVING SESSION - whilst attempting to derive a solution, the knowledge base rules and database components are searched for appropriate items of knowledge/data. When the system cannot find an appropriate item of data, an interactive question is generated for the user to answer. Once entered, data is again checked against a set of constraints.

3) SOLUTION REPORTING SESSION - any solutions found during the problem solving session are displayed to the user. An example solution determined by the system for a given set of data is shown in figure 2. The solution is for a two location bearing arrangement in which one bearing is to be used at each location. The bearing types are to be single row deep groove ball and a database search has established six feasible components to use.

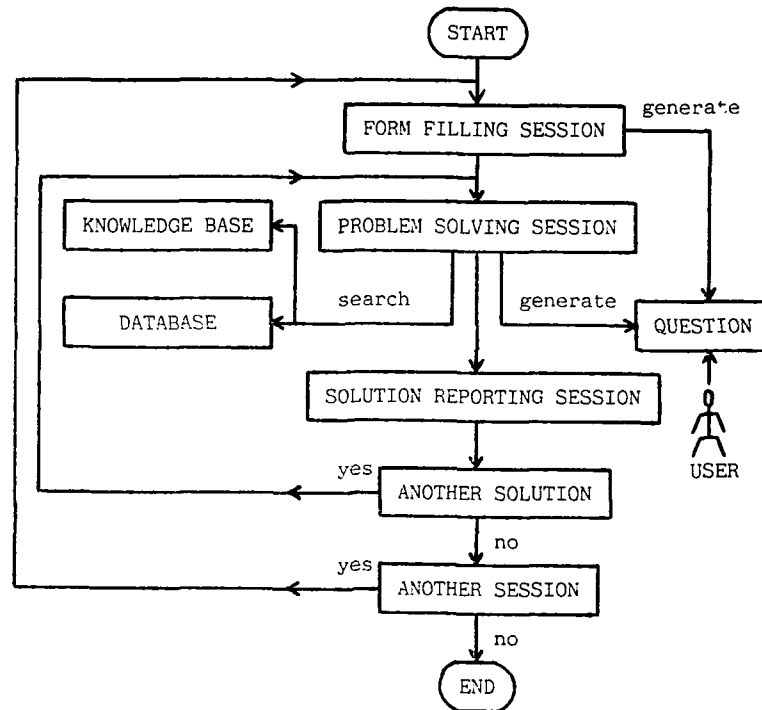


Figure 1 - Block diagram representation of system operation.

Data:

```

application_domain = OTHER
env_temp_changes_negligible
dist_fixed_free_negligible
angular_misalignment_required = very_small
degree_of_rigidity_required = very_low
applied_radial_load_magnitude_fixed_end = 3 kN
applied_radial_load_magnitude_free_end = 2 kN
applied_axial_load_magnitude = 2 kN
shaft_diameter_max = 500 mm
shaft_diameter_min = 258 mm
housing_bore_diameter_max = 600 mm
housing_bore_diameter_min = 510 mm
snap_ring_type = without
protection = none
rotational_speed = 750 rpm
environmental_temperature_max = 50 C
time_or_revs_life = revs
revs_life = 6 million revs
  
```

SOLUTION:

```

ARRANGEMENT : fixed_end = free_end
BEARING TYPE : single_row_deep_groove_ball
FEASIBLE COMPONENT NUMBERS : 6068, 6072, 6976,
                             6076, 6980, 6080
  
```

Figure 2 - Solution determined by system using given set of data.

SESSION XVI - (Paper (iii)) - FRIDAY 9th SEPTEMBER

TRIBOLOGY AIDS FOR DESIGNERS

by

C J Thijsse

(Philips Centre for Manufacturing Technology, The Netherlands)

SYNOPSIS

During the design phase of a construction, tribology is only one aspect that must be considered. The designer's tribological knowledge consists of single, more or less reliable facts. It therefore follows that it takes the designer a great deal of time to incorporate tribological aspects into his design, assuming he knows where to find these more or less established facts. What is needed is a logical collation of this knowledge. It is important to be able to assess whether a given design will encounter tribological problems by using some rules-of-thumb or simple computer programs. Insight into the tribological properties that play a part also need to be given, and ways must be indicated, along which solutions can be found.

For these reasons, we have divided tribology into four parts; **construction, lubricant, (surface) material and environment.**

Design specifications concerning dynamic and static behaviour, namely force, kind of motion, shape and permitted wear height, are reflected in the design.

The building blocks are formed by:

- a) the lubricant with viscosity and boundary lubrication properties as the important parameters and
- b) the (surface) materials with the important parameters of elasticity, hardness and roughness.

The environment forms the constraints within which the tribological system has to work.

We can now define the problem to be solved as follows: "What kind of building blocks should be chosen to meet the design specifications within the given environmental constraints?"

Plastic deformation, too much wear height and surface fatigue are considered as failure criteria .

To establish whether plastic deformation will occur in the contact, the admissible stress is compared with the actual stress. For counterformal situations, the contact stress is calculated according to Hertz. We have developed a computer program to calculate easily other contact situations than ball-ball or parallel cylindrical contact. Any necessary corrections can be made when a traction force is present.

To check that the admissible wear height is not exceeded, we compare the admissible wear factor (k -value) with the expected wear factor. Given the admissible wear height, the mode of motion of the surfaces relative to each other and of the contact place relative to the surfaces, the contact force and the shape of the contacting parts, one can easily calculate the admissible wear factor according to Archard, using a small computer program. For counterformal contacts, we have developed a computer program based on the work of Dowson and Higginson to calculate the situation of lubrication. Quick estimations for the expected wear factor can be made using a graph showing roughly the wear factors in relation to several tribo systems. For a more accurate prediction of the actual wear factor, we have built a database containing wear and friction results of approximately 600 series of (mainly pin-disc and pin-ring) experiments carried out in our own laboratory under varying circumstances. We are also building a similar system containing data from literature.

Plastic-metal systems can be tested for the permissible p_v -value or p_t -value, using a computer program based on the formulae from Erhard and Strickle.

Using data from literature, we have formed empirical formulae to establish whether there is a danger of surface fatigue. These formulae give, for metal surfaces, the relation between the contact stress, the number of load cycles during service lifetime, the situation of lubrication and the hardness of the material.

The above-mentioned formulae, graphs and PC programs give quick and easy insight into the feasibility of simple tribo systems. Also, to make the more complicated systems manageable, we have built a prototype expert system based on the tools mentioned, together with approximately 200 tribological rules(-of-thumb).

It should be clear from this approach that tribological expertise must not only be structured, but also simplified; indeed, this seems to be the only way for large groups of designers to learn about tribology. We hope to eliminate most of the trivial wear problems in this manner - in the event of very special tribological problems, the tribology experts are always willing to help.

15th LEEDS-LYON SYMPOSIUM ON TRIBOLOGY
THE TRIBOLOGICAL DESIGN OF MACHINE ELEMENTS
6th - 9th SEPTEMBER 1988

ACCOMMODATION

All delegates will be housed at Bodington Hall, a University of Leeds Hall of Residence, where technical sessions will also be held. The enclosed *FACT SHEET* will help delegates locate Bodington Hall - those arriving by air at Leeds/Bradford Airport should note that it is more convenient to take a taxi to the Hall than to use public transportation.

REGISTRATION

This will take place at Bodington Hall on the afternoon of Tuesday 6th September, commencing at 14.00. The Symposium registration desk will be located in the main entrance foyer at Bodington Hall and clear directions will be given on the precinct.

FIRST TECHNICAL SESSION

The Symposium Opening and Keynote Lecture to be presented by *PROFESSOR H.S. CHENG* will commence at 17.30 on the 6th September. Immediately afterwards at about 18.30 buses will leave Bodington Hall to take delegates to the Symposium Dinner to be held at the *MERCHANT ADVENTURERS HALL, YORK*.

DEPARTURE

Luggage may be left in the gym (see *FACT SHEET*) on the day of vacating. It would be appreciated if rooms could be cleared as soon as possible. We are able to arrange accommodation for those requiring it on the Friday night and indeed on Monday 5th September the day immediately preceding the Symposium.

SYMPOSIUM TELEPHONE NUMBER: (Leeds (0532) 670756).

OTHER DETAILS

There are some amendments to the provisional technical programme already distributed and details are enclosed. The final programme, together with the synopses of the papers and other material, will be available to delegates on registration. For any other information please telephone Leeds (0532) 332155.

We look forward to welcoming you to Leeds and to a fruitful and enjoyable Symposium.

D. DOWSON
C.M. TAYLOR
August, 1988

The University of Leeds

CONFERENCE FACILITIES FACT SHEET

BODINGTON HALL



Standing in 14 acres of private grounds in the attractive Leeds suburb of Adel, the Hall is a modern purpose-built conference and residential complex. Situated adjacent to the Leeds Outer Ring Road, an important advantage is the quick and easy access to all major incoming routes leading from the national motorway network and the close proximity of the international Leeds/Bradford Airport.

With the capacity to accommodate a maximum of 700 visitors, the Hall offers in-house facilities for self-contained conferences, seminars and special events for up to 300 delegates.

The central building provides all conference rooms, dining hall, sports and recreational areas. Close by lie eight houses, each with 75/80 bedrooms. The Hall overlooks a large expanse of lawned gardens and playing fields offering a wide range of opportunities for sporting tournaments, displays, demonstrations and similar outdoor events.

DAY SEMINARS—THROUGHOUT THE YEAR

The excellent location, wide range of meeting rooms and convenient layout of the Hall make it particularly suited for a one-day conference/seminar. This facility is available for up to 300 delegates and may be used throughout the year, including week-days during term time.

The Management and Staff have a wealth of experience in the

Conference Organiser's Office/Registration

The entrance lobby features a conference registration desk, porter's lodge and conference organiser's office for use throughout each event. Equipped with desk, external telephone line, etc., this facility provides the convenience of efficient communications on arrival and throughout each event.

Car Parking

Plentiful free car-parking is available throughout the extensive grounds.

Accommodation

Up to 700 guests can be accommodated in comfortable study bedrooms, the majority of which are single occupancy with a small number of twin rooms also available. Wash-hand basins are provided within 300 of the guest bedrooms, and each residential block contains a common room/lounge and a launderette. Each group of rooms shares a kitchen equipped with tea/coffee making facilities for visitors' use.

N.B. Residential accommodation is available only during vacation periods—normally July/August/September, End December/Early January, End March/April.

Audio Visual Equipment

The Hall provides a number of items of equipment free of charge for conference events, including:-

Rostrum and Lectern

PA System (Including Radio-Link Microphone)

Roll-Down Projection Screens

Flip-Charts and Blackboards

OHP and 35mm. Carousel Projectors

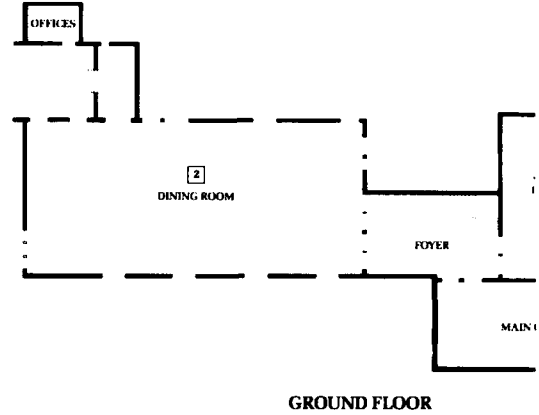
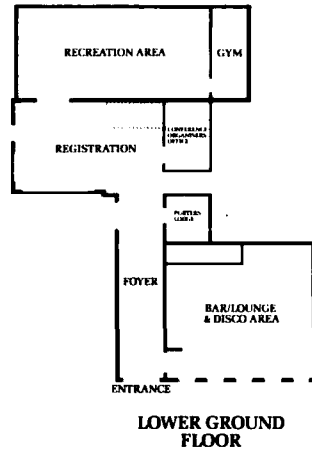
Additional equipment can be hired in from specialist outside suppliers on request.

Receptions

Private receptions, smaller dinners, etc. can be arranged within the Small Dining Room to provide a less formal atmosphere for up to 100 visitors.

organisation of this type of event, and our special Day Seminar package includes room hire charges (including syndicate rooms), audio-visual equipment, set conference lunch and refreshments between sessions.

Day seminar package currently charged at.....
per person per day, plus VAT at the appropriate rate.



Exhibition Facilities

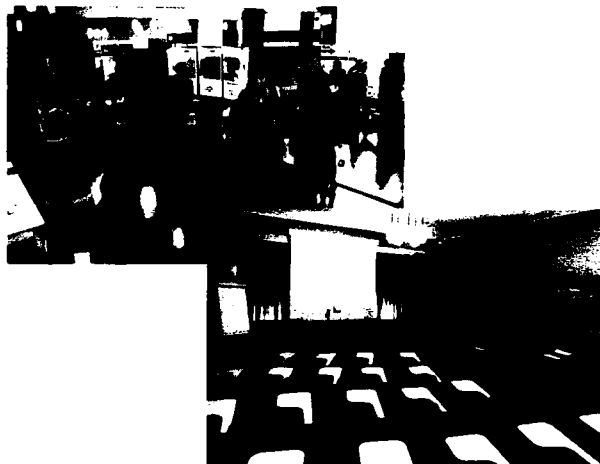
Adjoining the Main Conference Room lies the Small Dining Room, which offers flat-floored exhibition space of up to 1,800ft². This provides a convenient display area, which can be increased by the use of adjacent meeting rooms. Tea/coffee refreshments can be served between sessions within this area by arrangement.

The University has a comprehensive range of display panel boards, spotlights, tables and chairs etc., for hire, and can provide a complete "turnkey" exhibition system in this area.

Detailed floor plans are available for this and all ancillary rooms.

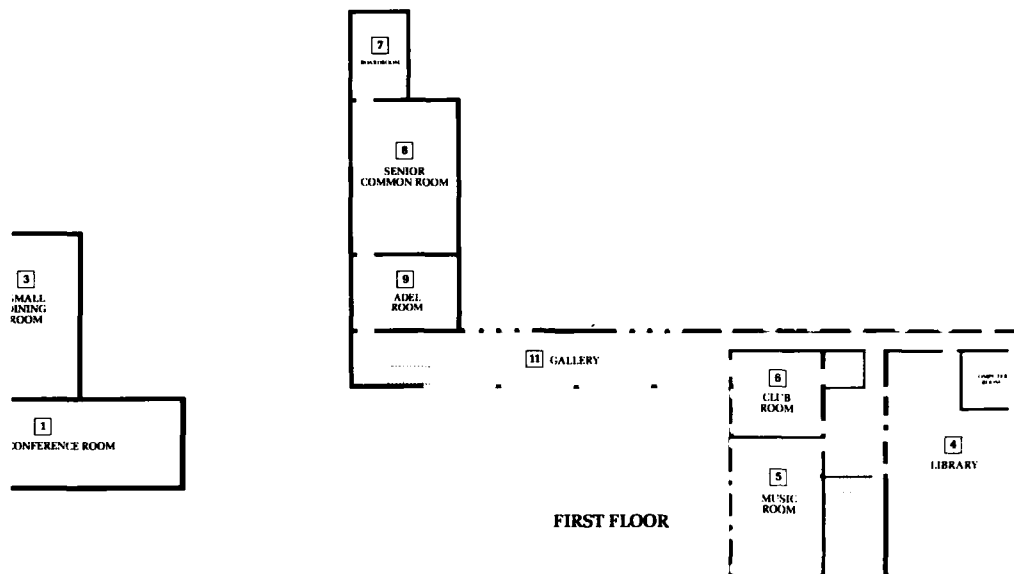
Meeting Facilities—Guide

All meeting rooms feature excellent natural daylight and include blackout curtains for audio visual work. All are flat-floored and can be provided with roll-down Projector Screens, PA System and Rostrum where applicable.



Key	Room	Dimensions	CAPACITY				Floor Area	Possible Uses
			Theatre Style	Boardrm Style	Recep'n	Dining		
1	Main Conference Room	80' x 27' 24.5 x 8.5m	300	—	450	—	240yds ² 202m ²	Main meeting/plenary sessions, usually equipped with Rostrum, PA System, Lectern, roll down Screens, etc.
2	Dining Room	101' x 50' 30.9 x 15.3m	—	—	600	350	561yds ² 473m ²	Formal style dining layout in either top table and sprigs, or in tables of 12 covers. Raised section to feature high table for 40.
3	Small Dining Room	52' x 35' 15.9 x 10.7m	150	—	250	120	202yds ² 170m ²	Exhibitions and displays, receptions pre or post-dinner.
4	Library	52' x 35' 15.9 x 10.7m	150	—	200	—	202yds ² 170m ²	Medium size meeting room for 150, also includes ante-room equipped with computer main frame connection point.
5	Music Room	38' x 24' 11.6 x 7.3m	80	30	100	—	101yds ² 85m ²	Large syndicate or smaller meeting room for up to 80 (theatre style).
6	Club Room	22' x 24' 6.7 x 7.3m	40	20	—	—	59yds ² 49m ²	Syndicate or large board room style for up to 40.
7	Board Room	15' x 19' 4.6 x 5.8m	—	12	—	—	32yds ² 27m ²	Committee meetings around board table for up to 12.
8	Senior Common Room	36' x 21' 11.0 x 6.4m	40	30	80	—	84yds ² 71m ²	Larger syndicate or committee meeting room, equipped with easy chairs and coffee tables.
9	Adel Room	17' x 14' 5.2 x 4.28m	30	15	—	—	26yds ² 22m ²	Syndicate or ante-room for small receptions, committee meetings etc.
10	Common Rooms (x14)	(variable)	(each) 25 +	(each) 12	—	—	—	Each house has one or two large common rooms, which offer light spacious facilities for syndicate work for up to 25/30 delegates.
11	Gallery	63' x 15'6" 19.2 x 4.72m	—	—	—	—	106yds ² 90m ²	Overlooking dining room, provides attractive space for poster/product displays.

All Dimensions are approximate.



SPORTS AND RECREATIONAL FACILITIES

Should the conference programme allow, residential visitors can make full use of the excellent range of sports and recreational areas:-

Snooker Two full sized tables together with a full range of equipment are available, with a small charge being made by means of metred lighting for the use of each table.

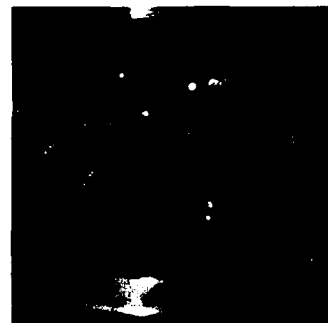
Squash Two full sized squash courts are available on the ground floor, with a small charge being made for each playing session.

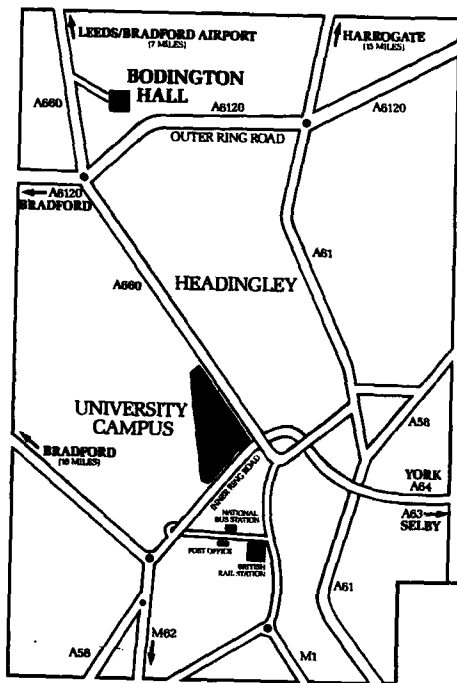
Table Tennis/Badminton Equipment can be provided within any suitable sized meeting room not otherwise in use, free of charge.

Pitch and Putt, Golf/Croquet A flat lawned area can be provided, in warmer weather, for either croquet or pitch and putt golf.

Sports Pitches Adjacent to the Hall complex lie several sports pitches which can be used by prior arrangement for football/rugby/hockey/cricket, with charges being made dependent upon playing numbers and duration of time in use. A large sports pavilion overlooks the playing field which can also be hired during vacation periods.

Bar/Lounge and Disco On the ground floor adjacent to the main entrance is a newly refurbished bar/lounge. Visitors are charged pub-type bar prices, and a dance floor area features disco lighting and sound system for social functions in the evening. A charge is made for provision of a disco to visiting parties.





From M62/M621, take signs for Harrogate/Wetherby/York from end of motorway along Inner Ring Road. After half mile take 'University' signs and drive straight on **past** University main entrance on left hand side. Continue for two miles and road becomes signposted A660 'Otley'. Straight over large roundabout at Outer Ring Road and after ¼ mile take slip road on right hand across carriageway into entrance drive.
(M621 - 6 miles).

From West and North West (Bradford), at junction of A6120 Leeds Outer Ring Road turn left, continuing until large roundabout, taking left turn signposted A660 'Otley'. After ¼ mile take slip road on right hand across carriageway into entrance drive.
(Bradford - 7 miles).

PUBLIC TRANSPORT

Rail B.R. Intercity Leeds Station - 4 miles
Air Leeds/Bradford International Airport - 6 miles
Bus (From B.R. Station and National Bus Terminal, board at City Square) - **Yorkshire Rider**
 No 1 - Stop at Lawnswood
 No 92 - Stop at Lawnswood
 No 95 - Stop at Bodington Hall
 10/15 minutes travelling time from City Centre/Station
Taxi 10/15 minutes travelling time from City Centre/Station

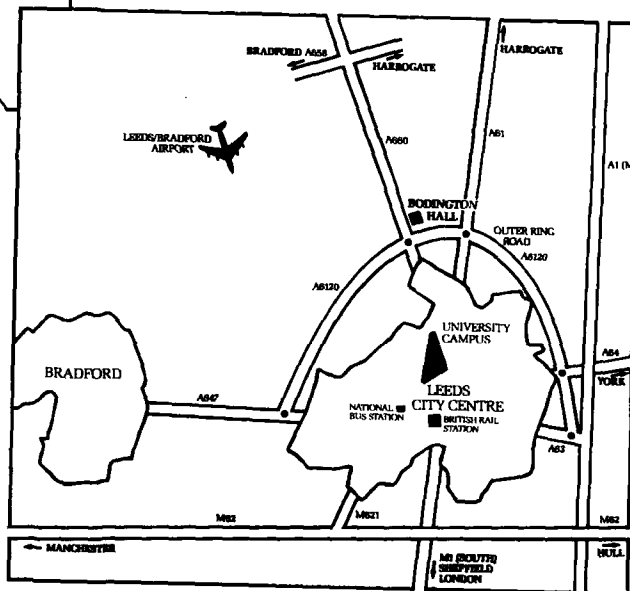
LOCATION

ACCESS BY ROAD

From North and North East (A61 Harrogate, A661 Wetherby, York), turn right on to A6120 at Leeds Outer Ring Road, continue until large roundabout, turn right onto A660 signposted 'Otley'. After ¼ mile take slip road on right, across carriageway into entrance drive.
(Harrogate - 14 miles, A1 North via A64 - 12 miles, York - 25 miles).

From A1 South, turn off A1 at A63, continue for five miles until city outskirts, turn right onto A6120 along Leeds Outer Ring Road until large roundabout, take right turn onto A660 signposted 'Otley'. After ¼ mile take slip road on right across carriageway into entrance drive.
(A1 South, via A63 - 14 miles).

From M1 South, take 'City Centre' signs from end of M1, approaching city centre take 'University' signs and drive straight on **past** the University main entrance on left hand side. Continue for two miles and road becomes signposted A660 'Otley'. Straight on at large roundabout at Outer Ring Road, and after ¼ mile take slip road on right hand across carriageway into entrance drive.
(M1 South - 6 miles, City Centre - 4 miles).



Postal Address

Bodington Hall, Otley Road,
 Leeds LS16 5PT
 Telephone (0532) 672521

The University of Leeds



Reservations and Enquiries

Commercial Office,
 University of Leeds,
 LEEDS LS2 9JT.
 Tel. (0532) 336100 or 459944
 Fax. (0532) 336017

(A Member of British Universities Accommodation Consortium)

15th LEEDS-LYON SYMPOSIUM ON TRIBOLOGY
THE TRIBOLOGICAL DESIGN OF MACHINE ELEMENTS
6th - 9th SEPTEMBER 1988

The Symposium will be held at Bodington Hall, University of Leeds, Otley Road, Leeds LS2 9JT

O U T L I N E P R O G R A M M E

TUESDAY 6th SEPTEMBER

07.30 - 08.15	Session I	Keynote Address			Clayton

WEDNESDAY 7th SEPTEMBER

09.00 - 10.30	Session II	Review Papers			Down Ditchford Froese Widmann Zimmer-Spahn

11.00 - 12.30	Session III	Seals			Salovey Cox Koh Gabelh Kambers Visscher Stakenborg van Gesten

13.00 - 15.00	Session IV	Cams			Gezon Froese Kambers Joll Dobson Tait

15.00 - 15.45	Session V	Belts			Childs Gerritt

16.15 - 17.30	Session VI	Gears			Harrop Tom Pryden O'Moiglu Velas Reilly

THURSDAY 8th SEPTEMBER

08.30 - 10.00	Session VII	Rolling Element Bearings			Konstantin Lambert Frost Scales Ioannides Hamer Ko

	Session VIII	Plain Bearings			Gethin Cooking Wilcock Booser Medwell

	<i>Session IX</i>	Wear	Kuno Waterhouse Evre Felder Briscoe Tweedale
10.30 - 12.00	<i>Session X</i>	Rolling Element Bearings	Han Winer Chatterjee Fischer Fisher Fischer Werner Fischer Werner
	<i>Session XI</i>	Plain Bearings	Han Fischer Briscoe Fischer Fischer Baker Bosker Chatterjee Tucker
	<i>Session XII</i>	Ceramics	Chatterjee Stolarski Kutelski Platen Raj Sasaki Date Fischer
<u>FRIDAY 9th SEPTEMBER</u>			
09.00 - 10.30	<i>Session XIII</i>	Review Papers	Chatterjee Chatterjee Roberts Bosker Fischer Muller
11.00 - 12.30	<i>Session XIV</i>	Hydrostatic Bearings	Xu Chen Van Heijningen Kantor Kolkman Fischer Weston Morton Rowe Ashman Parker Gardner
14.00 - 15.00	<i>Session XV</i>	Information Storage and Retrieval/Magnetic Bearings	Boushian Chen
15.00 - 16.00	<i>Session XVI</i>	Knowledge Based Systems	Ishi Hamrock Klinger Winfield Douglas Griffin Thijssen

15th LEEDS-LYON SYMPOSIUM ON TRIBOLOGY

VISIT to NORTH YORKSHIRE MOORS - 8th SEPTEMBER 1988

As indicated on the final programme a visit to the North Yorkshire Moors has been arranged for all delegates who wish to take part, on the afternoon and evening of **Thursday 8th September.**

The North Yorkshire Moors form an area of outstanding natural beauty, with many pretty inland villages and bounded on its eastern side by a rugged, high-cliffed coastline and picturesque fishing villages. We have arranged four separate visits, all including the North Yorkshire Moors, but visiting different places of interest. Delegates may, with certain limitations noted below, choose anyone of the four tours, but as the number of places on each tour is limited this choice must be on a "first come" basis. Lists for registering for the tours will be available at the Symposium. Choice of tour must be indicated not later than 11.00 a.m. Wednesday 7th September. All the tours conclude with Dinner at the Crown Hotel, Boroughbridge.

The four tours on offer are:-

KILBURN (Woodcarving) and WHITBY

RIEVAULX ABBEY and WHITBY

NORTH YORKSHIRE MOORS RAILWAY and WHITBY

FYLINGDALES EARLY WARNING RADAR STATION and RIEVAULX ABBEY

Detailed itineraries for the four tours, are given below:

(a) KILBURN and WHITBY

Coach from Bodington Hall to Kilburn Village arriving at approximately 2.00 p.m. Delegates will be able to visit the famous Thompson (Mouseman) furniture factory and see traditional, hand-crafted and hand-carved solid oak furniture being made and also to view the showrooms. Note that there is no organised 'tour' of the workshop but you will be free to wander. Departure from Kilburn is at 3.15.p.m. and the coach then goes directly to Whitby, arriving at approximately 4.30.p.m. Whitby is a large fishing village of great character and visual charm. It is split into two halves by the River Esk, and it was here that the explorer Captain Cook was born and learned his seamanship. Whitby has historical connections with the Victorian photographer, Frank Meadows Sutcliffe and was the setting for the original Dracula stories by Bram Stoker. St. Mary's church is an extremely interesting example of Norman architecture with a unique interior and is well worth a visit. From the churchyard magnificent views of Whitby may be enjoyed and immediately adjacent to the church are the ruins of the 13th century Abbey. A stone stairway with 199 steps leads down into the town. Delegates will have approximately 1½ hours free time in Whitby before the coach leaves at 6.00 p.m. to arrive at the Crown Hotel, Boroughbridge at approximately 7.30.p.m. for Dinner.

(b) RIEVAULX ABBEY and WHITBY

Coach from Bodington Hall to Rievaulx Abbey, arriving at approximately 2.15.p.m. Here delegates will be free to explore the Abbey at leisure. Rievaulx Abbey was founded in 1131 by Monks of the Cistercian order and the ruins which still stand have a soaring beauty which is awe inspiring, and are set in a steep, richly wooded valley.

The coach will leave Rievaulx at 3.30.p.m. to arrive at Whitby at approximately 4.30 p.m. Departure from Whitby will be at 6.00.p.m., giving delegates 1½ hours free time in the town. The tour will conclude at the Crown Hotel, Boroughbridge for Dinner.

(c) NORTH YORKSHIRE MOORS RAILWAY and WHITBY

Coach from Bodington Hall to Pickering, to arrive at approximately 2.30.p.m. Pickering is a small market town surrounded by attractive farming land to the south and moorland to the north and east. At Pickering delegates will board the North Yorkshire Moors Railway train to depart at 2.50.p.m. The steam hauled train will travel through wooded slopes, steep gorges, moorland and nature reserves to arrive at Grosmont at 3.55.p.m. The line was originally built by George Stephenson in 1836. At Grosmont delegates will once again join the coach for a short ride to Whitby arriving at approximately 4.30.p.m. Once again there will be approximately 1½ hours free time before departing Whitby at 6.00.p.m. for Dinner at the Crown Hotel, Boroughbridge.

(d) FYLINGDALES EARLY WARNING RADAR STATION and RIEVAULX ABBEY

[Please note that this tour is restricted to delegates who come from the NATO countries or from Australia and New Zealand].

Coach from Bodington Hall to Royal Air Force Fylingdales to arrive at approximately 3.00.p.m. Here delegates will take part in a guided tour of the establishment and will be able to see the current range of early warning radars and some of the engineering aspects of the radar superstructures including the advanced rolling element support bearings. Departure from Fylingdales is at 5.00.p.m. and the tour then goes to Rievaulx Abbey to arrive at approximately 5.45.p.m. Delegates will have 45 minutes to explore the Abbey before departing at 6.30.p.m. for the Crown Hotel for Dinner, arriving at Boroughbridge at approximately 7.15.p.m.

B. Jobbins

September 1988

15th LEEDS-LYON SYMPOSIUM ON TRIBOLOGY
THE TRIBOLOGICAL DESIGN OF MACHINE ELEMENTS
6th - 9th SEPTEMBER 1988

NOTE TO AUTHORS:

- [1] There have been some modifications to the preliminary programme already distributed. Please find enclosed an outline of the final programme indicating the time at which you will be making your presentation.
- [2] All technical sessions will be held at Bodington Hall, the University Hall of Residence where delegates are being accommodated.
- [3] The usual audio-visual facilities will be available in the main conference room:- blackboard, overhead projector, 2 x 2 slide projector, film projector and microphone (if required). For the parallel sessions an overhead projector and slide projector will be available and other requirements should be notified.
- [4] A projectionist will be available throughout the Symposium and slides may be handed to him before the session. Notice of any special requirements e.g. films, would be appreciated. Slides may be indexed by the presenter himself, or the projectionist, as required.
- [5] On this occasion only written discussions will be accepted for publication in the final proceedings. This will be circulated to authors by mid-October and replies must be provided by mid-November to meet the publishing deadline.
- [6] *TIMING*

The schedule for the Symposium is extremely tight and authors must limit themselves to 15 minutes presentation time. Session Chairmen will be asked to be firm in ensuring that their session runs to time and that each presenter has a fair share of the time available. Review papers may have slightly longer for presentation by agreement with the Chairman.

15th LEEDS-LYON SYMPOSIUM ON TRIBOLOGY
THE TRIBOLOGICAL DESIGN OF MACHINE ELEMENTS
6th - 9th SEPTEMBER 1988

NOTE TO SESSION CHAIRMEN:

- [1] The schedule for nearly all sessions is extremely tight and it would be appreciated if Chairmen would firmly limit those authors who run over their allotted presented time.
Presentations should be limited to 15 minutes or slightly more for Review Papers depending on the time wished for discussion.

- [2] It has been the tradition of Leeds-Lyon Symposia to have presentation of the papers in sequence by delaying discussion and questions until all the papers have been read. In this way each author should have a fair presentation time.

- [3] It would be appreciated if Chairmen could identify the presenter of the multi-author papers and introduce presenters with a few biographical details.

- [4] On this occasion only written discussions will be accepted for publication in the Proceedings together with authors replies. Could Chairmen please encourage such written discussion to be received in Leeds by early October at the latest.

Thank you.